DEPARTMENT OF THE ARMY
U.S. ARMY FOREIGN SCIENCE AND TECHNOLOGY CENTER
220 SEVENTH STREET NE.
CHARLOTTESVILLE, VIRGINIA 22901

TRANSLATION

In Reply Refer to:
FSTC-HT-23-0585-74
DIA Task No. T74180174

Date: 27 Feb 1974

AD783747

ENGLISH TITLE: CAVITATION DAMAGE IN DIESEL ENGINES

SOURCE: Kavitatsionnyye Razrusheniya v Dizelyakh, Mashinostroyeniye Press, Leningrad, 1970, 152 pp

AUTHOR: N. N. Ivanchenko, A. A. Skuydin, and M. D. Nikitin

LANGUAGE: Russian

COUNTRY: USSR

REQUESTOR: AMXBR-XA-FI

TRANSLATOR: Leo Kanner Associates, Redwood City, CA (AC)

ABSTRACT: The book deals with cavitation damage to diesel engine parts, methods of controlling this damage, and techniques for calculating and accelerated testing of parts for cavitation resistance. Principal factors leading to cavitation erosion in diesel engines are examined: water temperature in diesel engine cooling jackets, design factors, and operating factors. Methods of calculating vibrational acceleration of cylinder liners are outlined; estimates are presented of the possible amplitudes and critical accelerations of vibrations in the surfaces of parts swept by water in a diesel engine.

NOTICE

The contents of this publication have been translated as presented in the original text. No attempt has been made to verify the accuracy of any statement contained herein. This translation is published with a minimum of copy editing and graphics preparation in order to expedite the dissemination of information.

Approved for public release. Distribution unlimited.

TABLE OF CONTENTS

AUTHORS' ABSTRACT

Kavitatsionnyye Razrusheniya v Dizelyakh [Cavitation Damage in Diesel Engines], N. N. Ivanchenko, A. A. Skurdin, and M. D. Nikitin, Leningrad, Mashinostroyeniye Press, 1970, 152 pages; 21 tables, 83 illustrations, and 54 bibliographic references.

The book examines systematically processes of cavitation damage to diesel engine parts, methods of controlling this damage, and techniques of calculation and accelerated testing of parts for cavitation resistance. The main factors leading to cavitation erosion in diesel engines are analyzed; the effect on the damage rate of water temperature, design and operating factors, and the like on the damage rate is described.

The theoretical fundamentals of cavitation in the presence of vibrational fields are presented. Methods of calculating vibrational characteristics of systems are set forth; estimates are given of the possible amplitudes and critical accelerations of vibrations of surfaces swept by water.

The book is intended for engineering-technical personnel concerned with diesel engine designing and construction. It can also prove useful to students at higher educational centers in the appropriate specialties.

FOREWORD

Directives under the Five-Year Plan for the development of the national economy adopted at the Twenty-third Congress of the CPSU provide for increasing the capacity, operating economy, reliability, and longevity of machines, instruments, and equipment, and increasing the potential of motors by one and one-half to three times. Advances in modern diesel engine-building are related to the steady growth in the level of uprating engines by increasing the degree of supercharging and the engine rpm.

Increases in high speeds and the mean effective pressure, along with the trend toward reduction in weight and overall dimensions, lead to cavitation damage in diesel engine parts. Cavitation damage is encountered not only at surfaces of cylinder liners and the block swept by coolant fluid, but also at the surfaces of the main and connecting rod bearings, and at the parts of the fuel feed system and water pumps. Cavitation damage can be detected at the surfaces of parts operating in various conditions, and also in liquids with different properties. Therefore eliminating cavitation damage in diesels is a most important and urgent problem.

Various points of view have been expressed in the technical literature concerning the causes leading to the intensive failure of cylinder liners. Some investigators state that this is the result of electrochemical corrosion, while others attribute the failure to cavitation erosion. The complexity of the physicochemical processes leading to cavitation failure of cylinder liners hampers the direct study of individual stages of these processes.

Numerous experimental studies have dealt with the problems of cavitation and the damage it causes in machine building and shipbuilding. However, the problem of cavitation damage in diesels has not been sufficiently discussed in these works.

The present study examines problems involved in finding the causes responsible for cavitation and cavitation damage to the surfaces of the parts of diesel engines swept by water, as well as methods of investigating materials used in diesel engines and diesel engine parts for their cavitation resistance. A relationship is shown between diesel engine characteristics and cavitation damage. A method is outlined for calculating diesel engine cylinder liners with respect to cavitation resistance and measures to suppress cavitation damage to diesel engine parts which thus far have not been generalized.

The material for the book was provided by experimental studies conducted by the authors at different times in Central Scientific Research Diesel Engine Institute.

We request that all comments and suggestions concerning this book be sent to the publisher.

CHAPTER ONE

CAVITATION DAMAGE TO DIESEL ENGINE PARTS

1. Cavitation Damage to Water-Swept Surfaces of Cylinder Liners and Blocks of Diesel Engines

Diesel engines with high specific weight and built with thick-walled cylinder liners and blocks did not suffer intensive damage to water-swept surfaces of these parts. Later, as lighter-designed diesels were built and as they were uprated in their mean effective pressure and rpm, damage to cylinder liner walls and cylinder blocks began to be encountered in many engine models. This damage also shows up in the formation of local accumulations of deep pits, in most cases with a clean surface, without the presence of deposits of corrosion products. They develop independently of the general corrosion pitting of the cylinder liner walls and blocks which is observed in engines that are cooled with seawater.

In most cases, before clusters of pits appear on a cylinder liner wall, the wall is coated with an oxide film at the site of future damage.

With further operation of the engine, pits begin to appear, very rapidly enlarging, and in several cases continuous flaws are formed in the cylinder liner walls.

The first clusters of pits appear in the rocking plane of the connecting rod on the side in the direction of which the piston side pressure is applied in the power stroke. If one faces an engine so that the crankshaft rotates clockwise, the first local clusters of pits will appear on the left side of the cylinder (on the water jacket side). With further operation of the engine, the area of the damaged section enlarges, and sometimes even new zones of pit clusters appear.

The first investigators studying the causes for this defect (1935-1939) concluded that it was electrochemical in nature. They suggested that the effect is caused by unaven cooling, stagnant zones in the cooling system, metal contamination, the presence of dissimilar metals in the cooling system, and other similar factors. Therefore, they recommended controlling the pitting of liners by installing zinc protectors and by modifying the water flow direction in the cooling systems. The ineffectiveness of these measures compelled designers and researchers to study more closely the causes and conditions leading to pit clusters appearing on cylinder liners and blocks in diesel engines.

In 1948-1952 it became possible to establish [17, 22] that the cause must be sought for in cavitation processes brought about in diesel engines by high-frequency vibrations of the walls of cylinder liners. When the walls of cylinder liners and blocks in diesel engines are damaged by cavitation, failure and electrochemical erosion are observed [35].

The mutual role of these radically distinct processes depends on numerous factors and has not yet been adequately studied.

In several cases (damage to dielectrics, cavitation in chemically neutral liquids), cavitation erosion is manifested as mechanical damage without the presence of electrochemical processes. The progression of the damage is associated with surface fatigue of the metal. This is based on the fact that in the initial period the surface undergoes work hardening and only thereupon do pits appear [10]. In contrast to this point of view, other authors noted that fatigue phenomena do not play an appreciable role in the progression of cavitation damage. In their view, the chipping of material is caused by each of the individual conditions developing in the collapse of cavitation bubbles [cavities] [30].

Some theories state that the initiation of high temperatures in the latter stages of the compression of cavitation bubbles promotes the spread of damage.

At the present time it now has been reliably ascertained that damage to cylinder liner walls and cylinder blocks is caused by cavitation processes initiated in the cooling system of the engine by the action of high-frequency vibrations of cylinder liners excited by piston blows resulting from piston slap from one cylinder wall to the other on passing through the top dead center [17].

The presence of a heat gap between the piston and the cylinder liner leads to the piston striking the liner wall and causing it to undergo high-frequency vibrations in slap (change in direction of application of piston side pressure against the cylinder wall). When the liner walls

are in vibration, alternating elongations and compressions occur in the water jacket, leading to the formation and implosion of cavitation bubbles, which then causes cavitation erosion.

Depending on the model of the engine, the design of the cylinder liner, the ratio of the cylinder wall thickness to the cylinder diameter, the gap between the piston and the liner, and several other factors, the number and arrangement of the zones of pit clusters can vary. However, all cases have the common factor that the first clusters of pits appear in the rocking plane of the connecting rod. Thin-walled cylinder liners vibrate, forming several antinodes in the cross section, and in each of these a damage zone appears. Significant damage is also encountered at the sealing and support shoulders and in the blocks. Here the damage is accompanied by the formation not only of deep pits, but also of longitudinal depressions.

Thus, cavitation damage of two types appears at cylinder liners and blocks:

1) clusters of deep pits with clean surfaces in the rocking plane of connecting rods (when there is cavitation erosion caused by vibrations in the acoustic and ultrasonic ranges);

2) clusters of pits at the locations of water outflow and inflow (when there is corrosion damage caused by the combined action of hydrodynamic and vibrational cavitation); and

3) pitting of support and sealing shoulders (the result of the intensifying of cavitation processes in narrow water jackets with the probable participation of crevice corrosion).

Typical of cavitation damage in cylinder blocks is the fact that prevention of liner damage by applying a solid coating (chrome plating or nitriding) leads to intensified damage of blocks at locations that are opposite the zones of cylinder liners where their pitting had been earlier detected (before the coating).

The vibration of liners causes alternating elongation and compression of the water in the cooling jacket. This leads to the formation and closure of cavitation bubbles (cavities).

Figure 1 shows the cylinder liners of a diesel engine after 542 hours of operation. Clusters of deep pits are clearly discernable on their surfaces in the rocking planes of the connecting rods.

Figure 2 shows the damage in the zone of the seating shoulders. As the result of pits forming at the upper seating shoulders of liners, cracks appear often in the liners beneath the sealing shoulder, which completely impairs the liners.

An example of damage to a liner that had been in service for a total of 106 hours, in the water inflow location, is shown in Figure 3. The arrow points to the location of water inflow. This kind of cylinder liner damage differs appreciably from general liner pitting caused by erosion when cooled by seawater. The corrosion process accompanies severe electrochemical pitting of the entire liner surface, on which a patina of corrosion products and traces of graphite from the liner material (cast iron) remains. However, even here liner vibration leads to simultaneous cavitation damage, which aggravates the general damage to the external liner surfaces.

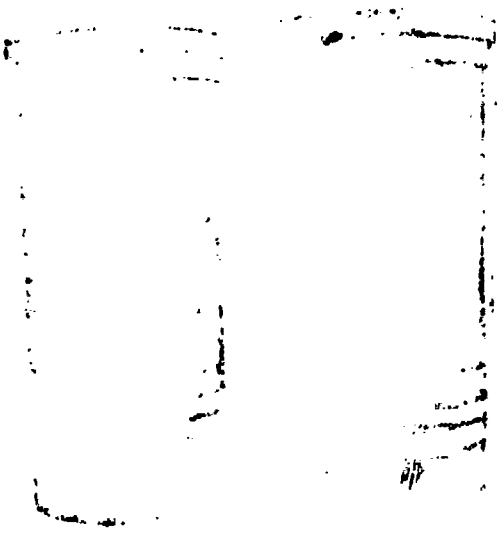

Figure 1: Cylinder Liners of the 1Ch 8.5/11 Diesel Engine After 562 Hours of Operation.

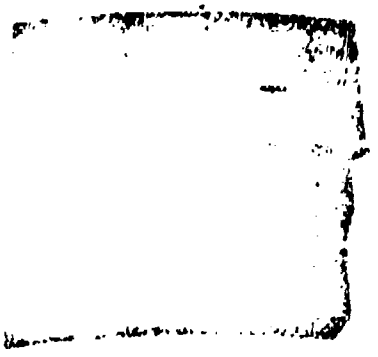

Figure 2: Damage to Cylinder Liners of 4Ch 17.5/24 Diesel Engine in the Area of the Upper Seating Shoulder

Figure 4 shows the cylinder liner of a marine diesel engine after 2500 hours of operation. Traces of cavitation damage over large areas can be noted on its surfaces, along with traces of corrosion and salt deposits.

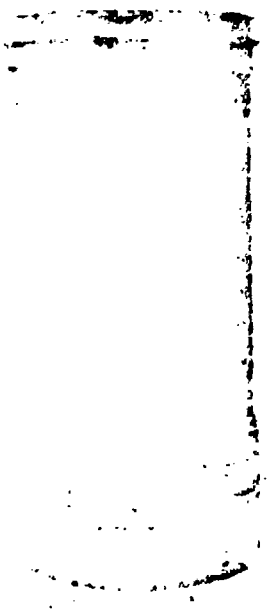

Figure 3: Liner Damage in the Area of Cooling Water Inflow

Figure 5 shows the initial stage of damage to a diesel engine block. Blocks made of cast iron undergo damage most intensively. Aluminum blocks prove to be more resistant to cavitation erosion than cast iron blocks.

Damage to the walls of cylinder liners and diesel engine blocks caused by cavitation erosion significantly reduces the service life and reliability of diesel engines, since such damage causes cracks and

sometimes continuous flaws to appear. This leads to water entering the oil and the diesel engine malfunctioning.

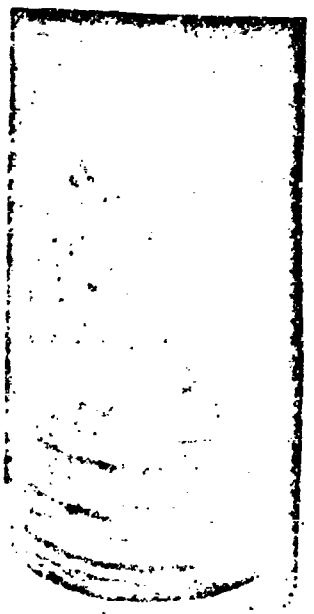

Figure 4: Damage to Cylinder Liner of a Marine Low-Speed Diesel Engine

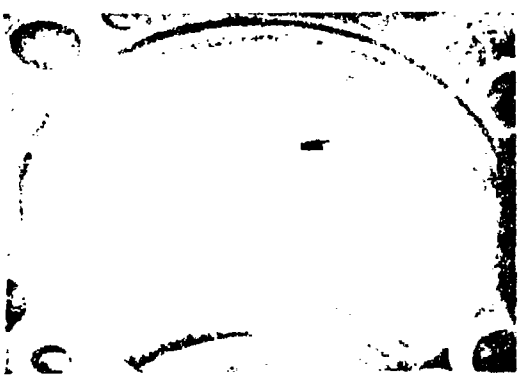

Figure 5: Damage to Cylinder Block of Diesel Engine

2. Cavitation Damage to Bearing Shells and Fuel Feed Equipment Parts

Increasingly, damage to the surfaces of crankshaft bearings is showing up in uprated diesel engines; this damage is caused by cavitation processes in the oil layer. Usually these consist of point chipping of the bearing material (most often lead bronze) situated in the zone of maximum pressures in its oil layer. By its nature, this chipping differs appreciably from the damage in bearings caused by other factors, for example corrosion, fatigue, and wear.

The location of the damage in the zone of maximum pressures in the oil wedge shows that cavitation phenomena caused by the abrupt rise in pressure in the oil layer of the bearing after the cavitation cavity leaves the minimum pressure zone represents the cause of this damage. Most often this damage begins at a slip rate of 9-10 m/sec and a specific pressure, $p = 200\text{-}250$ kg/cm^2. However, whereas cavitation damage depends on the design of the bearing shell and the material, for a given combination of all factors influencing cavitation, the damage can begin even for other combinations of velocities and pressures.

Cavitation damage to fuel system parts is relatively infrequent and is generally observed at the plungers of fuel pumps and nozzle needles.

Damage consists of pits and gouging of metal. The cause of this damage must be regarded as cavitation phenomena caused by abrupt fluctuations in pressure in the fuel. It must be noted that this damage quite rapidly causes the fuel equipment to malfunction and methods of controlling it are thus far inadequate.

This kind of damage is observed in fuel lines and refrigerator coils. In this case the cause evidently lies in the pressure changes in the liquid flow.

Quite often, the impellers of centrifugal water pumps of diesel engines and cooling unit covers undergo cavitation damage. The main reason for the damage is the improper designing of the part, causing separations in the liquid flow and the formation of zones with reduced pressure.

CHAPTER TWO

THEORETICAL ESSENTIALS OF CAVITATION AND CAVITATION DAMAGE IN DIESEL ENGINES

3. Cavitation and Essentials of Physicochemical Processes Occurring During Cavitation

This book examines the theory of cavitation erosion as applied to damage in liners of working cylinders in diesel engines.

Cavitation in a liquid medium refers to the hydromechanical process of the formation of voids in the continuity of a liquid at the flow locations where the pressure drops to the saturated vapor pressure of this liquid at a given temperature, or else to a certain critical pressure at which gases or air dissolved in the liquid begin to be evolved in the form of bubbles (cavities).

The formation of continuity voids (cavitation cavities), just as their annihilation, depends to a significant extent on various factors, the fundamental of which are those that lead to local, alternating increases and decreases in pressure in the liquid.

In diesel engines, variable pressure in a liquid is caused principally by vibrations in surfaces surrounding the liquid, and in a number of cases -- as the result of abrupt changes in flow velocity and direction.

Damage in surfaces surrounded by a liquid occurs in zones where cavitation bubbles collapse (are annihilated) under the effect of increased pressure. When this takes place, local pressure peaks develop, and surface damage occurs upon exposure to these pressure peaks.

Many studies [1, 12, 30] have dealt with problems of the theory of cavitation cavities as well as changes occurring in the physicochemical structure of a material subjected to cavitation failure. The aim of these studies was to establish a relationship between hydrodynamic characteristics of a flow and parameters describing the failure process.

In view of the complexity of physicochemical processes occurring during cavitation and cavitation erosion, it had not yet been possible to fully clarify the physical nature of the successive progression of these phenomena. Thus far there are various points of view as to the physical nature of cavitation damage.

Most investigators agree that the primary cause of failure is the impactive action of liquid against the surface of a metal occurring in the collapse of cavitation cavities. Views of workers differ widely on the role of electrical factors in cavitation damage, and also on problems associated with the kind of progression of successive stages of cavitation damage in the surfaces under attack.

Opinions differ concerning the causes leading to electrochemical processes during cavitation. For example, it is suggested that owing

to high temperatures in the implosion of cavitation cavities, thermoelectric effects are observed. The electric currents induced in a material are explained as due to the action of highly localized compressive stresses caused by the small area which the dynamic forces act against at the instant of cavity collapse. The hypothesis of the strong effect of purely oxidative processes on the trend of cavitation damage has many adherents. There are experimental data confirming this hypothesis, but directly contradictory facts, as well. Cavitation erosion develops in chemically neutral media and also on specimens made of glass, gold, and various plastics, that is, nonoxidizable materials.

In view of the extraordinary complexity of the phenomena in cavitation damage that are caused, on the one hand, by the rapidity of the processes of the last stages of failure, and on the other -- by the diversity of processes developing in different materials subjected to multiple exposure to a field of collapsing bubbles, cavitation erosion has not yet been fully studied. Moreover, there is not even a hydrodynamic theory of cavitation erosion that would permit estimating the order of magnitude of the developing conditions and the effect on them of such parameters of the medium as velocity, pressure, and so on.

During cavitation damage, depending on the intensity of the cavitation process (including the formation and collapse of cavitation cavities), the medium, the material of the internal cooling surfaces, and other factors, electrochemical processes can participate to a greater or lesser extent. However, we can state that local pressure peaks at microsurfaces are induced in cavitation erosion.

The main cause of cavitation and cavitation damage in diesel-cooling areas is the variable pressure in the medium caused by vibrations of cylinder liners.

Variable acoustic, and at times ultrasonic pressure in a liquid can cause, at a certain intensity, the formation and implosion of cavitation cavities, accompanied by hydraulic impacts, increased temperature in the zone of imploding cavities, and so on. We refer to all of this as the primary effect of cavitation, manifested directly in the coolant liquid. The action of these primary cavitation effects on enclosing surfaces causes their material to undergo stress peaks, heating, electrochemical processes, and so on, that lead to failure of the vibrating and fixed walls. We call these processes secondary effects.

In our further examination of primary and secondary cavitation effects caused by alternating acoustic pressure in a liquid, we made use of data obtained by the authors in studies conducted on cavitation damage in material specimens in MSV [magnetostrictive vibrators] in diesel engines, as well as the data of Spengler [46].

The interrelationship of phenomena occurring during cavitation is shown in Figure 6. Here all the primary effects that can be a cause of cavitation damage in cooled diesel engine surfaces are noted with thin hatching. The influence of other primary effects on surface damage has thus far not been studied.

Figure 6 shows that the phenomenon of cavitation damage to surfaces cannot be classified as due to only one of many factors. Evidently, in any case the cause of cavitation damage is not only the high pressures induced in the implosion of cavities and the increased temperatures, but

also the electrochemical and diffusion processes occurring at the liquid-vibrating surface interface.

The nature of the primary effect is extremely diverse. Let us first consider those that directly cause secondary effects leading to the failure of diesel engine cooling surfaces.

A rise in pressure in microvolumes of a medium is associated with the collapse of vapor and gas-vapor cavities induced during the elongation phase. We know that the pressures developing during the collapse of cavities many times exceed pressures required to form the cavities and again attain thousands and tens of thousands of atmospheres. The pressure rise in the microvolumes of the medium is accompanied by a temperature rise of the medium as a whole and, in particular, of its individual microvolumes.

Heating caused by surface friction is local, that is, it appears at the surface boundary. By the surface boundary we mean any surface at which external friction can arise. The absolute temperature rise of the medium as a whole is not detectable in the overall level. However, the local rise can be appreciable owing to its effect on other phenomena, for example, on chemical reactions occurring at medium boundaries.

Heating due to surface friction is very distinctly manifested. If, for example, we immerse a thermometer in a cavitation fountain, it will show +30° C (that is, the temperature of the liquid), however one cannot hold it with the hand owing to intense heating at the glass-skin interface.

Heating of the medium caused by sound absorption is another form of the effect. Here some of the acoustic energy is converted into thermal

energy, which then causes a rise in the temperature of the medium. Heating depends on the absorption coefficient and the intensity of the acoustic vibrations giving rise to cavitation.

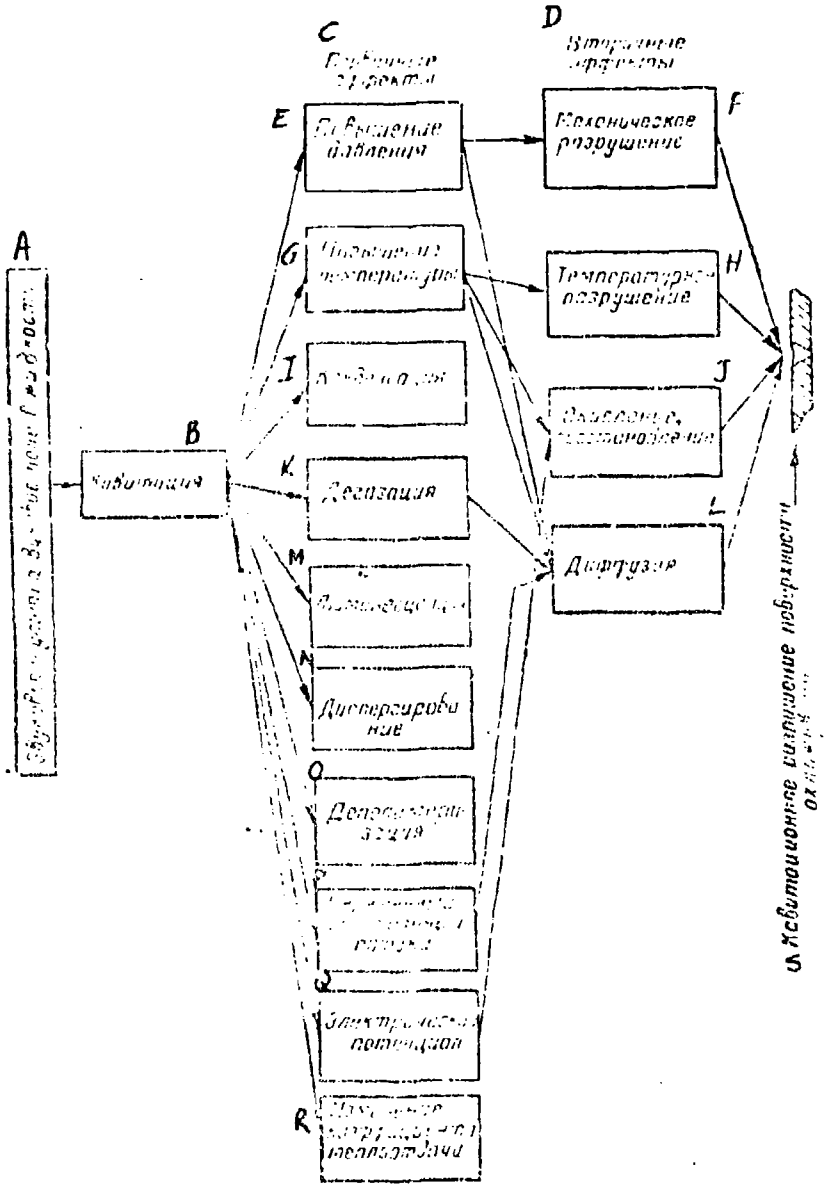

Figure 6: Systematization of Various Cav. ation Effects

[Key on following page]

Key: A. Acoustic and ultrasonic fields in a liquid
B. Cavitation
C. Primary effects
D. Secondary effects
E. Pressure rise
F. Mechanical damage
G. Temperature rise
H. Temperature damage
I. Condensation
J. Oxidation, reduction
K. Degassing
L. Diffusion
M. Luminescence
N. Dispersion
O. Depolymerization
P. Variable and constant flows
Q. Electric potential
R. Change in heat transfer coefficient
S. Cavitation damage to cooling surface

If some volume of the medium is subjected to acoustic and ultrasonic cavitation and within it total absorption of the energy thus developed occurs, the intensity of heat transfer N_ω is equal to the total acoustic intensity received by the vibrating surface N_{ac} [ac = acoustic] . Let the irradiated volume of the medium have the thickness s. Let the sound intensity on entering the layer be represented by I_1, on exiting from the layer -- I_2, the cross section of the acoustic field -- F, then the intensity of the sound developed in this layer is

$$N_\omega = (I_1 - I_2)F \tag{1}$$

is expended in heating the medium.

Using equation (1) and Beer's law of variation in sound absorption in a medium, we get

$$N_\omega = (I_1 - I_2)F = I_1F(1 - e^{-2\alpha s}), \tag{2}$$

where α is the absorptivity of the medium.

The rise in the water temperature, if we neglect thermal conductivity, is

where T is the heating time;

G is the weight of heated volume;

c_t is the specific heat capacity.

The temperature rise caused by the friction of layers of the liquid and by the absorption of acoustic energy can be appreciable.

During cavitation, high temperatures in microvolumes of collapsing cavities also develop due to the high pressures arising, which is sometimes accompanied by the glowing of indistinct areas in cavitation zones of the liquid. The temperature rise in the microvolumes of the collapsing cavities, significant as it is, does not lead to an appreciable rise in the mean temperature of the medium. However, local points with high temperatures are very dangerous since they cause the secondary effect of electrochemical erosion of metallic surfaces located in the cavitation zone. The nature of secondary effects is extremely diverse, but they are similar in that they all lead to damage of surfaces swept by the cavitating liquid.

As a result of the abrupt pressure rise in the microvolumes of the liquid adjoining a solid surface caused by collapsing cavities, gradual spalling of solid particles of the wall material occurs, which then leads to surface damage. This damage is usually local and occurs in areas where the cavitation cavities have collapsed. Damage can develop at a high rate, which depends entirely on the intensity of the cavitation process. In addition, temperature damage to the surface -- its melting

space -- may also occur since a sharp rise in the temperature of the microvolume corresponds to high pressures in the collapsing microvolumes of the liquid. In those cases when the collapsing of the cavities occurs at a liquid-surface interface and if the temperature of the microvolume exceeds the melting point of the wall (or a specimen) material, the surface melts. If the temperatures in the microvolumes of the liquid are below the melting points of the material of the wall, then changes in the surface color (opalescence color) are observed in the area of the cavitating volume of liquid.

Simultaneously, at the liquid-surface interface oxidation-reduction processes occur, ultimately also leading to damage.

The constant and variable flows in the liquid and the diffusion processes aggravate secondary effects -- effects of damage owing to acceleration in the entrainment of particles of the damaged surface. Thus far the specific role in surface damage of frequency of vibration and the material remains unexplained. Study of these relationships will make possible a precise selection of methods of control for given cavitation processes.

4. Causes of Cavitation in a Liquid and Cavitation Damage of Vibrating Surfaces Swept by This Liquid

The hydrodynamic theory of cavitation shows that for a gas-vapor cavity to appear and grow, an initial focus of a void in the continuity of a liquid is necessary.

In other words, an initial bubble is required, which under favorable conditions begins to grow in size, and then collapses in the higher-pressure zone. However, when the liquid is under dynamic stress, a void

can occur in the liquid during the elongation phase, accompanied by the formation of cavities, which collapse during the compression phase even without the presence of the initial void. To cause discontinuity in the liquid, the cohesive force of molecules must be overcome. In a degassed liquid not containing foreign impurities, stresses equal to several atmospheres are required to produce a void. But if these cavities collapse, then high pressures build up, which can be as high as several thousands of atmospheres. These pressures lead to the inception of numerous centers of secondary cavitation. The detrimental consequences of cavitation in equipment are well known, for example, damage to high-speed turbine blades, and vibrating cylinder liners and blocks of diesel engines even when made of the best materials.

Cavitation develops during the elongation phase of a liquid occurring with variable acoustic pressure in the acoustic and ultrasonic field of the liquid caused by a vibrating surface. Cavitation is accompanied by the noise it produces in the liquid.

Cavitation cannot arise in weak acoustic fields [35], since for cavitation to appear the minimum intensity must be exceeded, which is referred to as the critical threshold of cavitation.

This threshold value depends on the frequency of the sound, the amplitude of the vibrations of the liquid, and the forces of cohesion in the liquid, and increases with rise in the external pressure and with decrease in temperature. Cavitation proves to be especially severe at the interface of two media, since here only forces of cohesion are operative. The appearance of cavitation is particularly favored by the

presence in sound-irradiated liquid of cavitation nuclei, which may be substances dissolved in the liquid, small particles, and gas bubbles undetectable with the unaided eye. Near these nuclei the forces of cohesion are severely weakened. In purified, degassed liquids, due to the absence of (molecular) gas inclusions, the number of cavitation nuclei is at a minimum, therefore cavitation can appear in this instance at even higher vibration intensities. But if cavitation is induced in a liquid in which dissolved gas is present, under the effect of elongation this gas will be evolved in minute bubbles. These bubbles, due to hydrodynamic forces, merge into larger bubbles and rise to the surface of the liquid. If the frequencies of the free vibrations of the gas bubbles of a given size vibrating in the liquid arrive at resonance with the frequency of the hydro-acoustic field of the liquid, cavitation forces can be significantly increased. The resonance frequency of gas bubbles, according to the data of M. Mataushek, is determined approximately by the following relation:

$$f = \frac{1}{\pi d_1} \sqrt{\frac{3\kappa' p_0}{\rho}},$$

where ρ is the intensity of the liquid;

p_0 is the hydrostatic pressure in the liquid;

κ' is the ratio of the specific heat capacities for the gas in the bubbles (adiabat index);

d_1 is the bubble diameter.

In the range of ultrasonic frequencies, the frequency dependence of cavitation evidently is determined by the small inertia of the effect, since some time is required to form the cavities. Therefore at vibration frequencies up to 20 kHz, cavitation in diesel engines appears at lower

intensities than in the high-frequency range of vibrations.

At very high ultrasonic frequencies (above 5 MHz), cavitation has thus far not been produced by experimental means.

The critical threshold of cavitation rises with increase in viscosity of the liquid. When the actual value of this threshold was measured, extremely dissimilar are obtained.

Based on new studies [46], to excite cavitation in tap water at 20 kHz, an intensity of about 1 w/cm^2 is required, and at an intensity of 200 kHz -- 10 w/cm^2. Acoustic and ultrasonic cavitation induced in cooling jackets of diesel engines leads to the failure of vibrating and fixed surfaces of the diesel engines that are water-swept. Thus, when a high-intensity vibratory field is excited in a liquid, the initial cavities can appear in the absence of impurities in the form of suspended foreign particles and gases in the liquid due to the detachment of the vibrating surface from the liquid and due to voids within the liquid as the acceleration and velocity of the vibrations are increased to some critical threshold W'_{cr} [cr = critical] and V'_{cr}.

The level of vibration in diesel engine cylinders, as we know, is evaluated by dynamic factors such as amplitude, velocity, acceleration, and frequency of the vibratory process, which are specific for each particular diesel engine. On exposure to vibrations of the cylinder wall, a hydro-acoustic field is produced in the coolant liquid. When this happens, gas-vapor cavities appear, more precisely, the cavitation of the liquid begins. The intensity of cavitation depends on several variables, which include -- besides vibrations -- first of all the temperature of the

medium, the pressure at the given point, the viscosity of the medium, its flow rate, the presence of impurities in it, and its gas composition.

The cavitation process will begin also when there is a pressure drop at a given point in the medium down to the critical pressure or the saturated vapor pressure, p_d.

In a medium that has no displacements of the liquid flow (standing liquid) under the effect of the vibratory field, cavitation will begin at the instant when the velocity of the vibrational motion reaches a critical value V_{cr} at which the liquid suffers discontinuities and gas-vapor cavities form.

The critical velocity of vibrations depends to a large extent on the physicochemical properties of the liquid.

For a plane wave of vibrations, the pressure intensity in the acoustic range of vibration frequencies can be determined by the formula

$$I = \frac{1}{2}\rho c(\omega A)^2 = \frac{1}{2}\frac{\rho c}{\omega^2}W^2 = \frac{1}{2}\rho c V^2 = \frac{pV}{2}, \qquad (3)$$

where c is the speed of sound in the medium;

V is the amplitude of velocity of particle vibrations;

p is the amplitude of the variable pressure;

A is the amplitude of the vibrations;

W is the amplitude of the acceleration.

Vibrational motion of the medium particles, as the pressure wave propagates, lead to the inception in the medium of variable pressure p_1, which varies periodically at the frequency of the vibrations

$$p_1 = p \sin \omega t.$$

Here

$$p = \rho c A f.$$

If the plane pressure wave with intensity I impinges against an obstacle that completely reflects the pressure waves, it will exert the following overall pressure on the obstacle:

$$p = \frac{2I}{c}.$$

If the obstacle partially damps the vibrations, the overall pressure will be smaller.

The oscillations caused by the vibration of a surface lead to the particles of the surrounding liquid adjoining the surface to undergo vibrational motions relative to the equilibrium position and simultaneously cause their displacement, that is, a constant liquid flow. This phenomenon shows up in the form of intense currents leading to vigorous agitation of the medium and is brought about by the viscosity of the liquid. The nature of the flows observed during tests at the MSV is shown in Figure 7. According to experimental data obtained by the authors, and also from the work [25], the flow intensity increases with increase in radiation intensity. The direction of the flow remains unchanged.

The variable pressure in the acoustic range of vibrations and the constant flow play a major role in forming gas-vapor cavities, in the reduced-pressure zone, and in the collapse of these cavities in the increased-pressure zones. These phenomena are then responsible for cavitation damage to surfaces. As a rule, a vibrating surface and a fixed surface located in the zone of the variable pressure wave and the spouting liquid are damaged.

The vibrational intensity necessary to cause cavitation to begin is a critical value and depends on the frequency and amplitude of the

vibrations, as well as several other parameters characterizing the condition of the medium in which the vibrational processes take place.

Based on the equation determining the acoustic pressure, let us write an equation for the plane pressure wave in the liquid:

$$P_{ac} = [illegible] = -[illegible], \qquad (4)$$

where g is acceleration due to gravity.

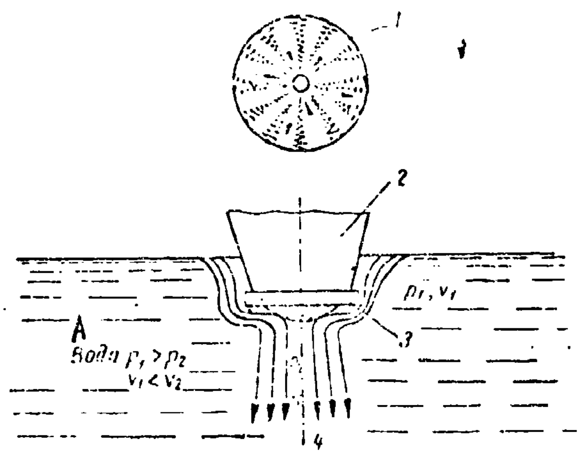

Figure 7. Scheme of Liquid Motion in the Region of a Vibrating Surface of a Specimen:

1 - Direction of motion of cavitation cavities

2 - Vibrator

3 - Specimen

4 - Direction of motion along specimen

Key: A: Water

A void develops in the liquid when there is a decrease in the pressure p_{ac} down to a specific limit at which it will be equal to the difference between the static pressure p_a at a given point in the liquid and the saturated vapor pressure at the given temperature:

$$p_a - p_d = \Delta p = \frac{v_{cr}^2 \rho^c}{g}.$$

Here

$$\Delta p = p_{ac} \quad \text{and} \quad p_a - p_d = p_{ac} = \frac{V'^2_{cr}}{g} \rho^c .$$

The velocity of the vibrational motion of the particles of the liquid will be assumed to be the critical value

$$V'_{cr} = \frac{g(p_a - p_d)}{\rho^c}.$$

The critical acceleration of the vibrational motion of water particles is

$$W'_{cr} = \frac{2\pi g (p_a - p_d) f}{\rho^c},$$

where p_d is the saturated vapor pressure at the specified temperature.

From this equation it follows that the critical velocity of vibrations of the liquid molecules depends only on the physicochemical properties and its temperature. Data characterizing the critical velocity of the vibrations in technically pure water will be as follows for various temperatures:

t in °C	5	10	20	30	40	50	60	70	80	90	100
V'_{cr} in cm/sec	7.15	7.13	7.1	6.99	6.7	6.34	5.7	4.77	3.46	1.98	0

As follows from these data, the critical velocities are not large and decrease with increase in temperature. At 100°C cavities can begin to

form spontaneously in the water, that is, the water begins to boil. Specific critical accelerations of the vibrations of the liquid, which increase with the vibration frequency, will correspond to these critical velocities. Values of W'_{cr} at 15°C when $V'_{cr} = 7.1$ are listed in Table 1.

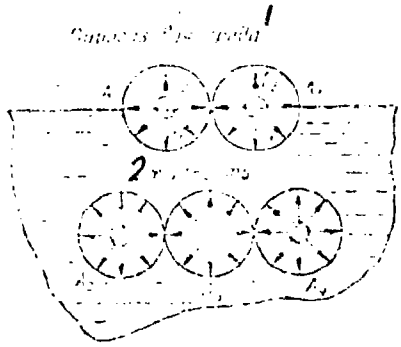

Figure 8. Diagram of Molecular Forces Within and at the Surface of a Liquid.

KEY: 1 - Gas-vapor medium

2 - Liquid

By examining Figure 8 we see that the interaction of the molecules A and A_1 in the surface layer of the liquid and situated within its volume (molecules A_2, A_3 and A_4) differs. In the surface layer the attractive force F_2 in the direction of the pair is many times smaller than the attractive force F_1 toward the bulk of the liquid. The difference of these forces, per unit surface, is the internal pressure and amounts to 11,000 atm. That is why water is so resistant to compression.

Damage to a fixed obstacle in the hydro-acoustic field of a liquid will occur the more rapidly, the higher the velocity of vibrations, given

the condition that it is higher than some critical velocity threshold V_{cr} at which damage begins. The proportionality of the intensity of damage at a fixed barrier in the liquid to the velocity of vibrations is observed because the pressure drop leading to discontinuity of the liquid is directly proportional to the velocity of the vibrational motion of particles of the liquid.

Table 1. VALUES OF CRITICAL ACCELERATION

A					
B	10	100	1000	5000	10 000
	446	4460	44 600	223 000	446 000
C	1,13	0,11	0,01	0,002	0,001

KEY: A - f in Hz
B - W'_{cr} in cm/sec^2
C - A in mm

The rate of damage at the vibrating surface which is the source of the hydro-acoustic field is proportional for a given liquid, to the acceleration of the vibrations of the surface, assuming the condition that the acceleration of the vibrational motion is higher than a specific critical acceleration threshold W_{cr} at which damage begins. This correlation in the damage at the a vibrating surface is accounted for by the fact that the void in the continuity and the collapse of a cavity results from the action of the inertial forces of the water. As shown in Figure 9, during the first period of the vibration of the surface, (position I),

the inertial forces induced in the liquid P^{v}_{i} [v = vibrating, i = inertial], do not exceed the forces of cohesion P_{coh}, therefore there is no void in the liquid and thus no cavitation. When during the first period (position II) of vibrations the forces P_{coh} are exceeded by the forces P^{v}_{i}, a void will occur in the liquid at point A and cavitation will begin. When during the second half-period of vibrations the forces required to collapse the cavity P_{col} are exceeded by the forces P^{v}_{i} (position III), closure of the cavities will begin at point B, and cavitation damage will set in.

Since the amplitudes, frequencies, and their derivatives (velocities and acceleration of vibrational motion) differ in magnitude for different diesel engines, depending on their design and operating conditions, cavitation processes in the liquid cooling the diesel engine and processes of cavitation damage can have different intensities for each type of diesel engine.

The vibrational acceleration is characterized by the following expression:

$$W' \sim A(2\pi f)^2,$$

that is, acceleration is a function of amplitude A and frequency f. Therefore for the same acceleration of the vibrational motion, where it is somewhat larger than W'_{cr} cavitation damage will always occur. However, here the amplitude of the vibrations must be somewhat larger than the threshold.

It can be assumed that in cavitation damage occurring in the range of relatively low frequencies to 2000 Hz, generally pressure forces will act destructively since due to the removal of heat to the ambient environment,

the temperature factor will not play a key role owing to the relatively low cyclicity of the temperature factor with a low exposure time. When cavitation occurs in the higher frequency range, to the mechanical factors is added the temperature factor, and as a result of which electrochemical processes are thus intensified.

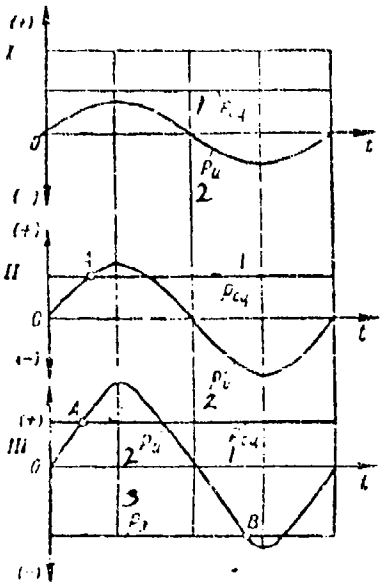

Figure 9. Plot of Cavity Formation and Collapse:

I - v = max, w = 0
II - v = 0, w = max
III - v = 0, w = max (A is the instant of discontinuity; B is the instant of collapse)

KEY: 1 - P_{coh}

2 - P_i

3 - P_{col}

We know that for a vibratory intensity of high-frequency devices of 1 kw at a frequency of 1600 Hz surface cleaning processes occur. When the intensity of the device is increased, at the same frequency, metals placed on the vibrator undergo heating and melting. At intensities of 20 - 30 kw, high alloy steel and refractory metals will melt on the vibrators.

In the general case, the intensity of cavitation damage (weight loss, ΔG) is a function of pressure p and temperature T in the microvolume, potential V', and current strength I between the heated microvolume of the ambient medium and the surface being damaged;

$$\Delta G = f(p, T, V', I).$$

However, the intensity of surface damage is also a function of several other factors. First of all they must be regarded as including the following: the material of the surfaces, the finish of the surfaces, the temperature and moisture content of the medium, the acoustic characteristics of the vibrations, and the flow rate of the medium.

For a preliminary estimate of the acceleration motion at which a liquid begins to experience a void in the layer directly next to the vibrating surface, let us examine the forces applied at the microvolume.

Let us delimit the microvolume Δv from the adjoining layer of liquid near the vibrating surface and executing motion according to the vibrational laws of this surface. It is assumed that discontinuity in a liquid with the formation and collapse of cavities directly at the vibrating surface, that is, at the interface surface-adjoining liquid layer, is the most dangerous from the standpoint of erosion. Here, the inertial force of the water $P^{w}_{i} = m\, dw/dt$, the cohesive force of the liquid P_{con}, the drag

of the layers, and the force of friction against the other layers will act at the delimited microvolume.

Neglecting the forces of drag and friction in view of their smallness [24], let us set up the equation of forces;

$$P^{W}_{i} = m_{at}\ dw/dt = P_{coh}\ ,$$

where m_{at} is the attached mass of liquid, assumed constant; and

dw is the acceleration of the hydrovolume of the liquid.

It is assumed that discontinuity of the liquid at the boundary of the microvolume will occur if the sum of forces applied at the microvolume exceed the cohesive forces of the liquid:

$$m_{at}\ dw = P_{coh}\ dt\ .$$

Integrating the equation we get

$$m_{at} \int_{0}^{w} dw = P_{coh} \int_{0}^{t} dt \quad \text{or} \quad m_{at}\ w = P_{coh}\ t.$$

The velocity of vibrational motion at which a discontinuity will occur will be

$$v = P_{coh}\ t/m_{at}\ .$$

Since the frequency of the vibrations is inversely proportional to the time $\omega = 1/t$, then $v = P_{coh}/m_{at}\omega$. Acceleration of the vibrational motion is

$$W = v\omega = P_{coh}/m_{at}\ .$$

Acceleration of vibrational motion at which the liquid suffers a discontinuity at the boundary of the vibrating surface is a constant,

independent of the vibration frequency.

The vibrational acceleration will depend only on the cohesive forces at the boundary of the vibrating surface with the liquid of the mass of adjoining water. Schematically, this can be shown by the diagram in Figure 10. No damage will occur in the subcritical region. When the acceleration of vibrations is increased beyond W_{cr}, cavitation damage will begin. This is valid for the formation of cavitation and erosion in diesel engines, since the vibrating surfaces execute vibrations in the high-frequency region where the adjoining mass of liquid is virtually independent of vibration frequency. Based on the data given in [42], the stress for discontinuity to occur is 3.6 kg/m^2 for water.

Therefore, the cohesive forces of water per cm^2 of surface amount to 0.36 g. To determine the critical acceleration, we must know the adjoining mass of liquid. It can be determined by the difference in the frequencies of the free vibrations of the given surface in air and in water. The mass of water per cm^2 of surface area is 0.00002 g · ec/cm^2. Based on the mass of the adjoining water, we can also determine the thickness of the adjoining layer, which proves to be 0.02 mm.

Therefore, acceleration of vibrational motion at which the liquid begins to experience discontinuities at the surface-water region is approximately 18,000 cm/sec^2 or 18 g.

The collapse of cavities and also the process of cavitation damage begin at somewhat higher accelerations. Experience in building diesel engines shows that at cylinder liner vibrations with an acceleration of 20 g, traces of the initial stage of cavitation damage are already detectable.

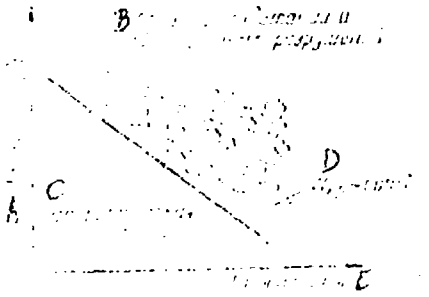

Figure 10. Plot of Critical Acceleration

KEY: A - lg amplitude
B - Region of cavitation and cavitation damage
C - Precritical region
D - W_{cr} = const
E - lg frequency

5. Cavitation and Conditions for Its Inception in a Medium Flowing Past a Body, in the Absence of Vibrations. Locations of These Effects in Diesel Engines

The critical pressure p_{cr} at which cavitation begins depends to a large extent on physicochemical properties of the liquid: viscosity, content of dissolved gases and of air, salinity, temperature, and so on. The saturated vapor pressure p_d usually is lower than the critical pressure and depends mainly on the temperature of the water. Values of p_d are given in Table 2 for various temperatures. Here the fraction which pressure p_d is of the atmospheric pressure p_a, in per cent, is shown, based on the data given in [1].

Cavitation processes in the cooling systems of diesel engines are caused mainly by high-frequency vibrations of cylinder liners. The changes in the flow velocities of the coolant fluid and the corresponding pressure decreases and increases that are induced can promote cavitation damage. This can be most graphically made evident at the locations close to the inflow of water into the water jacket. Cavitation processes induced when flow occurs past asymmetric-profile solid bodies (typical of propellers, turbines, pumps, and so on) are encountered in diesel engines in the water pump, especially at high intake heights.

Table 2. Saturated Vapor Pressure of Water at Various Temperatures

t in °C (A) / p_a in kg/m² (B)	0	10	20	30	40	50	60	100
	69	125	238	433	752	1258	2031	10 332
$\frac{p_a}{p_0}$ 100%	0,9	1,2	1,5	2,3	4,2	7,2	12,2	19,7	100

KEY: A - t in °C
B - p_a in kg/m²

The pressure change Δp at some point on the surface of the body swept by a liquid and immersed in it to a depth h_1 from the free surface is estimated by the dimensionless coefficient of local rarefaction:

$$\xi = \frac{\Delta p}{q} = \frac{p_0 - p_1}{q} = \left(\frac{v_1}{v}\right)^2 - 1.$$

Here $q = \rho v_1^2/2$ -- the velocity pressure of the incident flow (velocity head);

p_0 is the hydrostatic pressure at the particular point on the swept body;

p_1 and v_1 are the pressure and flow velocity at this same point.

The maximum rarefaction will occur at the point where the coefficient becomes a maximum, and the pressure at this point will be:

$$p_{1\text{-min}} = p_0 - \xi_{max} q.$$

The cavitation process will begin when $p_{1\text{-min}}$ becomes equal to the critical pressure p_{cr}, and then attains the saturated vapor pressure of water p_d at the given temperature.

The possibility of a cavitation process developing when a solid body is swept by a fluid is evaluated by the cavitation number χ by comparing it with the coefficient ξ_{max}

$$\chi = \frac{2(p_0 - p_{cr})}{\rho v_{cr}^2} = \left(\frac{\Delta p}{q}\right)_{max}.$$

From this expression we see that if ξ_{max} proves to be smaller than the cavitation number χ there will be no cavitation. It develops given the condition that $\chi \leqslant \xi_{max}$.

The value of χ corresponding to the initiation of the cavitation process can be taken as the critical cavitation number.

The critical velocities v_i at which the pressure in the flow of the fluid past the solid body is reduced to p_{cr} or p_d will be equal to the following, respectively, at ξ_{max}:

$$\xi_{cr} = \frac{2(p_0 - p_{cr})}{\rho v_{cr}^2} = \frac{p_0 - p_{cr}}{q};$$

$$\xi_d = \frac{2(p_0 - p_d)}{\rho v_{cr.d}^2} = \frac{p_0 - p_d}{q_{cr.d}}.$$

Depending on the pressure reduction in the stream at the surface of the swept body, in hydrodynamics a distinction is made between gaseous and

gas-vapor cavitation, and the latter can have two stages.

Gaseous cavitation ($\xi = \xi_{cr}$) begins when due to the diffusion of gases and air at the sites where the pressure reaches p_{cr} cavitation bubbles develop, which on moving along the swept body collapse under the effect of increased pressure.

The first stage of vaporous cavitation ($\xi = \xi_d$) begins if the local pressure drops to p_d (cold boiling of water). When this happens, the gaseous bubbles earlier formed will grow by being filled with vapor from the liquid. This stage in the development of cavitation represents a danger from the standpoint of possible rapid appearance of cavitation erosion.

The second stage of vaporous cavitation ($\xi < \xi_d$) is characteristic of a substantial expansion of the cavitation zone.

An experimental study of flow past various profiles in cavitation conditions shows that the instant of cavitation onset can be determined by the beginning of its first stage when $p_{1\text{-}min} = p_d$. Therefore the critical cavitation number can be expressed as: $\chi_{cr} = \xi_d = \frac{p_0 - p_d}{q_{cnd}}$.

The rarefaction peak at the surface of a segmented profile can be found from the plots (Fig. 11) of Shenkhetr from Gutsche's materials. Fig. 11 shows the dependence of the maximum rarefaction coefficient $\xi_{max} = (\Delta p/q)_{max}$ at the suction side of the profile (as applied, for example, to the blade of a water wheel), relative profile thickness $\delta = e/b$, and the lift coefficient calculated for a profile of infinite size.

At the present time problems of the combined role in cavitation erosion of high-frequency vibrations and both pressure drop and rise resulting from changes in flow velocity if they are not large and

cannot by themselves produce cavitation have not yet been adequately studied. This is because in vibrations the formation and collapse of cavitation cavity occurs at the same site. In a variable-velocity flow the formation of bubbles occurs in the section where the maximum flow velocity and the minimum pressure are found, while collapse occurs over the section where the flow velocity drops and the pressure rises. In estimating the combined effect of these factors responsible for cavitation erosion, in each individual case, depending on the intensity of vibrations, the hydrodynamic properties of the flow, and the general level of pressures and temperatures, one must make appropriate calculations to determine the conditions for the formation and collapse of cavitation bubbles. The most objective data here can be obtained by experimental means.

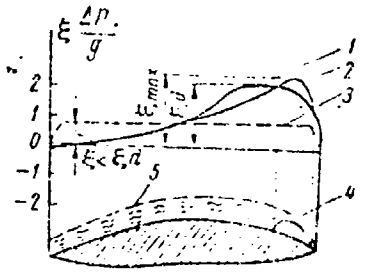

Figure 11: Effect of Cavitation on the Local Rarefaction Coefficient ξ at the Suction Wall of a Profile:

1 - ξ at the first stage of cavitation
2 - ξ in the absence of cavitation
3 - ξ in the second stage of cavitation
4 - propagation of eddy in the second stage of cavitation
5 - propagation of cavitation eddy in the second stage of cavitation

Studies made to determine the flow rate of coolant water showed that as a rule the flow rate is less than 1 m/sec and only at the locations of inflow in individual cases is the value as much as 2 - 8 m/sec, that is,

the critical values required for cavitation and cavitation damage to develop are not attained.

Thus, high-frequency vibrations are the main cause of cavitation erosion in diesel engines.

The hydrodynamic process of the formation of cavitation plays the main role in damage to crankshaft bearings of diesel engines, since the flow rate of the oil in the wedge of the main and butterfly bearings of diesel engines affects damage. As a result of a sharp pressure drop in the oil layer, gas-vapor cavities are formed in the oil wedge, which then collapse in the increased-pressure zone and damage the bearing surface. Cavitation phenomena in bearings (especially connecting rod bearings) are also affected by vibrations along the column of oil in the drilled lubricating passages in connecting rods.

Damage to bearings is still not widespread. However, with increase in the operating speed of diesel engines, cavitation damage to bearings can take on a more serious nature. Therefore bearings must be designed with allowance for the attainment of minimum flow rates of the oil wedge with minimum pressure drop.

The hydrodynamic process of cavitation is intrinsic also to the fuel equipment of diesel engines. There have been cases in which plunger pairs of uprated diesel engines have jammed due to cavitation damage. Damage caused by cavitation at fuel pump plungers is thus far quite an infrequent phenomenon. However, there is every reason to assume that continued uprating of diesel engines in terms of power (increasing the cycle feed) and in rpm (reducing the time required to feed a given portion

of fuel), that is, an increase in the dynamics of the cycle, would lead to intensified hydrodynamic processes of the formation of voids in the mass of fuel and to more frequent damage and jamming of plunger pairs.

6. Vibration of Cylinder Liners as a Source of Cavitation in Diesel Engines

Intensive vibrations of cylinder liners leading to cavitation in water jackets of diesel engines are caused by piston blows. When a piston passes the top dead center, the direction along which the side pressure force (sign) is applied changes and the piston shifts from one wall of the cylinder to the other opposite wall. Piston slap takes place. Since there is a gap between the piston and the cylinder liner, the slap occurs with impact. It is obvious that when there is a large gap between the piston and the liner and when the side force is large, the velocity at which the piston strikes the cylinder wall will be higher. The impact energy will increase.

Oscillography of liner vibrations and gas pressures in an engine cylinder and their comparison with the plot of side pressure forces for a piston reveal the following [17].

1. Bursts of intensive cylinder liner vibrations develop with each change in the sign of the side pressure forces P_s [s = side], causing piston slap. The greatest dispersion is found for liner vibrations caused by the piston impacting near the TDC [top dead center] when the forces P_s are large. Two additional bursts of intensified vibrations, but at an amplitude smaller than in the first case, develop when there are repeated

changes in the sign of side pressure forces.

2. The frequency of liner vibrations is practically independent of the load at which the engine is operated and its rpm. This has an effect only on the amplitude of the vibrations due to changes in the forces P_g and in the size of the gap between the piston and the liner.

3. Under the effect of the first piston impact (near the TDC) and the gas pressure forces in the cylinder, the liner wall undergoes significant bending. Flexural vibrations occur.

4. When liner vibrations characterized by appropriate amplitudes and frequencies occur, accelerations can reach values high enough so that the liquid is detached from the liner surface and also internal liquid voids occur, leading to cavitation.

5. These vibrations in most cases are vibrations of the liner wall with the piston pressed against it, or are natural vibrations of the liner distorted by the effect of the attached mass of the piston which impinges against the liner wall at an angle or with part of its lateral surface.

In approximate terms, a calculated determination of the vibration frequency can be made by the method of calculating the frequencies of transverse natural vibrations of a weightless beam with a single concentrated mass. In this case the number of vibrations per minute $n = 300/\sqrt{f_{st}}$ [f_{st} is static deflection at the point at which the concentrated mass (piston) is applied under the force of its weight, in cm].

6. Slap of the piston and the beginning of intensive liner wall vibrations occur not at the moment of change in the sign of forces P_g, but with some delay, determined by the time required for the piston to pass

from one wall to the other. The time t_2 of the transition of piston from one wall, to the other is found from the expression

$$t_2 = \sqrt[3]{\frac{\delta}{k'_0}},$$

where δ is the thermal gap between the piston and the liner; and

k'_0 is a coefficient.

Thus, to determine the piston slap time we must know the thermal gap for a given diesel engine operating regime and for a given mass of the parts in translational motion.

The studies [16, 34, 35] proposed a formula for estimating the intensity of vibrations of cylinder liners in diesel engines. During the slap of the piston in the power stroke of a diesel engine, the intensity of cylinder liner vibrations I induced by the impact of a piston against the cylinder wall, is evaluated by the ratio of the impact momentum S' to the area of piston contact with the cylinder liner F_v

$$I = a_0^2 \frac{S'}{F_v}.$$

The solution of several equations set up to determine the piston slap time, the velocity and acceleration at the instant of impact, and also several other quantities, made it possible to find an expression for the intensity of cylinder liner vibrations in a diesel engine at the instant of piston slap in the region of the working TDC

$$I = 0{,}78 \frac{k(1-k)}{F_v} a_0^2 \sqrt[3]{\frac{\omega^2 R^2 \cos\alpha}{g^2}} (P_z - P_j + P_G). \qquad (5)$$

Here k is the coefficient of restoration equal to the ratio of the velocities after the impact v_2 and before the impact v_1 ($k = v_2/v_1$);

n is the diesel engine rpm;

G is the weight of the parts in translational motion;

λ' is the ratio of the crank radius to the connecting rod length;

a_φ is the acceleration of the piston in sideward motion;

P_z is the force of gas pressure at the piston;

P_i is the inertia force; and

P_g is the weight force.

From equation [2] it follows that the intensity of cylinder liner vibrations in various diesel engines depends on a number of design and operating parameters which must be regarded as primarily including the rpm, cylinder size, combustion pressure, piston weight, material of the cylinder and the housing parts, thermal gap, area of piston contact with the liner at the instant of impact, and several others.

The extent of the area of piston contact with the liner is variable and depends on the overall moment $\sum M$ acting at the piston and rotating it within the limits of the thermal gap.

In the absence of piston skewing relative to the wristpin axis, the maximum area of contact is determined by the expression

$$F_c = l_t k_1 \pi D_{cy} ,$$

where l_t is the length of the trunk section of the piston; and

$k_1 \pi D_{cy}$ is the segment of the circumference along which the piston is in contact with the cylinder liner.

The coefficient k_1 lies within the limits 0.2 - 0.3 and depends on piston design.

The minimum area of contact is observed when a piston undergoes slap in an inclined condition, when the overall moment $\sum M$ acts on it, and is determined in practice by a line whose length is $k_1 \pi D_{cy}$. At this instant the specific stresses in the liner rise sharply, which then is the cause of more intense vibrations.

The magnitude and direction of action at the piston $\sum M$ are determined by the ratio of four moments of the force couples acting at the piston. They include the moments arising from the forces of gas pressure at the piston M_g and the piston rings M'_g, the moments arising from the forces of inertia of the head M^h_i and the piston trunk M^t_i induced as the piston changes its sideward direction.

The force P_z and the quantities dependent on it can be assumed constant for the small crank angle during which piston slap occurs (5 - 10°C). Accordingly, the components of the overall moment acting on the piston when the piston begins contacting the liner are represented by the following equations:

$$M^h_i = (G_h/g) a_j l_1 ;$$

$$M^t_i = (G_t/g) a_j l_2 ;$$

$$M_g = P_{tot} (\pi D^2_p/8) f ;$$

$$M'_g = P_{tot} \pi (D^2_{cy} - D^2_p)/4 \sum l ,$$

where G_h and G_t are the weight of the piston head and trunk;

l_1, l_2, f and $\sum l$ are the arms of the force couples;

P_{tot} is the total force acting at the piston;

D_{cy} and D_p are the diameters of the cylinder and the piston.

The total moment rotating the piston depends on several factors. The magnitude of the moment will be greater the greater the weight of the piston head and the shorter the trunk section.

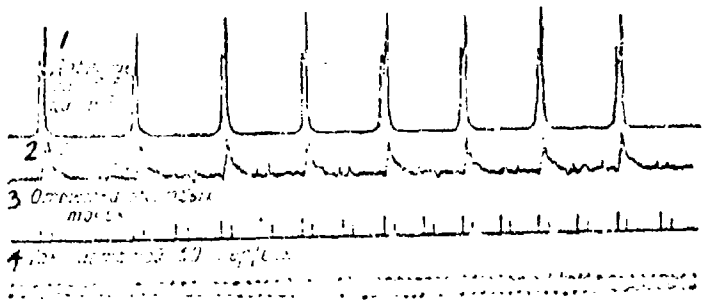

Figure 12. Oscillogram of Liner Vibrations of a 6 Ch 8.5/11 Diesel Engine (1500 rpm, 100% Load)

KEY: 1 - Pressure of gases in cylinder
2 - Liner vibrations
3 - Dead center markers
4 - Current with a frequency of 50 cycles per second

In confirmation of the fact that the vibrations of cylinder liners arising at the instants of piston slap can lead to detachment of the liquid from the vibrating surface and, as a consequence, can be the cause of cavitation in the cooling water and cavitation damage at surfaces swept by the water, measurements were made of liner vibrations in a number of diesel engines [17].

In the 6 Ch 8.8/11 diesel engine, the vibrations of the cylinder liners were recorded with the diesel engine operating according to the

external and generator characteristics. The vibration meter was mounted on the side at which the piston impacts in passing through the TDC at the beginning of the power intake. As we can see from the oscillogram shown in Figure 12, intense vibrations arise during each cycle of diesel engine operation. Interpretation of the oscillogram (Figure 13) shows us that the inception of intense vibrations coincides with the instants of piston impacting against the liner. Vibrations of cylinder liners occur at frequencies of liner free vibrations, whose first forms have values of 800-3000 Hz for various diesel engines.

The most intense fast-damping vibrations occur during the combustion period of the fuel when the normal pressure P_s causing piston slap from one wall to the other is considerable. Two additional bursts of vibrations with an initial amplitude that is smaller than in the first case coincide with the repeated changes in the sign of the side pressure forces and the repeated piston slap they caused.

At a constant rpm, the frequency of low-frequency vibrations is virtually independent of the load at which the diesel engine is operated. The dispersion of the vibrations increases somewhat with decrease in the diesel engine load (Figure 14). This is due to the fact that as the load is reduced the piston temperature drops and, as a consequence, the gap between the piston and the liner wall increases and the impact energy rises.

Liner vibrations even in a low-power diesel engine occur at accelerations that are many times greater than the acceleration due to gravity.

At some instant the liner vibrations are characterized by an amplitude that in some cases reaches 0.008 mm, and by a frequency amounting to 7500 periods per second at 1200 rpm. In this case, for the 6 Ch 8.5/11 diesel engine, the acceleration of the liner vibrations is 45 g, and cavitation damage to the liners occurs after 500-600 hours of operation to a depth of 1.3 mm.

When studies were made on the 4 Ch 10.5/13 diesel engine, 40 hp, at 1500 rpm, clusters of pits up to 1 mm in diameter and up to 0.5 mm in depth were found after 30 hours of operation, and 400 hours of operation proved to be sufficient for most of the surface of the liner to be damaged (the pits had diameters of 6-7 mm and were 5-6 mm deep).

Experiments conducted on 4 Ch 10.5/13 diesel engines established that the cylinder liners are subjected to pitting erosion as a rule when the 4 Ch 10.5/13 diesel engines operate with pistons made of AK 4 aluminum alloy. If the engine operates with cast iron pistons, no liner damage is observed. This is accounted for by the different gaps between the pistons and the liners. When an aluminum piston is used, the diametral gap in the cold state is 0.52 for the test diesel engine, and 0.15 mm -- for a cast iron piston.

The acceleration of liner vibrations during the operating time of the diesel provided with aluminum pistons was 58 g, and when provided with cast iron pistons -- 23 g (Figure 15).

Further tests made on diesel engines with different cylinder liner vibrations showed that damage is the more intense, the more intense the vibrations. For vibrations with accelerations below 18-20 g, no damage

within the limits of diesel engine service periods was detected. The greatest vibrations occur at the frequencies of free vibrations.

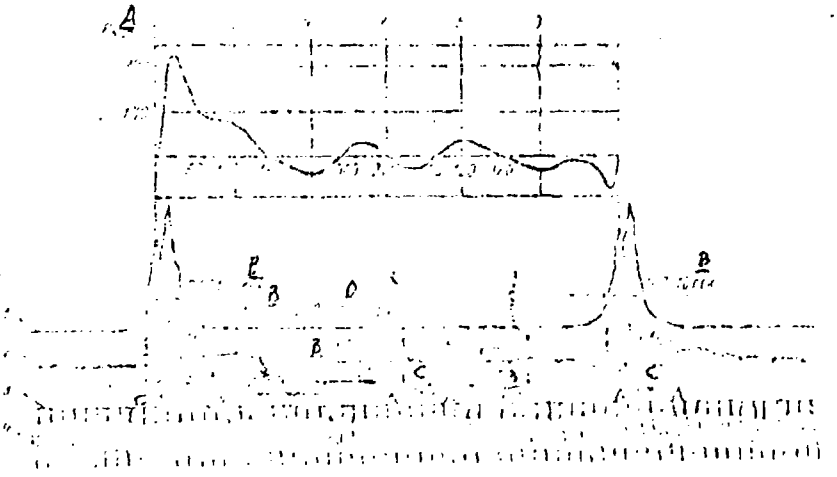

Figure 13. Oscillogram of Liner Vibrations in a 6 Ch 8.5/11 Diesel Engine (1500 rpm, 100% Load) and the Theoretical Plot of the Side Pressure Forces) at the Piston):

1 - Pressure of gas in cylinder 2 - Liner vibration 3 - TDC marker
4 - Time marker

KEY: A - P_4, kg

B - sec
C - TDC
D - 1300 periods/sec

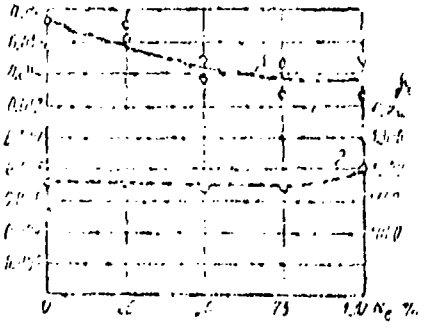

Figure 14. Dependence of Dispersion ϵ and Vibration Frequency γ of Liners in the 6 Ch 8.5/11 Diesel Engine on Power N_e:

1 - Aluminum piston
2 - Cast iron piston

KEY: A - I, II

It was found that the main factor in cavitation in diesel engines is the vibrations of surfaces swept by water. The intensity of vibrations can be estimated by equation (5). The magnitude of the vibrations is a function of numerous design and dynamic parameters. Eliminating cavitation is directly related to reducing the vibrations of surfaces swept by water.

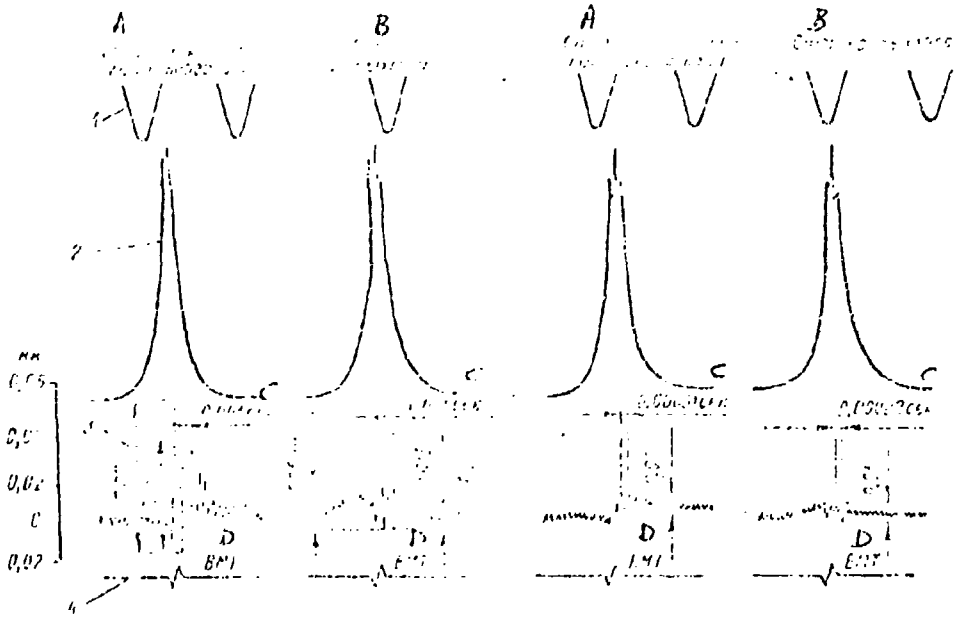

Figure 15. Oscillogram of Liner Vibrations in the 4 Ch 10.5/13 Diesel Engine (1200 rpm, 50% Load):

1 - Time marker 2 - Cylinder pressure 3 - Vibrations 4 - TDC marker

KEY: A - Camshaft side
B - Exhaust side
C - sec.
D - TDC

7. Theoretical Determination of Frequencies of Free Vibrations of Diesel Engine Cylinder Liners

A calculation of the frequencies of free vibrations as well as a theoretical determination of the possible amplitudes of free vibrations of

diesel engine cylinders is necessary for a theoretical evaluation of all vibration parameters of cylinder liners. This in turn in the future will permit a particular diesel engine design to be calculated from the standpoint of the engine's cavitation resistance.

Evidently, the maximum vibrational accelerations leading to the collapse of cavities and to intense damage of surfaces swept by water in the range 300-2000 hours can be observed in the region of high-frequency free vibrations, since processes of cavitation damage in the region of lower frequencies will take thousands and tens of thousands of hours to develop and therefore are not dangerous from the standpoint of diesel engine longevity.

To determine the accelerations of cylinder liner vibrations in diesel engines, we must first of all calculate their free-vibration frequencies with adequate precision. We can select several systems of calculation. The simplest system must be regarded as considering the cylinder liner as a prismatic rod. The frequencies of free vibrations determined in this fashion differ by an order of magnitude from those actually measured by resonance and other methods and therefore cannot serve as a basis for calculating liner accelerations. To determine the frequencies of free vibrations of liners, a more complicated but also most exact method of calculation is used, which amounts to considering the liners as thin-walled cylinders with different conditions of clamping (fixing) along their margins [43]. Calculations based on this method make it possible to determine the free-vibration frequencies of liners having the first form with an accuracy of 8-10%, which is quite adequate for practical calculations.

From the theory of vibrations of thin cylinders we know that when a cylinder wall of this kind is struck, flexural deformations and elongation of walls are observed [14]. In the sections perpendicular to the cylinder axis the vibrations are characterized by some number of waves distributed along the circumference. If the amount or if the number of waves in the plane of the circle is denoted by N_1, the first three shapes of the vibrations are of the form shown in Figure 16. The case when n_1 is less than two cannot occur for a cylinder liner, therefore we will consider the simplest case when $n_1 = 2$. Here there are four lines on the liner at which the radial motions are equal to zero. These lines are called the nodes of cylindrical vibrations.

However, owing to the tangential displacement, the nodes are not positions of absolute rest.

Actually, there can be the most diverse forms of vibrations, depending on the combinations of cylindrical waves n_1 and axial waves N.

The frequencies of free vibrations of diesel engine cylinders evidently lie within the range of free-vibration frequencies of identical cylinders with freely supported and rigidly fixed ends. Therefore it is useful to determine the boundary values of the free-vibration frequencies for these cases. The sequence of calculations in both cases is approximately the same.

We adopt the following notation for the calculations:

a is the mean radius of the cylinder

a_1 is the external radius of the cylinder

a_2 is the radius of the flange

b is the length of the axial half-wave

c' is the constant of the axial frequency coefficient

d is the thickness of the cylinder end

d_1 is the thickness of the flange

l_x, l_y, l_z are the normal strains

l_{xy}, l_{yz}, l_{xz} are the shear strains

$f_{fr} = \omega/2\pi$ is the frequency of cylinder free vibrations

g is the acceleration due to gravity

h is the thickness of the cylinder wall

k is the ratio of the hyperbolic component of vibration to sinusoidal component (fixed ends)

l is the cylinder length

m is the number of axial half-waves (m + 1) -- the number of nodes of axial half-waves

n_1 is the number of cylindrical waves ($2n_1$) -- the number of nodes of cylindrical waves

P_x, P_y, P_z are the components of normal stresses

P_{xy}, P_{xz}, P_{yz} are the components of the superimposed stresses

t is time

U; V', A' are the components of the displacement of the central point of a cylinder

X, Y, Z are the coordinates in the axial, radial and peripheral directions

A", B, C are the maximum amplitudes of the vibrations

E is Young's modulus

K_0, K_1, K_2 are the coefficients in the frequency equation (freely supported ends)

R_0, R_1, R_2 are the coefficients in the frequency equation (rigidly fixed ends)

S is the strain work (potential energy)

T_k is the kinetic energy

$\alpha = h/a$; $\beta = h^2/12a^2$ -- coefficients

$\Delta =$ is the frequency coefficient

ε_1, ε_2 are the normal strains in the central section of the cylinder

Θ_1, Θ_2 are the functions $\mu l/a$ (fixed ends)

$\lambda = m\pi a/l$ is the coefficient of the length of the axial wave (freely supported ends)

$\lambda_e =$ is the equivalent coefficient of the length of the axial wave

μ is the coefficient of the length of the axial wave (fixed ends)

ρ is the density

σ is Poisson's ratio

φ is the angular coordinate, and

$\omega = 2\pi f$ is the circular frequency.

For a cylinder with freely supported ends, the displacements in the direction of the X, Y, and Z axes (Figure 17) based on the data in [43], are adopted in the form of the following equations:

$$\left.\begin{aligned} U &= A' \cos\frac{m\pi x}{l}\cos n_1\Phi\cos\omega t;\\ V &= B\sin\frac{m\pi x}{l}\sin n_1\Phi\cos\omega t;\\ A' &= C\sin\frac{m\pi x}{l}\cos n_1\Phi\cos\omega t. \end{aligned}\right\} \qquad (6)$$

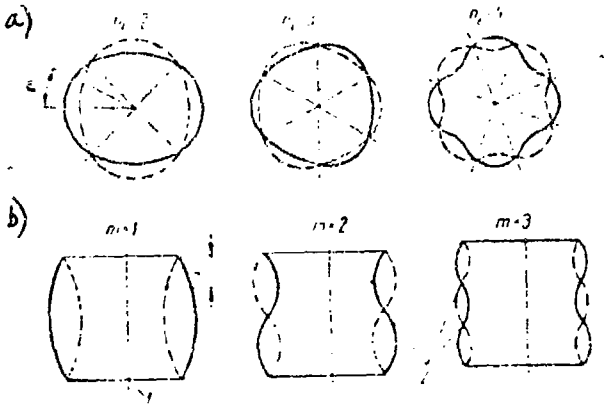

Figure 16. Forms of Vibrations of Cylindrical Shells and Liners of Diesel Engine Cylinders: a - cylindrical vibrations in the plane of the circle; b - axial vibrations (1 -- liner axis; 2 -- node of vibrations)

It is shown that equations (6) satisfy the conditions at the ends and are compatible with the relative strain.

The vibrations take on a more complicated form for cylinders with fixed ends. The following conditic is must be satisfied at each cylinder end:

$$U = 0; \quad V = 0; \quad W = 0; \quad \frac{\partial w}{\partial x} = 0.$$

This shows that the radial displacement occurs according to a sinusoidal law, just as do the axial displacements caused by these radial displacements.

To simplify the analysis of cylinders with fixed ends, let us assume a point in the central plane of the cylinder and let us consider individually two conditions for the even and odd number of nodes of axial vibrations. Professor R. N. Arnold proposes that the displacement in the

axial and radial directions be considered in the following form for the even number of nodes:

$$\left.\begin{aligned} U &= \bar{U}\left(-\sin\frac{\mu x}{a} + k\sinh\frac{\mu x}{a}\right)\cos n_1\Phi; \\ V &= \bar{V}\left(\cos\frac{\mu x}{a} + k\cosh\frac{\mu x}{a}\right)\sin n_1\Phi; \\ W &= \bar{A}_0\left(\cos\frac{\mu x}{a} + k\cosh\frac{\mu x}{a}\right)\cos n_1\Phi. \end{aligned}\right\} \quad (7)$$

Here the quantities $\bar{U}$, $\bar{V}$, and $\bar{A}_0$ are functions only of time, and $k = \frac{\sin\frac{\mu l}{2a}}{\sinh\frac{\mu l}{2a}}$ and the value of μ is given as $\operatorname{tg}\frac{\mu l}{2a} = \operatorname{th}\frac{\mu l}{2a}$.

The roots of the equation will be $\frac{\mu l}{a} = 1{,}506\pi;\ \frac{7}{2}\pi;\ \frac{11}{2}\pi;\ \frac{15}{2}\pi \ldots$ in accordance with the number series 2, 4, 6, 8..., corresponding to the nodes of vibrations.

Let us consider an element of a cylindrical shell having length l, thickness h and with mean radius a. This element is bounded by two planes shown in Figure 18, perpendicular to the X axis and at a distance dx, and by two radial planes at the angle $d\Phi$ to the axis. The stresses P_x, P_y, and P_z are applied at the cylinder element parallel to the X, Y, and Z axes. The sheer stresses P_{xy}, P_{yz}, and P_{xy}, which are determined on analogy with the first-named stresses, are applied along a plane perpendicular to the X axis in the direction of Y. The strains in the direction of the axes can be estimated by l_x, l_y and l_z. Neglecting the trapezoidal form of the surface in the direction perpendicular to the X axis, the work of cylinder strain can be written as

$$S = \int_0^{2\pi}\int_0^{l}\int_{-\frac{1}{2}h}^{+\frac{1}{2}h} \frac{1}{2}(P_x l_x + P_y l_y + P_{xy} l_{xy})\, a\, d\Phi\, dx\, dz. \quad (8)$$

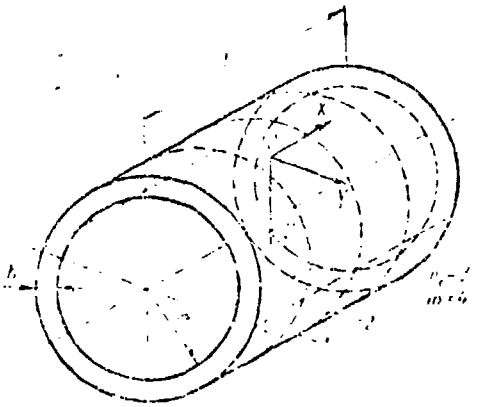

Figure 17. Nodes of Cylindrical 1 and Axial 2 Vibrations of a Cylinder

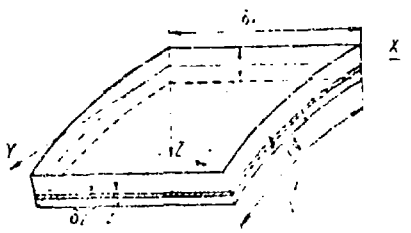

Figure 18. Element of Cylindrical Shell

Professor A. Love [48] showed that to the first approximation stresses P_z and shearing strains l_{yz} and l_{xz} are equal to zero. Based on Hooke's law, we have

$$P_x = \frac{E}{1-\sigma^2}(l_x + \sigma l_y); \quad P_y = \frac{E}{1-\sigma^2}(l_y + \sigma l_x);$$

$$P_{xy} = \frac{E}{2(1+\sigma)} l_{xy}.$$

After substituting these values into equation (8), we get the expression

$$S = \frac{E}{2(1-\sigma^2)} \int_0^{2\pi} \int_0^{l} \int_{-\frac{1}{2}h}^{\frac{1}{2}h} \left[l_x^2 + l_y^2 + 2\sigma l_x l_y + \right.$$

$$\left. + \frac{1}{2}(1-\sigma)\, l_{xy}^2 \right] a\, d\Phi\, dx\, dz. \qquad (9)$$

Let us additionally designate ε_1 as the strain in the X-axis for the central surface of the cylinder, and ε_2 as the strain in the Y axis for the central surface of the cylinder, and let k_1 stand for the curvature of the surface along the X axis, and k_2 -- along the Y axis.

We will denote the strain in shearing by γ, and the strain in torsion by τ. The strains then at the distance Z from the central surface are determined from the following expression

$$l_x = \varepsilon_1 - z k_1; \quad l_y = \varepsilon_2 - z k_2; \quad l_{xy} = \gamma - 2z\tau.$$

Let us assume that U, V' and A' are the instantaneous displacements of a point in the central surface in the directions X, Y, and Z, while the strain and curvature can be given in terms of displacement, and their derivatives can be given as follows:

$$\left.\begin{aligned} \varepsilon_1 &= \frac{\delta U}{\delta x}; \quad k_1 = \frac{\delta^2 A'}{\delta^2 x}; \\ \varepsilon_2 &= \frac{1}{a}\frac{\delta V'}{\delta \Phi} - \frac{A'}{a}; \\ k_2 &= \frac{1}{a^2}\frac{\delta^2 A'}{\delta \Phi^2} + \frac{1}{a^2}\frac{\delta V'}{\delta \Phi}; \\ \gamma &= \frac{\delta V'}{\delta x} + \frac{1}{a}\frac{\delta U}{\delta \Phi}; \quad \tau = \frac{1}{a}\frac{\delta^2 A'}{\delta x\, \delta \Phi} + \frac{1}{a}\frac{\delta V'}{\delta x}. \end{aligned}\right\} \qquad (10)$$

In expression (10) Φ determines the angular positions of the point of interest. By expressing the strain in these equations in terms of U, V', and A', inserting the data obtained into equation (9) and integrating

it, we get the following equation for the strain work

$$S = -\frac{\pi E a l}{4a(1-\sigma^2)}\left\{\mu\Theta U^2 + \beta\mu^2\Theta_1\bar{A}_0 + \right.$$
$$+ \Theta_1\left[(n_1V-\bar{A}_0)^2 + \beta(n_1V-n_1^2\bar{A}_0)^2\right] +$$
$$+ 2\sigma\Theta_2\left[-\mu n_1UV + \mu U\bar{A}_0 + \beta\left(\mu^2n_1^2\bar{A}_0^2 + \mu^2n_1\bar{V}\bar{A}_0\right)^2\right] +$$
$$+ \frac{1}{2}(1-\sigma)\Theta_2\left[n_1^2U^2 + \mu^2V^2 - 2\mu n_1UV + \right.$$
$$\left.\left. + 4\beta\left(\mu^2V^2 + \mu^2n_1^2\bar{A}_0 - 2\mu^2n_1V\bar{A}_0\right)\right]\right\}. \qquad (11)$$

Here

$$\beta = \frac{\mu^2}{12k^2}; \quad \Theta_1 = 1 + k^2; \quad \Theta_2 = 1 - k^2 + \frac{2a}{\mu l}\sin\frac{\mu l}{2}.$$

The expression for the kinetic energy in any case of clamping [fixing] can be represented as follows

$$T_\kappa = -\frac{\rho}{2g}\int_0^{2\pi}\int_0^{l}\int_{-\frac{1}{2}+\Delta}^{\frac{1}{2}-\Delta}\left[\left(\frac{\delta\bar{U}}{\delta t}\right)^2 + \left(\frac{\delta\bar{V}}{\delta t}\right)^2 + \left(\frac{\delta\bar{A}_0}{\delta t}\right)^2\right]a\,d\Phi\,dx\,dz =$$
$$= -\frac{\pi E a l}{4g}\left\{\Theta_1\bar{U}^2 - \Theta_1(\bar{V}^2 + \bar{A}_0)\right\}.$$

Since $\bar{U}$, $\bar{V}$, $\bar{A}_0$ are independent variables, using Lagrange's equation we get

$$\frac{d}{dt}\left(\frac{\delta T_\kappa}{\delta\bar{U}}\right) - \frac{\delta T_\kappa}{\delta U} = -\frac{\delta S}{\delta\bar{U}}$$

and two analogous equations for V and A_0.

Inserting $\quad U = A''\cos\omega t; \quad V = B\cos\omega t; \quad \bar{A}_0 = C\cos\omega t$

and writing

$$\Delta = \frac{\rho(1-\sigma^2)\omega^2a^2}{Eg},$$

we get the following equations:

$$\left.\begin{aligned}
&\left[\mu^2\Theta_1 + \frac{1}{2}(1-\sigma)n_1^2\Theta_2 - \Delta(\Theta_2)\right]A'' - \\
&- \frac{1}{2}(1-\sigma)\mu n_1\Theta_2 B + \sigma\mu\Theta_2 C = 0; \\
&\left\{n_1^2\Theta_1 + \frac{1}{2}(1-\sigma)\mu^2\Theta_2 - \Delta\Theta_1 + \right. \\
&\left. + \beta\left[n_1^2\Theta_1 + 2(1-\sigma)\mu^2\Theta_2\right]\right\} B - \\
&- \frac{1}{2}(1-\sigma)\mu n_1\Theta_2 A'' - \\
&- \left[n_1\Theta_1 + \beta\left[n_1^3\Theta_1 + (2-\sigma)\mu^2 n_1\Theta_2\right]\right] C = 0; \\
&\sigma\mu\Theta_2 A'' - \left[n_1\Theta_1 + \beta\left[n_1^3\Theta_1 + (2-\sigma)\mu^2 n_1\Theta_2\right]\right] B + \\
&+ \left[\Theta_1 - \Delta\Theta_1 + \beta\left(\mu^4\Theta_1 + n_1^4\Theta_1 + 2\mu^2 n_1^2\Theta_2\right)\right] C = 0.
\end{aligned}\right\} \qquad (12)$$

For an odd number of nodes of axial vibrations, the displacement is represented by the following equations:

$$\left.\begin{aligned}
U &= A'\left(\cos\frac{\mu x}{a} - k\cos h\frac{\mu x}{a}\right)\cos n_1\Phi\cos\omega t; \\
V &= B\left(\sin\frac{\mu x}{a} - k\sin h\frac{\mu x}{a}\right)\sin n_1\Phi\cos\omega t; \\
W &= C\left(\sin\frac{\mu x}{a} - k\sin h\frac{\mu x}{a}\right)\cos n_1\Phi\cos\omega t;
\end{aligned}\right\} \qquad (13)$$

In equations (13), the quantities μ are expressed in terms of

$$\operatorname{tg}\frac{\mu l}{2a} = \operatorname{tg} h\frac{\mu l}{2a}.$$

The roots of equation (13), $\frac{\mu l}{a} = \frac{5}{2}\pi;\ \frac{9}{2}\pi;\ \frac{13}{2}\pi; \ldots$ **then correspond to the number series 3, 5, 7, ...**

The considerations concerning the odd number of nodes of vibration along the cylinder axis are analogous to equation (12) for the maximum amplitude A", B and C and are applicable for any number of nodes of axial vibrations given the condition that

$$\Theta_1 = 1 + (-1)^{n+1}k^2;$$
$$\Theta_2 = 1 + (-1)^{n+1}\left(\frac{2a}{\mu l}\sin\frac{\mu l}{a} - k^2\right).$$

If we cancel out the quantities A', B and C from equation (12) we get the cubic equation

$$\Lambda^3 + R_2\Lambda^2 + R_1\Lambda - R_0 = 0,$$

for which the frequency of free vibrations is

$$f_{fr} = \frac{1}{2\pi} \sqrt{\frac{E\Lambda}{\rho(1-\sigma^2)}}. \qquad (14)$$

Here the coefficients R_0, R_1 and R_2 will be as follows:

$$\left.\begin{aligned}
R_0 &= \frac{1}{2}(1-\sigma)\left[1-\sigma^2\left(\frac{\Theta_2}{\Theta_1}\right)^2\right]\mu^4 + \\
&+ \beta\left[\frac{1}{2}(1-\sigma)(\mu^2+n_1^2)\right] + \left[(1-2\sigma)\frac{\Theta_2}{\Theta_1} + \frac{\Theta_1}{\Theta_2}\right]\times \\
&\times(\mu^4 n_1^2 + \mu^2 n_1^4) + \left[3-\sigma-2\sigma\left(\frac{\Theta_2}{\Theta_1}\right)^2\right]\mu^2 n_1^2 - \\
&-(2-\sigma)\left[2-(1-\sigma)\sigma\left(\frac{\Theta_2}{\Theta_1}\right)^2\right]\mu^2 n_1^2 - \\
&-\left[2\frac{\Theta_2}{\Theta_1} + 2(1-2\sigma)\frac{\Theta_1}{\Theta_2}\right]\mu^2 n_1^2 - (1-\sigma)n_1^6 + \\
&+\left[2(1-\sigma) - 2\sigma^2(1-\sigma)\left(\frac{\Theta_2}{\Theta_1}\right)^2\right]\mu^4 + \\
&+\left[(1-2\sigma)\frac{\Theta_2}{\Theta_1} + \frac{\Theta_1}{\Theta_2}\right]\mu^2 n_1^2 + \frac{1}{2}(1-\sigma)n_1^4; \\
R_1 &= \frac{1}{2}(1-\sigma)(\mu^2+n^2) + \left(\frac{\Theta_1}{\Theta_2} - \sigma\frac{\Theta_2}{\Theta_1}\right)\mu^2 n_1^2 + \\
&+\frac{1}{2}(1-\sigma)n_1^2 + \left[\frac{1}{2}(1-\sigma-2\sigma^2)\frac{\Theta_2}{\Theta_1} + \frac{\Theta_1}{\Theta_2}\right]\mu^2 + \\
&+\beta\left\{\left[\frac{1}{2}(1-\sigma)\frac{\Theta_2}{\Theta_1} + \frac{\Theta_1}{\Theta_2}\right]\mu^2 - \right. \\
&\left.+\left[\frac{1}{2}(7-\sigma) - (1-\sigma)\left(\frac{\Theta_2}{\Theta_1}\right)^2\right]\mu^2 n_1^2 + \right. \\
&\left.+\left[\frac{1}{2}(7-3)\frac{\Theta_2}{\Theta_1} + \frac{\Theta_1}{\Theta_2}\right]\mu^2 n_1^2 + \frac{1}{2}(3-\sigma)n_1^4 + \right. \\
&\left.+2(1-\sigma)\mu^2 - \left[(3-\sigma^2)\frac{\Theta_2}{\Theta_1} - \frac{\Theta_1}{\Theta_2}\right]\mu^2 n_1^2 - \right. \\
&\left.-\frac{1}{2}(3+\sigma)n_1^4 + 2(1-\sigma)\frac{\Theta_2}{\Theta_1}\mu^2 + n_1^2\right\}; \\
R_2 &= \left[\frac{\Theta_2}{\Theta_1} + \frac{1}{2}(1-\sigma)\frac{\Theta_2}{\Theta_1}\right]\mu^2 + \\
&+\frac{1}{2}(3-\sigma)n_1^2 + 1 + \beta\left[\mu^4 + 2\frac{\Theta_2}{\Theta_1}\mu^2 n_1^2 + n_1^4 + \right. \\
&\left.+2(1-\sigma)\frac{\Theta_2}{\Theta_1}\mu^2 + n_1^2\right].
\end{aligned}\right\} \qquad (15)$$

The equation for the determination of the frequency of free vibrations of cylinders with freely supported ends can be derived as a particular case from the theory of the frequencies of free vibrations of cylinders with rigidly fixed ends when $\Theta_1 = \Theta_2 = 1$. Here the axial form of the wave becomes sinusoidal, in turn agreeing with the freely-supported end case. Then equation (15) becomes simplified:

$$\Delta^3 + K_2\Delta^2 + K_1\Delta + K_0 = 0, \tag{16}$$

where

$$f_{fr} = \frac{1}{2\pi r}\sqrt{\frac{E\Delta}{\rho(1-\sigma^2)}}$$

The coefficients K_0, K_1 and K_2 will be as follows:

$$\left.\begin{aligned}
K_0 &= \frac{1}{2}(1-\sigma)^2(1-\sigma)\lambda^4 + \frac{1}{2}(1-\sigma)\beta\left[(\lambda^2+n_1^2)^4 - \right.\\
&\quad - 2(4-\sigma^2)\lambda^4 n_1^2 - 8\lambda^2 n_1^4 - 2n_1^6 - 4(1-\sigma^2)\lambda^4 + \\
&\quad \left. + 4\lambda^2 n_1^2 + n_1^4\right];\\
K_1 &= \frac{1}{2}(1-\sigma)(\lambda^2+n_1^2)^2 + \frac{1}{2}(3-\sigma-2\sigma^2)\lambda^2 + \\
&\quad + \frac{1}{2}(1-\sigma)n_1^2 - \beta\left[\frac{1}{2}(3-\sigma)(\lambda^2+n_1^2)^3 + \right.\\
&\quad + 2(1-\sigma)\lambda^4 - (2-\sigma^2)\lambda^2 n_1^2 - \frac{1}{2}(3+\sigma)n_1^4 + \\
&\quad \left. + 2(1-\sigma)\lambda^2 + n_1^2\right];\\
K_2 &= 1 + \frac{1}{2}(3-\sigma)(\lambda^2+n_1^2) + \\
&\quad + \beta\left[(\lambda^2+n_1^2)^2 + 2(1-\sigma)\lambda^2 + n_1^2\right].
\end{aligned}\right| \tag{17}$$

Since Δ^3 and $K_2\Delta^2$ are small in comparison with other terms in the cubic equation, the following linear equation can serve as suitable approximation:

$$\Delta = -\frac{K_0}{K_1} + \frac{K_2}{K_1}\left(\frac{K_0}{K_1}\right)^2,$$

in which the coefficient K_0, K_1 and K_2 are determined by the following equations:

$$
\left.
\begin{aligned}
K_0 &= \frac{1}{2}(1-\sigma)^2(1+\sigma)\lambda^4 + \frac{1}{2}(1-\sigma)\beta\,[(\lambda^2+n_1^2)^4 - \\
&\qquad - 8\lambda^2 n_1^4 - 2n_1^6 + n_1^4]; \\
K_1 &= \frac{1}{2}(1-\sigma)(\lambda^2+n_1^2)^2 + \frac{1}{2}(3-\sigma-2\sigma^2)\lambda^2 + \\
&\qquad + \frac{1}{2}(1-\sigma)n_1^2 + \frac{1}{2}(3-\sigma)\beta(\lambda^2+n_1^2)^3; \\
K_2 &= 1 + \frac{1}{2}(3-\sigma)(\lambda^2+n_1^2).
\end{aligned}
\right\} \qquad (18)
$$

A solution to the system of equations (15) provides a very inexact result, since very awkward expressions result for coefficients in the equation of the frequency of free vibrations of a cylinder with fixed ends, while in actual operating conditions in a diesel engine the supports of a liner execute vibrations together with the block and therefore are not absolutely rigid. Since the theory of fixed ends does not fully correspond to the actual conditions, exact calculations are difficult to perform. More exact calculations are obtained when the system of equations (18) is solved for variants with freely supported ends. Professor R. N. Arnold [43] considers it quite obvious that a given cylinder with length l, fixed at its ends and excited with a periodic force can be replaced by another equivalent cylinder with freely supported ends of the same cross section and having the same frequency of vibrations if its length is $l - l'$. In this case

$$\lambda_l = [illegible] \qquad \text{and} \qquad \lambda = [illegible].$$

This in turn, makes it possible to set up the relation

$$[illegible] \qquad (19)$$

Here c_1 = [illegible] is a function of n and n_1 and also of cylinder size.

Based on the data in [43], the optimal value of c_1 is 0.3 for various cases. The calculation is performed with the same procedures for a cylinder with flanges, but only the equivalent diameter d is calculated according to the formula

$$[illegible]$$

where [illegible]

The equivalent axial frequency coefficient is determined by the expression

$$[illegible]$$

Based on these theoretical prerequisites, the procedure for determining the frequencies of free vibrations of cylinder liners in diesel engines can be as follows:

1) the quantities E, ρ, and μ must be selected for the liner material; and

2) then the coefficient of the length of the axial wave λ, the coefficients K_0, K_1 and K_2, the frequency coefficient Δ, the frequency of the free vibrations of the cylinder liner f_{fr}, the coefficients of the attached mass of water, and the coefficient [illegible] must be determined.

For the case $\eta\lambda > 1.1$, the calculation was made for the frequency of free vibrations of a liner with allowance for the flange, and the frequency of free vibrations of a cylinder liner was calculated with allowance for the coefficient of the attached mass of water.

In the second step the calculations were made for cases of freely

supported and rigidly fixed ends of a liner for different combinations of axial and cylindrical forms of vibrations.

As an example, we present the calculation of the frequencies of free vibrations of a cylinder liner in a 6 Ch 15/18 (Figure 19). For this engine we have

$a = 78.25$ mm, $h = 6.5$ mm,

$l = 276$ mm, $a_2 = 87.5$ mm,

$a_1 = 81.5$ mm.

Figure 19. Linear Dimensions of a Liner in a 6 Ch 15/18 Diesel Engine

The liner was made of 38 Kh MYu A alloy steel, for which we assume

$E = 2 \cdot 10^4$ kg/mm^2;

$\rho = 8.4 \cdot 10^{-6}$ kg/mm^3;

$\sigma = 0.26$;

$\beta = h^2/12a^2 = 42.3/12 \cdot 6120 = 0.000577$.

Inserting the ρ and σ from above into the system of equations (17), we get the coefficients:

$$K_0 = 0{,}345\lambda^4 + 0{,}000214\,[(\lambda^2 + n_1^2)^4 - 8\lambda^2 n_1^4 - 2n_1^2 + n_1^4];$$
$$K_1 = 0{,}37\,(\lambda^2 + n_1^2)^2 + 1{,}3\lambda^2 - 0{,}37 n_1^2 + 0{,}00079\,(\lambda^2 + n_1^2)^3;$$
$$K_2 = 1 + 1{,}37\,(\lambda^2 + n_1^2).$$

For a given cylinder liner, we have $f_{fr} = \frac{5{,}01 \cdot 10^4}{2{,}375 \cdot 25}\sqrt{\Lambda} = 10\,680\sqrt{\Lambda}.$

For a cylinder liner with freely supported ends when $m = 1$, $n_1 = 2$

$$\lambda = \frac{\pi \cdot 75 \cdot 2}{270} = 0{,}89;\ \lambda^2 = 0{,}792;\ \lambda^4 = 0{,}627.$$

Here $K_0 = 0.282$, $K_1 = 0.028$, and $K_2 = 7.56$.

The frequency coefficient is

$$\Lambda = \frac{0{,}282}{11{,}028} + \frac{7{,}56}{11{,}028}\left(\frac{0{,}282}{11{,}028}\right)^2 = 0{,}0213.$$

Thus, the frequency of free vibrations of a liner with respect to the first form will be

$$f_{fr-1} = 10\,680\sqrt{0{,}0213} = 1560 \text{ Hz}.$$

For $n_1 = 3$ and $m = 1$, the values of the quantities are as follows:

$$\lambda = 0{,}89;\ \lambda^2 = 0{,}792;\ \lambda^4 = 0{,}627.$$
$$K_0 = 1{,}736;\ K_1 = 40{,}5;\ K_2 = 14{,}41;$$
$$\Lambda = \frac{1{,}736}{40{,}5} + \frac{14{,}41}{[illegible]}\left(\frac{14{,}41}{[illegible]}\right) = 0{,}0[illegible]1,$$

and the frequency of the free vibrations in the second form is

$$f_{fr-2} = 10\,680\sqrt{[illegible]} = 2270 \text{ Hz}.$$

When $n_1 = 2$ and $m = 2$, the values of the quantities are as follows:

$$\lambda = 1{,}78;\ \lambda^2 = 3{,}17;\ \lambda^4 = 10{,}05;$$
$$K_0 = 3{,}9;\ K_1 = 24{,}9;\ K_2 = 10{,}85;$$
$$\Lambda = \frac{3{,}9}{24{,}9} + \frac{10{,}85}{24{,}9}\left(\frac{3{,}9}{24{,}9}\right)^2 = 0{,}167,$$

and the frequency of the free vibrations of the third form is

$$f_{fr-3} = 10680 / \sqrt{0,157} = 4300 \text{ Hz}.$$

When we consider a liner as a cylinder with fixed ends, we must again determine the values of these quantities. For the first form of vibrations, when $n_1 = 2$ and $m = 1$, we have

$$\lambda_1 = 1,150; \quad \lambda_2 = 1,41; \quad \lambda_3 = 1,5;$$
$$K_0 = 0,739; \quad K_1 = 15,9; \quad K_2 = 8,52 \quad \Delta = 0,0543,$$

and the frequency of the free vibrations of the first form will be

$$f_{fr-1} = 2490 \text{ Hz}.$$

For the second form of vibrations when $n_1 = 3$ and $m = 1$, we have

$$\lambda_1 = \lambda_2; \quad K_0 = 2,59; \quad K_1 = 45,8; \quad K_2 = 15,2; \quad \Delta = 0,058,$$

and the frequency of free vibrations of the second form is

$$f_{fr-2} = 2570 \text{ Hz}.$$

For the third form of vibrations when $n_1 = 2$ and $m = 1$, we have

$$\lambda_1 = 1,21; \quad \lambda_2 = 3,28; \quad \lambda_3 = 10,76;$$
$$K_0 = 4,2; \quad K_1 = 25,64; \quad K_2 = 10,97 \quad \Delta = 0,1745,$$

and the frequency of free vibrations is

$$f_{fr-3} = 4450 \text{ Hz}.$$

The most exact results in determining the frequency of free vibrations is given by calculating a liner with freely supported ends.

Since $\eta = 87.5/81.5 = 1.075$, which is less than 1.1, we do not have to determine the frequencies of free vibrations of a liner as a cylinder with flanges at its ends.

In a similar fashion, the frequencies of free vibrations of cylinder liners in other diesel engines are carried out. These calculations were

made when the medium surrounding the liner was water. Actually, the cylinder liners swept with water, some of which participates in the vibratory process. And the mass of the liner must actually be increased, and the frequency of the free vibrations somewhat reduced.

The ratio of the frequency of free vibrations of a body in air with respect to the frequency of free vibrations of the this same body in another medium, or when its mass is increased, is called the coefficient of attached mass.

According to the data of P. N. Lefonova, a formula for determining the coefficient of the attached mass of water is as follows:

$$\nu^2 = 1 + \frac{\rho_0 a_1}{\rho h \sqrt{n_1^2 + \alpha^2}}, \qquad (20)$$

where ν is the coefficient of the attached mass of water

a_1 is the external radius of the cylinder

ρ_0 is the density of the liquid (water)

ρ is the density of the cylinder material

h is the thickness of the cylinder wall

n_1 is the number of nodes of cylindrical half-waves;

$$\alpha = \frac{\pi a_1}{l}.$$

Here l is the length of the liner in contact with the water.

The calculated values of the coefficients of the attached mass of water are listed in Table 3 for several diesel engines.

Therefore, with consideration of the theoretically calculated values characterizing the attached mass of water, the frequency of free vibrations of cylinder liners $f_{fr,at}$ [at. = attached] will be somewhat lower, since

$$f_{fr,et} = \nu f_{fr}.$$

Table 4 presents the frequencies of free vibrations of cylinder liners of diesel engines designed for the case of freely supported ends, and frequencies of free vibrations with consideration of the attached mass of water.

When a liner is rigidly fixed in the block, the frequencies of free vibrations will increase, however, according to the data in [18] we must also take account of the attached mass of the piston, which in turn again reduces the frequencies of the free vibrations.

Table 3. Coefficients of Attached Mass of Water for Several Diesel Engines

1	2				13				
	3	3	3	4					
5									
6									
7									
8									
9									
10									
11									
12									

KEY:
1 - Diesel engine model
2 - Assumed numerical values
3 - in mm
4 - in $kg/mm^2 \cdot 10^6$
5 - Ch 8.5/11
6 - Ch 10.5/13
7 - Ch 12/14
8 - Ch 15/18
9 - Ch 18/20
10 - Ch 23/30
11 - D 23/30
12 - Note. The following values were assumed for diesel engines shown in the table: $n_1 = 2$, $\rho_0 = 10^{-6}$ kg/mm^3
13 - Calculated values

Table 4. Frequencies of Free Vibrations

1 Тип двигателя	2 f_{fr}			γ	3 $f_{fr,at}$		
	$n_1=2$; $m=1$	$n_1=3$; $m=1$	$n_1=2$; $m=2$		$n_1=2$; $m=1$	$n_1=3$; $m=1$	$n_1=2$; $m=2$
4 [illegible]	1737	[illegible]	4370	1,32	1310	[illegible]	[illegible]
5 [illegible]	1630	[illegible]	3570	1,255	1290	[illegible]	2850
6 [illegible]	1630	[illegible]	3730	1,24	1320	[illegible]	[illegible]
7 [illegible]	1560	[illegible]	[illegible]	1,20	1270	[illegible]	[illegible]
8 [illegible]	1320	[illegible]	3430	1,305	985	[illegible]	2530
9 [illegible]	710	[illegible]	1850	1,28	580	1120	1540
10 [illegible]	735	[illegible]	1650	1,21	640	1220	1370

KEY: 1 -Diesel engine model
2 - f_{fr}
3 - $f_{fr,at}$
4 - Ch 8.5/11
5 - Ch 10.5/13
6 - Ch 12/14
7 - Ch 15/18
8 - Ch 18/20
9 - Ch 23/30
10 - D 23/30

It is difficult to determine the attached piston mass, since according to the data in [34, 35], during the operating time the piston can be in a canted position and not rest fully against the liner.

Therefore, we adopt as an assumption in our calculations that the increase in the frequency of free vibrations resulting from the more rigid fixing of cylinder liner ends is compensated by a drop in frequency due to the attached piston mass.

As shown by experience, the actual frequencies of free vibrations of cylinder liners in diesel engines, determined by the resonance method as well as by the impact method is closest (with a small error) to calculations

made assuming freely supporting ends.

Table 5. Calculated and Experimental Frequencies of Free Vibrations of Cylinder Liners in Diesel Engines

1 Тип дизеля	2 Расчетные частоты для $f_{fr,at}$			3 Экспериментальные значения для f_{fr} по формам		
	$n_1=2$; $m=1$	$n_1=3$; $m=1$	$n_1=2$; $m=2$	1	2	3
4 Ч8,5 11	1310	2400	3350	1100	2900	4000
5 Ч10,5 13	1200	2500	2850	1050	2500	--
6 Ч15 18	1230	1800	3100	1200	2000	7000

KEY: 1 - Diesel engine model
2 - Calculated frequencies for $f_{fr,at}$
3 - Experimental values for f_{fr} for the indicated forms
4 - Ch 8.5/11
5 - Ch 10.5/13
6 - Ch 15/18

A comparison of calculated and experimental data for the frequencies of free vibrations of cylinder liners for a number of diesel engines Ch 8.5/11, Ch 10.5/13, and Ch 15/13 is shown in Table 5. These data indicate that when the coefficient of the attached mass of water γ is taken into account, the first vibrational form agrees thoroughly well. Therefore, this method of calculation is entirely suitable when estimating the frequencies of the first vibrational form. Calculated data for frequencies of free vibrations in air without allowing for the attached mass of water are closer to the frequencies of free vibrations of higher orders, since the attached mass of water depends on the frequency of vibrations of cylinder liners and evidently γ is close to unity for

vibration frequencies above 3000 Hz.

8. Theoretical Estimate of Accelerations of Cylinder Liners at Free-Vibration Frequencies

For a theoretical estimation of the vibrational accelerations, we must determine, in addition to the free-vibration frequency, also the maximum amplitude of vibrations at this frequency.

To determine the amplitude of free vibrations of cylinder liners and thus accelerations of vibrations, we must consider the displacement of a liner acted on by side force P applied by the piston against the liner according to an increasing linear law P = kt (Figure 20).

Let us assume that a load increasing during the time T from zero to its maximum P_{max} according to a linear law, that is,

$$P = p(t) = k_0 t = P_{max} \frac{t}{T},$$

is applied at a liner is in equilibrium when the piston is at the TDC (T = 0; A_0 = 0; v = 0) under the action of a force.

The displacement of the liner for the time interval t < T can be found from the expression

$$A = \frac{1}{M\omega} \int_0^t P(\xi) \sin \omega (t - \xi) d\xi = \frac{1}{M\omega} P_{max} - \int_0^t \xi \sin \omega (t + \xi) d\xi. \quad (21)$$

According to the data in brackets [37], we assume, instead of P (ξ), the expression P_{max} ξ /T. Integrating equation [21] by parts, we get

$$\int_0^t \xi \sin \omega (t - \xi) d\xi = \frac{1}{\omega} \left(t - \frac{1}{\omega} \sin \omega t \right);$$

$$A_0 = \frac{P_{max}}{M\omega^2} \left(\frac{t}{T} - \frac{1}{\omega T} \sin \omega t \right).$$

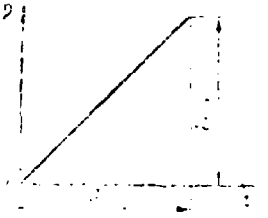

Figure 20. Variation of Side Force Acting at Piston in the Region of the Working TDC

Note that $\frac{P_{max}}{M\omega^2} = A_{st}$, that is, the static displacement of a liner corresponding to the maximum normal force P_{max}.

Therefore,

$$A_0 = A_{st}\left(\frac{t}{T} - \frac{\tau}{2\pi}\sin\frac{2\pi t}{\tau}\right),$$

where $\tau = \frac{2\pi}{\omega}$ is the vibrational period.

The displacement velocity of the liner is

$$v = \frac{A_{st}}{T}\left(1 - \cos\frac{2\pi t}{\tau}\right).$$

From this equation it follows that when $t \leq T$, the velocity of liner vibrations will remain positive. The greatest displacement will occur in the subsequent displacement of the liner, that is, when $t > T$.

The displacement of the liner when $T > t$ i

$$A_1 = \frac{1}{M\omega}\int_0^t P(\xi)\sin\omega(t-\xi)\,d\xi = \frac{1}{M\omega}\int_T^t P_{max}\sin\omega(t-\xi)\,d\xi =$$

$$= \frac{1}{M\omega}\cdot\frac{P_{max}}{T}\left[\frac{\xi}{\omega}\cdot\frac{1}{\omega}\cos\omega(t-\xi) + \frac{1}{\omega^2}\sin\omega(t-\xi)\right]_0^T +$$

$$+ \frac{P_{max}}{M\omega}\left[\frac{1}{\omega}\cos\omega(t-\xi)\right]_T^t = \frac{P_{max}}{M\omega^2}\left[\cos\omega(t-T) + \frac{1}{\omega T}\times\right.$$

$$\times \sin\omega(t-T)-\frac{1}{\omega T}\sin\omega t+1-\cos\omega(t-T)\Big]=$$

$$=A_{st}\left\{1-\frac{1}{\omega T}\left[\sin\omega(t-T)-\sin\omega t\right]\right\}=A_{st}\times$$

$$\times\left[1-\frac{2}{\omega T}\sin\frac{1}{2}\omega T\cos\frac{1}{2}\omega(2t-T)\right]=$$

$$=A_{st}\left[1-\frac{\tau}{\pi T}\sin\frac{\pi T}{\tau}\cos\frac{\pi}{\tau}(2t-T)\right].$$

In its final form, we have

$$A_0=A_{st}\left[1-\frac{\tau}{\pi T}\sin\frac{\pi T}{\tau}\cos\frac{\pi}{\tau}(2t-T)\right]. \qquad (22)$$

When T decreases to zero, equation (22) becomes simplified and is transformed into the expression for the liner displacement when it is acted on by an instantaneously applied load

$$A=A_{st}\left(1-\cos\frac{2\pi t}{\tau}\right).$$

Equation (22) shows that the displacement of a liner when $t<T$ is a harmonic vibration occurring in the vicinity of its static equilibrium position A_{st} with a period equal to the period of free vibrations τ and an amplitude equal to the difference between the deflections of the liner when a force variable according to the assumed law is applied and its deflections when the maximum force P is applied statically.

Therefore, we have

$$A=A_0+A_{st}.$$

According to the data of engineer I. S. Anishchenko, the greatest liner displacement will occur when $\cos\frac{\pi}{\tau}(2t-T)=\pm 1$, where the sign next to numeral 1 must be taken as the opposite of the sign of $\sin\pi T/\tau$. Thus, the maximum amplitude is

$$A_{max}=A_{st}\left[1+\left(\frac{\tau}{\pi T}\sin\frac{\pi T}{\tau}\right)\right]. \qquad (23)$$

The quantity appearing in the parentheses in expression (23), is the ratio of the maximum displacement of the liner body A_{max} to its greatest static displacement A_{st} and characterizes the dynamicity of the load. It can be called the coefficient of load dynamicity.

$$K_d = 1 + \left(\frac{\tau}{\pi T} \sin \frac{\pi T}{\tau}\right).$$

Since an exact determination of the ratio T/τ is virtually impossible, then by assuming an error within a safe margin, it is quite natural to assume the coefficient of load dynamicity K_d to be as follows, for practical purposes:

$$K_d = 1 - \frac{\tau}{\pi T}.$$

The formula

$$A_{st} = P_{max}/M\omega^2 = P_{max}/K_d$$

includes liner mass M. This mass must be applied at the point whose deflection is under consideration. Let us determine the reduced stiffness of the cylinder liner

$$C_{red} = \omega^2 M_{red} \quad [red = reduced].$$

The point on the cylinder liner corresponding to the center of the piston wristpin when the diesel engine crankshaft rotates by 30° is used as the point of reduction, that is, at the instant the maximum side force P is applied.

It can be shown that $M_{red} = \sum m i^2$, that is, the reduced mass of the body is equal to the sum of the products of the masses of all points by the square of their displacements i, which they acquire when the reduction point equal to unity is deflected.

For the assumed displacement along the Z axis, we can express the function i as follows

$$i = \frac{\sin^2 \frac{m\pi x}{l}}{\sin^2 \frac{m\pi c_1}{l}} \cos n_1 \Phi,$$

where c_1 is the distance from the upper edge of the cylinder liner to the point corresponding to the position of the axis of the piston wristpin for a 30° crank angle ($c_1 = c_0 + x$);

c_0 is the distance between the upper edge of the cylinder liner and the wristpin axis when the piston is at the TDC;

x is the distance that the piston traverses when the crankshaft rotates by the angle $\alpha = 30^\circ$ without allowing for Briks correction (H is the piston travel).

Earlier it was assumed that the maximum side force P will occur when the crankshaft has rotated by 30°, that is;

$$x = \frac{H}{2}(1 - \cos 30^\circ) = 0{,}067H.$$

Then

$$c_1 = c_0 + 0{,}067H.$$

Inserting the value i into the equation for M_{re}, we get the following expression:

$$M_{re} = \int_0^l \int_0^{2\pi} n \frac{\sin^2 \frac{m\pi x}{l}}{\sin^2 \frac{m\pi c_1}{l}} \cos^2 n_1 \Phi \, dx \, d\Phi = \frac{n}{\sin^2 \frac{m\pi c_1}{l}} \times \int_0^l \sin^2 \frac{m\pi x}{l} \, dx \int_0^{2\pi} \cos^2 n_1 \Phi \, d\Phi;$$

$$\int_0^{\frac{\pi l}{2}} \sin^2 \frac{\pi x}{l} dx = \frac{\pi}{2} = \frac{1}{\frac{\pi}{l}} \sin^2 \frac{\pi}{l} \frac{l}{2} = \frac{l}{2};$$

$$\int_0^{2\pi} \cos^2 \omega_1 t \, d(\omega_1 t) = \frac{\omega_1 t}{2} + \frac{1}{4\omega_1} \sin 2\omega_1 t \Big|_0^{2\pi} = \pi.$$

Thus,

$$M_{red} = \frac{\frac{\pi l}{2} m_0}{\sin^2 \frac{\pi}{l} \frac{m_0 l}{l}},$$

where m_0 is the unit mass $\left(m_0 = \frac{\Delta\rho}{2}\right)$.

Therefore,

$$M_{red} = \frac{\frac{\pi}{2} \frac{\Delta\rho}{2}}{\frac{\pi^2}{l^2} \sin^2 \frac{\pi}{l} \frac{m_0 l}{l}}. \tag{24}$$

To determine the maximum deflection of a liner when acted on by force P, in addition to ω_{f_1} and M_{red}, we must calculate the displacement velocity of the piston as it slaps within the limits of the thermal gap. Using the data in [1], we find that over the section from 0 to 30° of CA [crank angle], the force P rises from zero to the maximum approximately linearly, that is, $P = k_0 t$ (t is the time corresponding to the crank angle of 30°).

The acceleration of the piston displacement from one cylinder wall to the other is

$$\ddot{x}_p = \frac{P_1}{m_0} = \frac{k_0 t}{m_0}.$$

The piston velocity during slap is

$$\dot{x}_p = \int \frac{k_0 t}{m_0} dt = \frac{k_0}{m_0} \int t \, dt = \frac{k_0 t^2}{2 m_0} + C_1.$$

The piston travel is equal to the diametral gap

The values of the integration constants are obtained from the initial conditions for which t = 0, δ = 0. and V_t = 0 at the beginning of the motion, here $C'_1 = C_2 = 0$.

Thus, the piston travel velocity at the instant of impact is

where t is the time required for the piston to pass from one wall to the other, determined by the expression

The maximum normal force corresponding to a 30° CA is found to be as follows

Here λ = R/L (R is the crank radius and L is the length of the connecting rod)

p_e is the mean effective pressure;

F_p is the piston area.

The diametral gap δ between the piston and the liner, which is usually given for the cold diesel engine, appears in the formula for the determination of t. We must know the thermal gap when the diesel engine is in operation. Taking as an example, the fact that the liner wall temperature rises by an average of 100° C for a 100% load, and the

temperature of the piston trunk rises to 170° C, we find the gap in the heated state.

The diameter of the liner during heating increases by

$$\delta_1 = D_{cy} (100 - 20) \alpha_{li}$$

where α_{li} is the coefficient of the temperature expansion of the liner.

The diametral gap between the piston and the liner will be as follows when the diesel engine is in the heated state:

$$\delta = \delta_x + \delta_1 - \delta_p$$

where δ_x is the diametral gap in the cold state.

Table 6 gives gap values for working diesel engines.

The reduced liner masses are determined based on formula (2.5). The values of the reduced masses are given in Table 7 for several diesel engines. We next find P_{max}, t, and v, whose values are given in Table 8.

The maximum deflections when acted on by a statically applied force P_{max} are determined on the basis of conclusions made by Yu. A. Shimanskiy [37],

$$A_{st} = P_{max}/k_{re},$$

where $k_{re} = \omega^2 M_{re}$ is the reduced stiffness of the liner.

Calculations of A_{st} are shown in Table 9.

To obtain the amplitude of accelerations of cylinder liner vibrations, let us use the expression

$$A_{max} = A_{st} K_d \qquad [d = \text{dynamicity}].$$

Here A_{max} is the maximum deflection of the liner acted on by force

$$P = P_{max} t/T;$$

$A = A_{max} - A_{st}$ is the amplitude of the vibrations; and

$K_d = 1 + \tau / \pi T$ (T is the time during which the normal force rises from 0 to P_{max}).

Table 6. Table of Values for Calculating the Thermal Gap Between Piston and Liner

1	2	3			4	5	6
7	85	0,1	10	22	0,063	0,28	0,2
8	105	0,15/0,2	10	[illegible]	0,04	0,157/0,33	0,08/0,27
9	120	0,1	10	16	0,096	0,18	0,32
10	[illegible]	0,5	12	[illegible]	0,11	0,215	0,33
11	[illegible]	0,8	12	11	0,173	0,155	0,37
12	230	0,6	10	11	0,181	0,185	0,3
13	[illegible]	[illegible]	12	[illegible]	[illegible]	0,33	0,26

14 [illegible]

KEY: 1 - Diesel engine model
2 - D_{cy} in mm
3 - δ_K in mm
4 - δ_i in mm
5 - δ_p in mm
6 - δ in mm
7 - Ch 8.5/11
8 - Ch 10.5/13
9 - Ch 12/14
10 - Ch 15/18
11 - Ch 18/20
12 - Ch 23/30
13 - D 23/30
14 - Note. The numerator corresponds to a cast iron piston, and the denominator -- to an aluminum piston for Ch 10.5/13 diesel engines.

Table 7. Determination of the Reduced Masses of Liners in Several Diesel Engines

1	2	2	3	4	5	6	5	5		7
8 [illegible]	[illegible]	[illegible]	[illegible]	7	110	[illegible]	7,5	[illegible]	[illegible]	[illegible]
9 [illegible]	[illegible]	[illegible]	6,5	7	[illegible]	[illegible]	9,0	76	[illegible]	[illegible]
10 [illegible]	64	[illegible]	8,[illegible]	7	110	[illegible]	9,5	61,5	0,8	[illegible]
11 [illegible]	[illegible]	[illegible]	6,5	[illegible]	150	71	12	83	[illegible]	[illegible]
12 [illegible]	93	[illegible]	6,9	[illegible]	[illegible]	[illegible]	13,5	95,5	[illegible]	[illegible]
13 [illegible]	[illegible]	[illegible]	15,25	7	[illegible]	[illegible]	20	[illegible]	[illegible]	1,2[illegible]
14 [illegible]	121,5	[illegible]	13	[illegible]	[illegible]	[illegible]	20	225	[illegible]	1,7[illegible]

KEY: 1 - Diesel engine model
2 - in mm
3 - in kg/mm^3
4 - in kg/mm^2 · 10^{-6}
5 - in mm
6 - c_0 in mm
7 - M_{red} in kg·sec^2 · m
8 - Ch 8.5/11
9 - Ch 10.5/13
10 - Ch 12/14
11 - Ch 15/18
12 - Ch 18/20
13 - Ch 23/30
14 - D 23/30

The final calculated value of the vibrational acceleration of a cylinder liner in diesel engines is determined by the expression

$$W_{cal} = A(2\pi f_{fr})^2 \text{ Hz} \qquad [\text{cal} = \text{calculated}].$$

Calculated and experimental values of the accelerations for cylinder liner vibrations in several diesel engines are listed in Table 0.

The calculated maximum amplitudes and accelerations of free vibrations of cylinder liners acted on by normal force P agrees quite closely for several diesel engines with the actually measured quantities. Some

imprecision in the calculated and experimental data is due to certain assumptions that were made in the calculations. They include the following:

1) in determining the maximum dynamic deflection it was assumed that the force P acting via the piston against the liner varies from zero to its maximum when the piston is pressed against one of the sides of the cylinder liner, though this actually is not always so; and

2) the greatest deflections of the cylinder liner from the dynamic and static action of the normal force P will occur at the location corresponding to the position of the piston wristpin axis for a crank angle of 30°, that is, when the force reaches the maximum P_{max}. However, in various diesel engines the side force reaches its maximum for crank angles somewhat different from 30°, and the angle depends on design factors.

Table 8. Calculation of P_{max}, t, and v for Several Diesel Engines

1		2	3	4	5	6	7	8	9	10
11 [illegible]	[illegible]	1,81	[illegible]	136	1/[illegible]	5,7	0,17	0,[illegible]2	0,00153	0,392
12 [illegible]	[illegible]	[illegible]	[illegible]3	510	1/[illegible]	9,[illegible]	0,[illegible] / 0,21[illegible]	0,0[illegible]8 / 0,027	0,0[illegible] / 0,0016	0,19 / 0,[illegible]
13 [illegible]	[illegible]	[illegible]	116	[illegible]	1/[illegible]	12	[illegible]	0,052	0,0019	0,492
14 [illegible]	[illegible]	1,72	17[illegible]	[illegible]	1/[illegible]	18,9	[illegible]	0,033	0,0[illegible]187	0,5[illegible]
15 [illegible]	0,2[illegible]	[illegible]	[illegible]	[illegible]	1/[illegible]	[illegible]	[illegible]	[illegible]	0,0017	0,555
16 [illegible]	0,26[illegible]	5,1	415	161	1/200	52,2	2,54	0,[illegible]3	0,0024	0,38
17 [illegible]	[illegible]2,8	5,[illegible]	[illegible]	[illegible]	1/17[illegible]	[illegible]	[illegible]	0,025	0,003	0,273

[Key to Table 8 is on the next page]

KEY:

1 - Diesel engine model
2 - P_e in kt/cm^2
3 - F_p in cm^2
4 - P_{max} in kg
5 - t_1 in sec
6 - k_0 in kg/sec$\cdot 10^4$
77 - m_0 in kg/sec
8 - δ in cm
9 - T in sec
10 - v in cm/sec
11 - Ch 8.5/11
12 - Ch 10.5/13
13 - Ch 12/14
14 - Ch 15/18
15 - Ch 18/20
16 - Ch 23/30
17 - D 23/30

Table 9. Calculation of Static Deflection of Liner When Acted on by a Force

Тип дизеля 1	2	3	$n_1=2$, $m=1$	$n_1=3$, $m=1$	$n_1=2$, $m=1$	$n_1=3$, $m=1$	$n_1=2$, $m=1$	$n_1=2$, $m=1$
			4		5		6	
7 Ч8,5/11	140	0,065	8,25	15,1	9,41	15,6	0,0132	0,0125
8 Ч10,5/13	310	0,17	8,1	15,7	11,2	41,6	0,27	0,0074
9 Ч12/14	400	0,192	8,29	15,6	13,9	46,7	0,0303	0,0085
10 Ч15/18	630	0,29	7,75	11,3	17,3	37,1	0,0364	0,017
11 Ч18/20	1570	0,592	6,53	6,91	14,75	18,7	0,1065	0,084
12 Ч23/30	1650	1,24	3,65	7,54	16,5	61,4	0,0975	0,0262
13 Д23/30	1550	1,79	3,83	8,25	26,3	123,2	0,0526	0,0115

[Key to Table 9 is on the next page]

KEY: 1 - Diesel engine model
2 - p_{max} in kg
3 - M_{red} in $kg \cdot sec^2 \cdot M$
4 - ω_{red} in $sec^{-2} \cdot 10^3$
5 - k_{red} in $kg \cdot 10^6$
6 - A_3 in mm
7 - Ch 8.5/11
8 - Ch 10.5/13
9 - Ch 12/14
10 - Ch 15/18
11 - Ch 18/20
12 - Ch 23/30
13 - D 23/30

In spite of these assumptions, this method of calculation makes it possible to obtain a theoretical estimate of the vibrational field of a cylinder liner. This estimate, in turn, when combined with data on the extent of damage as a function of vibrational field intensity, enables us to formulate a method for calculating cavitation damage to cylinder liners in diesel engines.

9. Values of Accelerations Beyond Which Intensive Cavitation Corrosion Begins

Analysis of damage caused by cavitation in diesel engines of various models operating in various climatic zones and different situations showed that diesel engines with increased vibrational levels are most subject to damage and breakdown. Diesel engines with low vibrational levels are less subject to erosion damage. The vibrational level depends not only on the design execution of the diesel engine, but also on the operating regime. The poorest conditions involve operating in idle,

Table 10. Calculated Amplitudes and Accelerations of Liner Vibrations in Diesel Engines and Their Experimental Values

1		2	3	4	5	6	7	8	9
		z_1 2; m 1							
		z_1 3; m 1							
	T		0,[illegible]	[illegible]	0,0029	0,0045	0,007	[illegible]	[illegible]
		z_1 2; m 1	0,150	[illegible]	[illegible]	0,13	[illegible]	[illegible]	0,173
10	$\frac{T}{3T}$	z_1 3; m 1	[illegible]	[illegible]	[illegible]	0,095	0,101	0,117	[illegible]
		z_1 2; m 1	1,150	[illegible]	[illegible]	1,148	1,161	[illegible]	1,171
	P	z_1 3; m 1	[illegible]	[illegible]	1,00	1,095	1,101	1,117	[illegible]
		z_1 2; m 1	[illegible]	[illegible]	[illegible]	0,91	0,1263	[illegible]	[illegible]
	A_{max}	z_1 3; m 1	0,0132	0,008 / 0,00795	0,009	0,018	0,097	0,029	0,012
		z_1 2; m 1	0,0142	0,027	0,03	0,036	0,1063	0,035	0,052
	A_{cp}	m 1, z_1 3	[illegible]	[illegible]	[illegible]	0,017	[illegible]	0,026	0,011
10	A	z_1 2; m 1	0,0078	[illegible]	[illegible]	0,005	0,02	[illegible]	0,009
		z_1 3; m 1	[illegible]	[illegible]	[illegible]	[illegible]	[illegible]	[illegible]	[illegible]
	ω	z_1 2; m 1	[illegible]	36 27	29	30	[illegible]	39	15
		z_1 3; m 1	25	18 13	15	26	65	15	6
11	A		0,008	0,001		0,0017			0,01
	ω		45	17		38			12,6

[Key to Table 10 is on the next page]

KEY: 1 - Calculated and experimental data
2 - Diesel engine model
3 - Ch 8.5/11
4 - Ch 10.5/13
5 - Ch 12/14
6 - Ch 15/18
7 - Ch 18/20
8 - Ch 23/30
9 - D 23/30
10 - Calculated values
11 - Experimental values

with low cooling temperatures, and with frequent load changes. Therefore, under otherwise equal conditions diesel engines operating in these regimes begin to be damaged by cavitation earlier.

As an example, Figure 21 a, b, and c present photographs of cylinder liners of a diesel engine after 1000 hours of operation with various vibrational characteristics.

Figure 21a shows the cylinder liner with initial stages of damage at a surface in the connecting rod rocking plane. The depth of the cavitation pits over a small area is 0.2 - 0.3 mm. Specific damage areas amount to 0.05 g/cm^2. The thickness of the liner wall is 7 mm. The thermal gap between the piston and the liner is 0.32 mm.

The cylinder liner in Figure 21b also served in a diesel engine for 1000 hours with 30 g vibra[illegible]s. The pit depth is 1.6 mm. The area of damage is much greater than in the liner that had operated with 25 g vibration. Specific damage amounts to 0.45 g/cm^2 and the liner wall thickness is 6.5 mm. The thermal gap is 0.45 mm.

Much greater damage is obtained for a cylinder liner of a diesel operating for 1000 hours with 40 g vibration, (Figure 21c). The damage extended to a greater area along the height of the liner. The pit depth was 2.5 - 3 mm. The specific damage was 0.98 g/cm^2.

These results graphically show the intensified damage for the same operating time when there are different levels of cylinder liner vibration in a diesel engine.

It was experimentally established that up to 18 - 20 g accelerations of vibrational motion of cylinder liners processes of erosion damage occur slowly and do not cause dangers with respect to damage, since the erosion damage time is longer than the cylinder wear time. Under these conditions a cylinder liner can serve for 5000 - 6000 hours. If the accelerations of the liner vibrations exceed 20 g, the processes occur more intensively. At accelerations of 35 - 40 g, marked damage begins already after 300 - 400 hours of operation, and in 2000 - 2500 hours of operation the liner must be replaced because of erosion damage to the maximum allowable values.

Thus, experimental data on the accelerations of vibrations beyond which corrosion damage processes begin to be intensified agree with theoretical data.

It must be considered that under otherwise equal conditions, a 20 g acceleration is the critical acceleration of vibrations.

Figure 22 presents generalized data on the damage to the surfaces of liners swept by water, as a function of the operating time and the vibrational level, enabling us to make an estimate of how much time for a given vibrational regime will elapse before damage of the extent we are

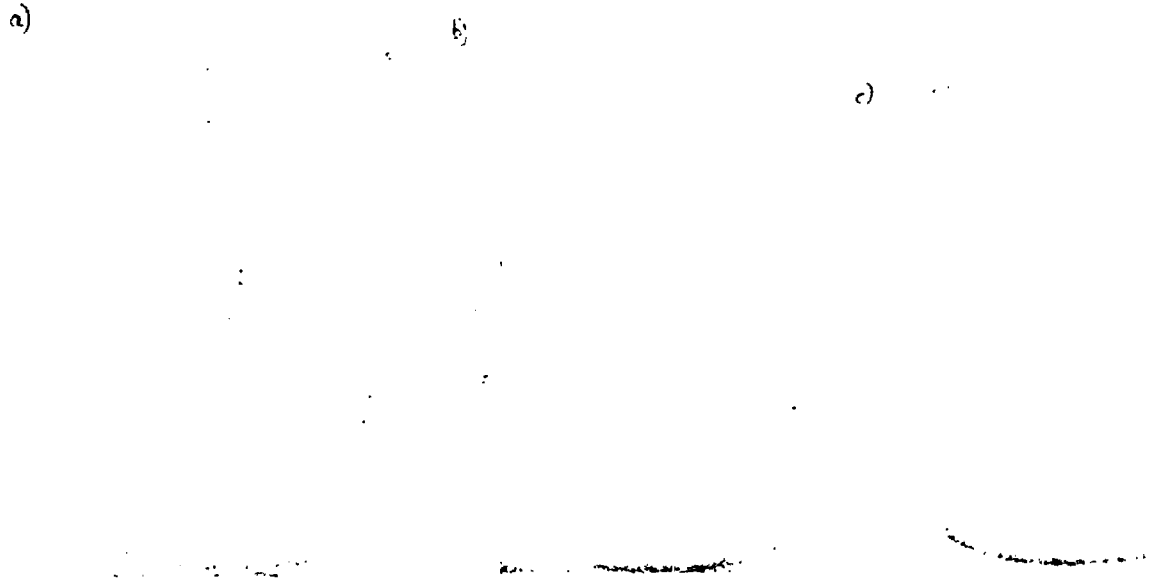

Figure 21. Cavitation Damage to Cylinder Liners of Diesels After 1000 Hours' Operation:

a - 25 g vibration b - 30 g vibration c - 40 g vibration

interested in wall appear. Several factors affecting the cavitation damage to surfaces were constant for the experimental points of the curves. The flow rate of the water was 0.5 m/sec. The water temperature was 40° C. The surface finish was ▽3.

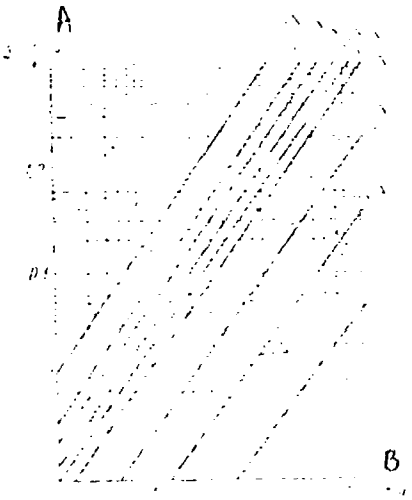

Figure 22. Weight Losses Δg of Samples of Materials (1) When Tested on Magnetostrictive Vibrators, and Samples of Liners (2) in Spent Diesel Engines as a Function of the Acceleration of Vibration W and the Operating Time

KEY: A - g/cm^2
B - t, hours

CHAPTER THREE

METHODS OF INVESTIGATING CAVITATION DAMAGE

10. Modern Methods of Investigating the Resistance of Specimens of Various Materials When They Undergo Cavitation Damage

The complexity of processes occurring in actual conditions when propellers, various kinds of hydraulic machines and devices, as well as

parts of diesels undergo cavitation damage hampers studies to find the effect particular factors have on the intensity of cavitation erosion and to find effective ways of controlling cavitation damage. In several cases pits on parts subjected to cavitation erosion appear after a relatively long operating time for the machine or mechanism. In these conditions studies on the phenomena occurring in cavitation erosion become very lengthy. Therefore several methods of accelerated investigation using various kinds of simulating stands were developed.

Methods of evaluating the cavitation resistance of materials include the following: the impact of a jet against rotating and fixed specimens; tests of the erosion resistance of materials in conditions of hydrodynamic cavitation at the specimen surface; study of the erosion resistance of materials for fixed specimens with circular vibratory exciters; and study of cavitation erosion with magnetostrictive vibrators.

Impact of jets against a rotating specimen. The sample is secured on the periphery of a rotating disc and in each revolution intersects a jet of water or wet steam perpendicular to the plane of the disk, (Figure 23).

A device of this kind is called an impact stand. Tests are conducted on it for different tip speeds of specimen revolution and for water jet diameters of 5 - 10 mm. In the papers [10, 38] the tests were conducted at a tip velocity of 78 m/sec. Increasing the tip velocity to 225 m/sec led to a significant acceleration of the damage process. It has been reported that at the present time tests are conducted at tip velocities up to 600 m/sec. These devices are most advantageous in studying erosion in steam and gas turbines since the conditions for specimen damage in

them are analogous to damage to turbine blades. These devices are unsuitable for investigations dealing with diesel engine parts since the process of cavitation damage in this case is not simulated with these devices.

Impact of jet against a fixed specimen. This method is analogous to the preceding technique in terms of the conditions of specimen damage and is most suitable for simulating damage to turbine blades. The study [36] presents results of tests made at jet velocities up to 600 m/sec, and the paper [33] presents the results of tests made at velocities up to 1050 m/sec, which led to intensifying the damage process. The device is shown schematically in Figure 24. This stand cannot be used to simulate damage processes in diesel engines since the kinetics of the process do not take account of the specific details of damage caused by cavitation in diesel engines.

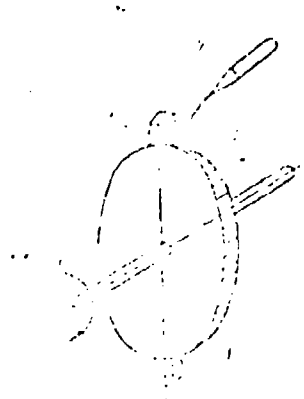

Figure 23. Stand with Rotating Specimens:

1 - Specimen 2 - Nozzle 3 - Water jet

Tests of the erosion resistance of materials in conditions of hydrodynamic cavitation at the surface of a specimen. Cavitation tubing and

nozzles are used for this purpose. Figure 25 shows one of the possible designs described in the studies [10, 30].

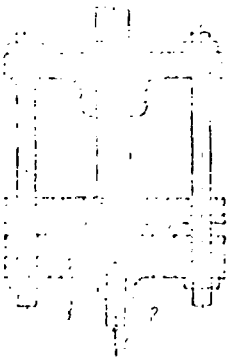

Figure 24. Stand With Fixed Specimen

1 - Specimen 2 - Nozzle 3 - Water inflow

The sharp decrease in the flow-through cross section in the nozzle causes a rise in the flow rate and a drop in the pressure in the flow down to a value leading to cavitation. The test specimen 2 is mounted in the diverging section of the nozzle where the pressure in the flow is increased and cavitation bubbles collapse. When this method is used, the process of cavitation erosion caused by hydrodynamic cavitation phenomena is simulated. A disadvantage of this method is that the time required to test each of the specimens proves to be relatively long.

Investigation of erosion resistance of materials with fixed specimens using a circular vibratory excitor. The stand (Figure 26) consists of a cylindrical beaker filled with water, with a barium titanide ring. When an alternating electrical field is applied to the surface of the ring, the volume of the ring changes in proportion to the frequency of the

field vibrations. Standing waves are formed in the liquid, which yield a greater amplitude of vibrations and greater pressures close to the plate at which the specimens are secured. Cavitation develops in the liquid, and the specimen is subjected to cavitation erosion. This is a relatively newly developed method [50, 51]; its use makes it possible to reproduce the erosion of a specimen that represents a fixed barrier in a hydro-acoustic field. The conditions for specimen failure with this test method approach the actual conditions in the cavitation erosion of cylinder liners if they are regarded as a fixed barrier. By this method rapid tests can be made in from several minutes to 2-3 hours. However, the device is cumbersome and inconvenient for testing a large number of specimens.

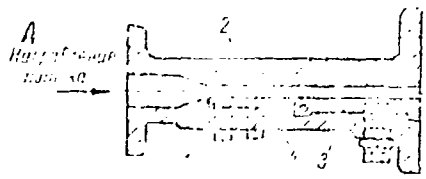

Figure 25. Scheme of Cavitation Nozzle:

1 - Set screw 2 - Cavitation zone 3 - Throttle 4 - Specimen

KEY: A - Flow direction

Investigation of cavitation erosion on magnetostrictive vibrators. Essentially, this method consists in securing the test specimen on the end of a nickel tube (or concentrator), immersed in the working liquid, where the nickel tube executes longitudinal vibrations at frequencies from 5000-25,000 Hz and higher with different amplitudes (Figure 27).

The vibrations of the rod or concentrator occur under the action of a variable magnetic field produced by the excitation winding. The tests of the cavitation erosion of materials with magnetostrictive vibrators (MSV) are of interest due to their identity of the processes with those occurring for cylinder liners of diesel engines, and also owing to the rapidity and possibility of conducting tests with variations made in parameters such as temperature, viscosity, and flow rate of the medium. Use of these instruments makes it possible also to conduct investigations at various accelerations, amplitudes, velocities, and frequencies of vibrations, that is, for different values of the number $S_c = vf/g$, and variations in several other parameters.

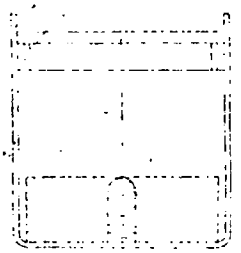

Figure 26. Scheme of Device With Circular Excitor:

1 - Beaker 2 - $BaTiO_3$ ring 3 - Plate 4 - Specimen

The specimen test time is limited to minutes or hours, and the erosion damage to material is estimated from the difference in the weight before the experiment and the weight after the experiment, and also based on the depth of cavitation pits. A small amount of water and low power levels not exceeding 2.5-4 kw are required for the tests. This method

is described in a number of sources [30, 35]. This apparatus with various ranges of excitation frequencies was used by the authors for rapid investigations of the cavitation erosions suffered by materials of cylinder liners and blocks in diesel engines.

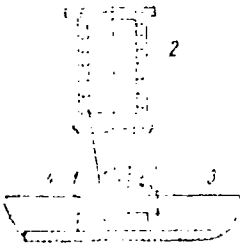

Figure 27. Scheme of Magnetostrictive Vibrator (MSV):

1 - Vibrating specimen 2 - MSV 3 - Water 4 - Fixed specimen

From a brief description of the various methods of rapid laboratory tests it follows that in the first two cavitation erosion occurs directly due to the impact of a jet or droplets into which the jet breaks up. This quite precisely simulates the damage to blades of steam and gas turbines and does not correspond to damage conditions in diesel engines. Thus, these two methods are unsuitable in investigating cavitation erosion in diesel engines.

The next three methods each simulates the individual processes occurring in the cavitation damage in diesel engines in their own individual ways. However, the last method (the method of investigation based on MSV) makes it possible to study the process with the greatest approximation to the damage conditions in diesel engines as various parameters are varied, with the minimum outlay of time. Therefore in addition

to full-size tests, it has found the greatest application in research.

The question arises as to whether it is possible to compare the results of testing the resistance of materials obtained on the various stands. Several investigators have made comparisons of this kind. For example, De Haller, and later Mousson [49], after comparing damage to a sizeable number of various metals on the impact stand and in the cavitation tubing, concluded that when tested by both methods materials are ranked in the same order in terms of erosion resistance. S. A. Keller reached similar conclusions based on results of tests made with the jet technique and with the magnetostrictive vibrator.

L. A. Glikman [10] has reported on the analogy of the comparison of test results with the MSV and with the impact stand for specimens of various steels, cast irons, brasses, and bronzes. However, it must be noted that when cavitation erosion occurs, in several cases, mechanical (playing the fundamental role) as well as electrochemical factors participate in metal damage; the electrochemical factors evidently do not occur when specimens are tested for erosion resistance on the jet impact stands. Therefore it must be noted that when comparative tests are conducted carefully (in various conditions and media) using devices that differ, such as those described earlier, a difference can be detected in the nature and intensity of damage to the test specimens.

Mechanical factors are paramount in specimen damage. Therefore in making a comparison of the results of tests made with the various methods, the authors obtained the identical sequence of the ranking of test materials by corrosion resistance, in all cases.

In estimating resistance to cavitation erosion for a particular material, one must also take account of the intensity of cavitation processes. Material that is resistant to erosion at a certain level of cavitation intensity can prove not to be resistant when the intensity is increased.

In the study [35] it was shown that the degree of damage to a specimen secured to a concentrator rises with increase in the vibrational accelerations produced with different amplitudes and frequencies. However, there are certain threshold accelerations and amplitudes up to which specimen damage is not observed.

The presence of threshold amplitudes is accounted for by the fact that even for high levels of accelerations of the vibrational process in the liquid and at very low amplitudes, the tensile stresses required to form cavitation bubbles are not induced. This becomes especially sensitive when the damage to a fixed specimen placed in a liquid at some distance from a vibrating specimen secured on the MSV is investigated. This specimen, acting as a shield, simulates the wall of a cylinder block. Here it was concluded that the intensity of damage to the fixed specimen increases with the velocity of the vibrational process. In studies made of the resistance of materials and different coatings using the MSV, comparable (qualitatively and quantitatively) results can be most clearly obtained.

11. MSV for Cavitation Damage Tests

The vibrational spectra of diesel engine parts subjected to cavitation damage lie in the broad range of frequencies from 5 to 10,000 Hz. The

most intense tonal components of the vibration exceeding the critical accelerations as a rule lie in a narrower frequency range from 800 to 8000 Hz, and for certain diesel engines they are situated in various spectral regions, related to the design and dynamic parameters of each specific diesel engine. Therefore, in rapid tests made of samples of materials or coatings, it becomes necessary to conduct the tests in different frequency spectrum ranges, including the higher region of vibrations than is emitted by the diesel engine, that is, with different MSV.

Vibrations of a test material specimen on the MSV are produced due to the magnetostriction effect. This effect consists of elongation and compression strains being induced in a rod of a ferromagnetic material placed in a variable magnetic field oriented along the rod. The strains as functions of the magnetic field have been studied and discussed in close detail in the literature. The magnetostriction effect depends on temperature. It decreases with increase in temperature, so the MSV stacks are water-cooled.

The amplitudes of MSV vibrations when it is excited at the fundamental frequency are of the order of 10^{-4} l_s (l_s is the length of the stack). The highest frequency at which relatively intense vibrations can still be excited is 60 kHz.

In building the MSV, only those materials that in addition to a well-pronounced magnetostrictive effect, also have high mechanical strength can be used. Pure nickel has proven itself particularly excellent as well as the alloy Permendur, consisting of 2% vanadium, 49% iron and 49% cobalt.

A sheet made of Permendur alloy is the most suitable in fabricating MSV for practical use in the laboratory. The MSV consists of a stack (rod) fabricated of Permendur, an electrical winding of a conductor in a moisture-resistant braiding, and a concentrator. The concentrator is needed to increase the amplitude of the vibrations of the MSV face, since the amplitude of the stack vibrations is negligible and does not exceed 5-20 μ.

When testing specimens of materials used for diesel engine parts, MSV of any frequency range can be built. MSV for 5, 10 and 20 kHz and several vibrators at intermediate frequencies have found the greatest use.

The overall dimensions of a MSV depend on the frequency of its vibrations. Thus, a 5 kHz MSV has a 380 mm long stack and a 570 mm long concentrator. A 10 kHz MSV has a 150 mm long stack and a 200 mm long concentrator, while a 20 kHz MSV has a 120 mm long stack and a 130 mm long concentrator.

The specimen of material to be subjected to failure at the threading can be mounted in the concentrator and immersed in water. In this case the conditions of damage to the vibrating surface are simulated.

A specimen clamped under the concentrator simulates the conditions of damage at a fixed surface.

MSV designed for 5-20 kHz encompass the entire range of vibrational spectra of diesel engine parts subjected to damage and with them conditions of damage observed in diesel engines can be reproduced.

Each MSV has its own amplitude characteristics, which is determined with optical instruments for MSV designed for up to 8 kHz. The frequency of vibrations is recorded with an audio generator, and the amplitude --

with a microscope, from the size of the blur of a calibration mark made with a diamond cutter on the lateral surface of the concentrator end.

The amplitude-frequency characteristic of MSV designed for above 8 kHz is measured with a vibro-measuring device. To record characteristics of MSV up to 10 kHz, A-3 vibrotransducers are suitable. Transducers built by the Bruel and Kjer Danish company are used in the higher frequency range.

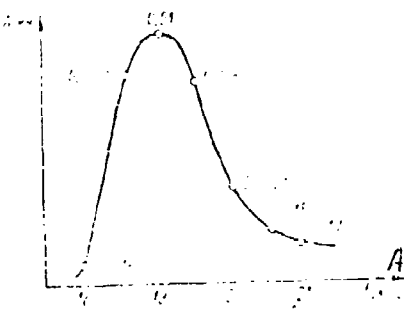

Figure 28. Amplitude-frequency Characteristic of a 19 kHz MSV

KEY: A - kHz

Figure 28 shows the amplitude-frequency characteristic of a 19 kHz MSV. The maximum amplitude of the vibrations for this MSV is at the frequency 19 kHz. However, tests with this vibrator, as with any other, can be conducted over a broader frequency range.

When conducting tests at a frequency differing from the resonance value, the test time is increased since the amplitude of the vibrations and the vibratory acceleration drop off.

Specimens of the test materials are placed in special baths in which the temperature of the medium and the pressure are measured in MSV tests.

A study of damage can be carried out either on the vibrating specimen or else on a fixed specimen placed under the concentrator of MSV.

12. Calculation of MSV Components Necessary for Experiments

A MSV, by transmitting elastic mechanical vibrations of acoustic or ultrasonic frequency (from the location of their generator) to the point of application (specimen undergoing damage) is the main component of the device. The calculation of oscillatory system components is made based on the methods outlined in the study [4]. As a result of calculation for a MSV with a specified vibration frequency, the amplitude of the stack vibrations is determined, along with stack cross section, number of turns and the cross section of the turns of the excitation winding. However, we know that to obtain an amplitude of stack vibrations greater than 20 μm is not possible for appropriate stack dimensions. Increasing the amplitude of the vibrations at a given frequency can be achieved by using transformers of the longitudinal elastic vibrations. Sometimes they are called vibration concentrators. Their function is to increase the amplitude of the vibrations to the required value, exceeding the amplitude of the vibrations of the end of the MSV stack by several times. Increasing the amplitude of vibrations at a given frequency leads to an increase in the vibration accelerations and to higher intensity of the damage of the test specimens.

The increase in the amplitude at the end of the concentrator is characterized by the transformation factor N. This factor is determined by

the ratio of the diameters (for the case of a cylindrical concentrator) of the input face d'_0, which is large in cross section, connected to the MSV stack, to the output face d'_1, which bears directly the material specimen undergoing damage,

The gain factor increases linearly, for an exponential concentrator, with increase in the ratio of the input to the output dimensions. The exponential concentrator is calculated in the following sequence. The translation factor is determined from the assigned diameters d'_0 and d'_1. Thus, for the concentrated use in a 20 hKz MSV bearing a stack with an 80 x 80 mm^2 cross section and for a 30 mm diameter damage specimen, N is 80/30 = 2.66.

Based on N, one determines the length of the concentrator using the following formula

[illegible]

where c is the speed of sound in the metal, which is $5.1 \cdot 10^5$ cm/sec; and

f is the resonance frequency of the MSV stack.

The length of a concentrator in a 20 kHz MSV, for a 30 mm diameter specimen, is 13.3 cm.

The following formula is used to calculate the exponent of the concentrator:

$$d'_x = d'_0 1^{-\beta x}_{con} ,$$

where d'_x is the diameter of the concentrator in the cross section

calculated by length; $\beta = \ln N/l_{con}$.

In the calculation we must divide the length of the concentrator into n sections (see Figure 30) and find for each section along the concentrator length the value of d'_x. The concentrator of a 20 kHz MSV is divided into 13 sections in the calculations. Thus, x varies in the calculations from 1 to 13.

When a concentrator is in operation, heat is released due to mechanical strains and the concentrator temperature rises. With increase in temperature, the vibration amplitude becomes smaller and the concentrator efficiency suffers. To eliminate this phenomenon, some of the concentrator together with the MSV stack is water-cooled.

The lower face of the cooling jacket is connected to the concentrator with soldering and welding and must necessarily lie in the node of the concentrator vibrations. Figure 29 shows the lower sleeve A of the cooling jacket made as one piece with the concentrator. The node of the vibrations for this concentrator lies (4.5 m [sic] from the face of the stack.

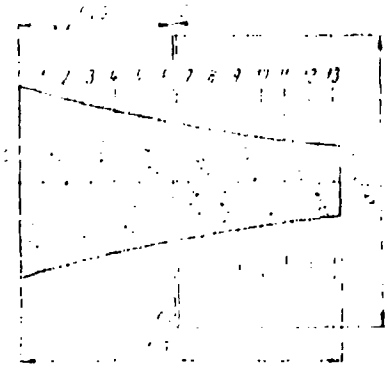

Figure 29. Concentrator for the Stack of a 20 kHz MSV

Using concentrators for any MSV stacks makes it possible to increase by two - five times the vibration amplitude, and to equally increase the vibration acceleration and significantly intensify the damage done to specimens of materials and coatings in accelerated tests using the MSV.

13. Determination By Calculation and Experimental Means of the Free-Vibration Frequencies of Test Specimens and Vibration Amplitudes with MSV

To conduct tests with the MSV, the weight and overall dimensions of specimens must be selected so that the adjustment frequency of the MSV stack and its concentrator do not change abruptly.

In practice it proves sufficient if the specimen diameter does not exceed 30-35 mm for a plate thickness of up to 4 mm. Usually round specimens 30 mm in diameter and 3 mm thick are used. Other specimen dimensions can also be used, but to estimate the intensity of specimen failure one must record the amplitude-frequency characteristic of the MSV together with the test specimen. It is desirable that the MSV-specimen system be selected so that the amplitude of the vibrations at the concentrator face with the specimen mounted on it is not reduced. This necessitates determining the free-vibration frequency of the test specimen and comparing it with the adjustment frequency of the MSV, which is achieved by the appropriate selection of specimen dimensions. The test specimen is a round plate bearing a threaded stem for mounting on the concentrator. From the paper [14] we have an expression for

calculating the free-vibration frequency of a plate with this kind of emplacement.

A round plate of radius R with mass per unit area μ_1 has the following free-vibration frequency:

$$\omega_{pl} \quad (26)$$

where a' is the coefficient that allows for the method of securing the plate;

$I =$ is the flexural stiffness of the plate ($E = 2.1 \cdot 10^6$ kg/cm^2 is the Young's modulus for steel, $E = 1.2 \cdot 10^6$ kg/cm^2 is the Young's modulus for cast iron, and for aluminum, $E = 0.7 \cdot 10^6$ kg/cm^2);

$\sigma \approx 0.3$, Poisson's ratio for steel, $\sigma = 0.25$ for cast iron, and for aluminum, $\sigma = 0.34$; h is the plate thickness); and

$\mu_1 = \gamma h/g$ (here γ is the specific weight of the material, g is the acceleration due to gravity).

The coefficient α' has various values, depending on the methods of mounting and the types of vibrations. When mounted in the center with the edges free and when the form of the vibrations is umbrella-shaped, a' = 3.75. When mounted in the center with three edges and with the vibrations in the form of two perpendicular nodal diameters, a' = 5.25. When a specimen is mounted in the center with its edges free and when the vibrations are in the form of a unimodal circle, a' = 9.07.

The free-vibration frequencies of specimens 30 mm in diameter and 3 mm in thickness, made of various materials, when a' = 3.75, are as follows:

Specimen Material	Frequency of Vibrations of the First Form in Hz
Steel	12,700
Aluminum	12,500
Cast Iron	9,550

In practice, the value of a' is selected in each specific case in relation to the kind of mounting. The effect of specimen mounting is checked on calibration or magnetostriction stands.

To estimate the error of calculating the free-vibration frequencies of specimens of different sizes, experiments can be conducted to determine them experimentally on vibratory audio-frequency range calibration stands. A VK-ID model stand, which has a working frequency range of 50-15,000 Hz, can be recommended.

Fine quartz sand is used for the visual determination of the instant of resonance-onset, and the resonance frequency is recorded with an audio-generator.

The experimental verification of the free-vibration frequencies of specimens shows that the error in their calculated determination does not exceed 5%.

Since studies on cavitation damage of specimens can be conducted with various MSV, with resonance frequencies of 5000, 10,000, 12,000, 19,000, and 20,000 Hz, and therefore, with various vibration amplitudes, one must find the amplitudes of specimen vibrations for each MSV. They are determined in the frequency range to 10,000 Hz by an acoustic method using instruments of the type IVPSh, PIU, and so on, and in the higher

frequency range -- by an optical technique using special microscopes. The amplitude characteristics of stacks are recorded as a function of the output indicators of the amplifiers to determine the vibration amplitudes by the optical method.

14. Results of Testing Specimens of Various Materials for Cavitation Damage

MSV are widely used by various authors to determine the effect of numerous factors on cavitation damage in vibrating and fixed specimens. Properties of the material, effect of the medium, vibration characteristics, and other parameters on cavitation damage are studied. Since the MSV used for these purposes produce significantly more intense vibrational fields than the vibrational fields of diesel engines, the damage processes of the test specimens take place very rapidly. Detectable damage sufficient to estimate their extent begins even in 0.1-3 hours. As an example, in Figures 30-32 are shown photographs of specimens of some materials used in diesel engine construction after several hours of testing. Damage pits can be clearly seen on the specimens, as deep as 1.7 mm. The area of the surface of a specimen subjected to damage depends on the experimental conditions and the method of mounting the specimen. For all materials without exception, the extent of damage increases in proportion to the test time and vibration acceleration. The extent of damage is affected by the hardness and microstructure of the material, surface finish, temperature of the medium, viscosity, gas content of the liquid, and its impurity content, electroconductivity of the liquid, and other factors. A hyperbolic function is observed between the extent of damage to a specimen

(weight loss) and the test time (Figure 33). The weight loss of a materia specimen is characterized by the following function

$$\Delta G_x = a' \Delta G_0 S^{n1} (t_x/t_0)^k , \qquad (27)$$

where a' is a coefficient that depends on the specimen material;

ΔG_0 is the weight loss taken as the zero threshold (0.1 mg);

$S_c = W_p/g$ is a dimensionless coefficient characterizing vibration acceleration (W_p is the acceleration of vibrations of the concentrator face);

t_x is the specimen test time;

t_0 is the time taken as the zero threshold (1 min); and

n and k are exponents.

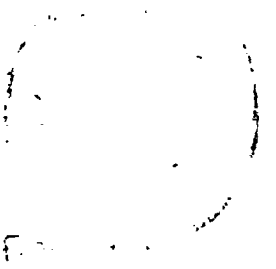

Figure 30. Specimen of AK 4 Material After 9 Hours of Testing on a MSV (Weight Loss 50 mg, Initial Weight 7.79 g, Final Weight 7.74 g)

Tests made on various construction materials used in diesel engine building for cylinder liners and cylinder blocks, using MSV, showed that the greatest weight losses in the same test time for the same vibration

acceleration and for other equal conditions are recorded for aluminum alloys. Then come cast iron and steel material. The least damage is found for specimens of material coated with opal and hard chromium.

Figure 31. Specimen of SCh Cast Iron After 14 Hours of Testing on a 12 kHz MSV

Figure 32. Specimen of 38KhMYuA Steel After 3 Hours Testing on a 10 kHz MSV

An analysis of experimental data showed that the ratios recorded for material damage agree with those of other experimentors investigating the damage of specimens at different times.

Adopting as unit damage the damage suffered by a specimen of 38 KhMYuA steel, given otherwise equal conditions the damage to a specimen

of gray cast iron SCh 24-48 will occur 6,8-7 times faster, and 10 times faster for an aluminum specimen, that is, an aluminum alloy is the least cavitation-resistant as we can see from the curves in Figure 33.

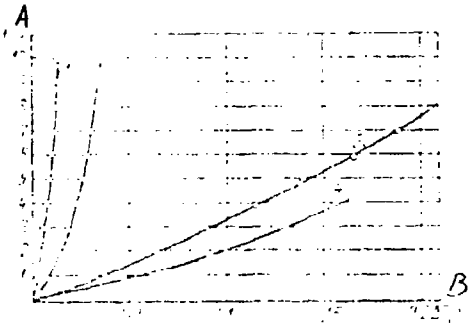

Figure 33. Damage to Specimens of Various Materials Determined a MSV:

1 - Steel coated with opal chromium 2 - 38 KMYuA steel 3 - SCh 24-44 [Text in paragraph gives 24-45] cast iron 4 - AK 4

KEY: A - t, hours
B - ΔG, g

From Figure 34 we see that after 3 hours' testing of steel specimens with different excitation frequencies and vibration amplitudes, the greatest damage resulted when maximum accelerations were applied.

In conducting tests of specimens on vibrators, it was noted that sometimes the progression of cavitation damage to specimens dies out after some time following the beginning of tests. This is associated with the change in the amplitude characteristic of the MSV, which is pencil-shaped. The maximum amplitudes are observed at the resonant frequencies. Thirty mm

specimens were selected for the test and they exhibited free-vibration frequencies in the range 7500-12,700 Hz, depending on the specimen thickness and its material. The free-vibration frequencies of the specimens depend on their thickness and mass.

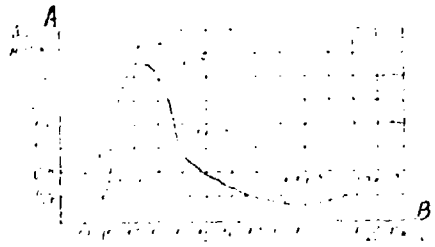

Figure 34. Damage to Steel Specimens at Constant Water Temperature as a Function of Various Accelerations (The Numerical Values Next to the Curve Stand for the Vibration Amplitude, in μm)

KEY: A - mg/cm^2
B - kHz

With increasing weight loss during the damage process, specimen thickness and mass change, which causes a change in the free-vibration frequency and shifts the system from the resonance zone into the lower-acceleration region. Here the damage rate is significantly slowed or halted altogether. Damage occurs more intensively in materials if the surface finish is reduced. Under otherwise equal conditions, a variation in surface finish from the second to the fifth class reduces the damage by 5-10%.

Thus, tests of specimens on the MSV permit an estimate of cavitation damage to a material specimen, in a very short time interval, under given

conditions, without conducting expensive and laborious tests in diesel engines.

15. Use of Data From MSV Tests of Specimens of Materials and Coatings to Determine the Cavitation Resistance of Cylinder Liners of Diesel Engines

We know that in diesel engines the process of cavitation damage develops over hundreds and thousands of hours. This process proceeds more intensively in diesel engines with high vibro-activity. Therefore it appears advantageous in the finishing of diesel engines to study phenomena of cavitation damage in conditions of the more intense course of the process, that is, on MSV.

Different values of MSV amplitude-frequency characteristics permit obtaining failure in specimens over several minutes or hours that are commensurable with damage in cylinder liners obtained in diesel engines over hundreds of hours.

Studies of the cavitation damage to material specimens on the MSV and diesel engine cylinder liners show that in either case the extent of the damage ΔG obeys the same law, which has the following form

$$\Delta G = a' S^{\alpha} n$$

where a' is a coefficient that depends only on the specimen material; and α and n are exponents.

Under this law one can calculate, approximately, what damage will occur in diesel engines for other values of vibrational acceleration

when the extent of damage to material specimens obtained on a MSV is known.

The damage ΔG will occur in the time interval t if the ratio of the acceleration of vibrational motion of the surface being damaged to the acceleration due to gravity is the quantity S_c.

Hence

$$t = \left(\frac{\Delta G}{a^{\alpha} S_c^{\alpha}} \right)^{\frac{1}{\alpha}}$$

to obtain the same damage ΔG but for a different ratio of the acceleration of the vibrational motion of a surface to the acceleration due to gravity, S_{c_1}, a different time interval is required:

$$t_1 = \left(\frac{\Delta G}{a^{\alpha} S_{c_1}^{\alpha}} \right)^{\frac{1}{\alpha}}.$$

From these expressions it follows that with increase in S_c, the time t during which the same extent of damage occurs will be shorter.

To compare the results of studying damage in various specimens of materials obtained with a MSV, with the results of tests made on diesel engine cylinder liners constructed of materials under comparison, it appeared necessary to establish the time required to obtain the same extent of damage for different accelerations. Knowing the ratio of these times is also necessary to estimate the results of accelerated tests of a diesel engine for cavitation erosion and to estimate its normal operating time until the onset of the same extent of damage as in accelerated tests. Here the time scale M is determined, approximately, by the relation:

$$M = \frac{t_1}{t} = \frac{\left(\frac{\Delta G}{a^{\alpha} S_{c_1}^{\alpha}} \right)^{\frac{1}{\alpha}}}{\left(\frac{\Delta G}{a^{\alpha} S_c^{\alpha}} \right)^{\frac{1}{\alpha}}} = \sqrt[\alpha]{\frac{S_c^{\alpha}}{S_{c_1}^{\alpha}}}. \qquad (28)$$

Studies showed that one can use the root $\gamma = 2$ for practical purposes, with adequate precision.

Therefore, the same extent of damage ΔG for the values S_c and S_{c1} characterizing the acceleration of the vibrational motion of surfaces will be obtained in the time t and t_1, which are found in a relationship as

[illegible] (29)

On establishing the mathematical dependence of the time factor for the same extent of damage as a function of the acceleration of vibrational motion, one must present the true values of the scale factor when working in different frequency ranges with different accelerations of vibrational motion.

Calculated and actual time scale data for the extent of damage ΔG = 100 mg = const are presented in Table 11.

The data in Table 11 show that the error in calculating the time scale in the range of working accelerations in diesel engines and in vibrators up to 1000 g does not exceed 10-12%, therefore formula (29) can be used for approximate calculations.

Thus, the results of cavitation tests of construction material specimens (aluminum alloys, steel, cast iron, and so on) on MSV can be reconverted to the operating conditions of diesel cylinder liners by using the appropriate scale.

Figure 35 presents the curve of the dependence of the extent of damage to a specimen of SCh 24-44 cast iron on the service time for tests made on a 12 kHz MSV at S_c = 5100 with a vibrational amplitude of 10 μm, and

Figure 36 shows the calculated service time of liners made of the same cast iron, for different accelerations. The agreement between the calculated and experimental data is satisfactory. In the same fashion all kinds of coatings, for example, damping, solid, and refractory coatings can be tested on HSV and be calculated for diesel engine performance.

Table 11. Calculated and Actual Time Scale Data

	1	2	3	4	5	6
				2.25	2.15	4.5
			10	3.32	2.3	4
				7	6	12
					9.5	7
				0.535	0.7	9.5
				0.111	0.105	5
				0.255	0.255	0
				0.78	0.8	2.5

7 [illegible]

1 - t_1 in hours

2 - t in hours

3 - t_{epx} in hours [exp = experimental]

4 - M_{cal} [cal = calculated]

5 - M_{ac} [ac = actual]

6 - Errors in per cent

7 - Remark. The following notation was adopted: t_{exp} is the actual experimental time; M_{cal} is the calculated scale factor; and M_{ac} is the experimental scale factor.

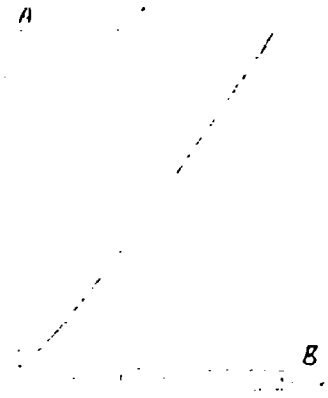

Figure 35. Failure of a SCh 24-44 Cast Iron Specimen on a 12 kHz MSV

KEY: A - t, hours

B - $\Delta g, g/cm^2$

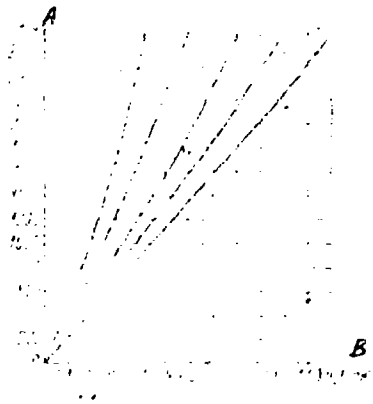

Figure 36. Calculated Weight Loss Curves of SCh 24-44 Cast Iron Liners When Serving in Diesel Engines With Different S_c Values: o o o -- Damage to a Cast Iron Liner of a Ch 10.5/13 Diesel Engine for Vibration With S_c - 20

KEY: A - t, hours ; B - Δ :, g/cm^2

16. Advantages and Disadvantages of Accelerated Specimen Test Methods

An advantage of accelerated tests of material specimens on MSV is the rapidity of the tests and the low outlays in conducting them. These tests provide comparable results for the extent of damage in the same construction material with respect to another. MSV tests make it possible to find how physicochemical properties of the liquid medium, its gas saturation, and several other factors affect failure. Satisfactory results are also provided by such tests in studying the resistance of hard and refractory coatings and also all kinds of elastic damping coatings applied on surfaces subject to failure. The results of these tests can serve as the basis for estimating the efficiency of a material or a coating in service conditions in a diesel engine.

The disadvantages of the accelerated test method must be regarded as the fact that it does not afford an estimate of efficiency over an extended time interval. As a result of MSV tests of additives for diesel engine coolant water, the relative effect of various additives on reducing damage is ascertained. However, MSV tests do not enter the question as to the serviceability of an additive in time, that is, its practical suitability. In actual experience it turns out that the additives that are most stable in time, that do not decompose into constituents, and that do not precipitate in 150-200 hours have the greatest effect on reducing cooling surface damage. Therefore one cannot judge the efficiency of additives from MSV tests since results contradicting actual data from diesel engine tests can be obtained.

MSV tests also do not permit a full estimation of the effect that mechanical, electrochemical and temperature factors have on the overall

damage of a surface, since the tests are conducted in the high-frequency range and at very high accelerations.

17. Acceleration Methods of Testing Diesel Engines for Cavitation Damage

Whereas in tests made of the cavitation damage of specimens on MSV it becomes possible to increase the vibratory field by tens and hundreds of times and thus to sharply intensify the process of specimen damage, in an actual diesel engine the cavitation damage process proceeds slowly -- takings hundreds and thousands of hours.

When studies were made on a diesel engine to select active agents protecting against cavitation erosion, to shorten the test time of each variant it often proves useful to intensify the cavitation processes, which is achieved by increasing the gap between the piston and the cylinder liner in order to raise the energy of piston impact against the liner, and this acceleration in testing is also achieved by running the diesel engine in regimes during which cavitation erosion is intensified. This makes it possible to intensify the process of damage to parts swept by water in the test diesel engine by several times and to reduce the test duration by an equal number of times.

By intensifying the damage process by fourfold, damage can be produced in 500 hours that is equivalent to the damage in a series-built diesel obtained after 2000 hours of operation.

To intensify the process of damage to cylinder liners in the Ch 15/18 diesel engine, one must triple the liner vibrational level, which is achieved by increasing the thermal gap between the piston and the liner by 0.25 mm.

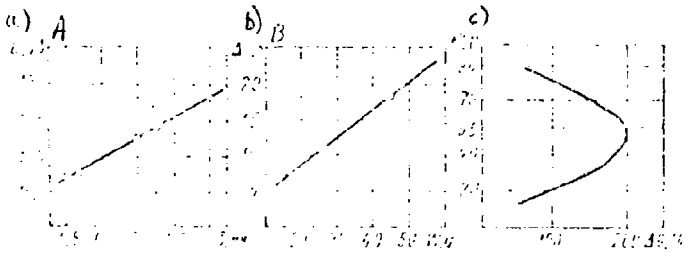

Figure 37. Dependence of Damage on Vibration and Temperature: a - Change in Vibration of Cylinder Liner of the Ch 15/18 Diesel on the Thermal Gap Between the Piston and the Liner; b - Increase in Weight Loss as a Function of Liner Vibration; c - Increase in Damage as a Function of Medium Temperature, for 1.05 atm Pressure in the Medium

KEY: A - L, db
B - Δ G, g

When the vibrational level of a liner is tripled, the rate of its cavitation damage increases by about twofold.

Operation of a diesel engine in the cooling temperature range 55-60° C as compared to 78-80° C with normal operating conditions also intensifies the failure process by a factor of 2.

Thus, a threefold increase in the liner vibrational level and operating the diesel engine in the cooling temperature range 55-60° C means a fourfold increase in the cavitation damage process, which in turn makes it possible to shorten the diesel engine test time by a factor of four.

Figure 37 presents functions characterizing the extent of acceleration of the cavitation damage process in accelerated testing. Figure 37a

shows the increase in liner vibration with increase in the thermal gap between the piston and the liner, and Figure 37b shows an increase in damage with a rise in vibrations. When vibrations are increased from 15 to 44 g, damage climbs by a factor of 2

Figure 37a shows the dependence of damage on cooling temperature. A temperature rise from 20 to 55° C increases damage by twofold. In tests on Ch 15/18 diesels and other models by the method of increasing the vibrational level and selecting the appropriate cooling temperature, the test time for each of the variants of diesel engine design considered for cavitation resistance can be appreciably shortened. These tests are accelerated and are conducted under a 500 hour program, instead of 2000-2200 hours.

To intensify the cavitation damage process by a higher factor, one must additionally increase the vibrational level of the surfaces being damaged by selecting the appropriate diesel engine operating regime, increasing the roughness of the surfaces undergoing damage to the second finish class, and cooling the diesel with an open cooling system, which increases the gas content in the water.

13. Visual Estimation of Cavitation Processes and the Initial Stage of Cavitation Damage in Diesel Engines

Estimating the extent of damage to surfaces swept with water, cylinder liners, and blocks of diesel engines is usually carried out after they have been run for a certain number of hours.

Diesel engines, both experimental as well as those operated in the national economy, run for different time intervals in different regimes. And this means changes in the vibratory fields of diesel engines, their cooling regime, and other parameters that can strongly affect the buildup of cavitation damage to surfaces.

The intensity of the vibration of a cylinder liner (of a specific diesel engine model) depends on its operating regime. As the load is increased, the side pressure force rises. Under otherwise equal conditions, this increases the rate at which the piston slaps from one cylinder wall to the other (with a change in the sign of the side pressure forces), and, therefore, the energy of its impact against the liner, but on the other hand, as the load goes up the temperature of the piston rises and the gap between it and the liner (especially for aluminum pistons) decreases Therefore the intensity of liner vibration can increase and decrease with rise in load, depending on the type of diesel engine.

One of the indirect characteristics by which one can evaluate the intensity of cavitation erosion to surfaces is the intensity of the vibratory field.

In evaluating damage based on vibrational parameters, naturally the effect of other parameters affecting surface erosion is not taken into account.

Transparent windows are built in the block for direct observation of the cavitation process in diesel engine cooling jackets (Figure 3). The windows are made of plexiglas. The configuration of the internal surfaces in the cooling system, when the windows are installed, must be kept unchanged.

Figure 38. Transparent Window in a Diesel Engine Block for Observation of the Stage of Cavitation Buildup

To estimate the first (initial) stage of cavitation damage, liners in a test block are coated with a thin layer of bakelite varnish with white nitro dye. This coating very rapidly breaks down when subjected to cavitation erosion and in 3-5 hours of operation dark pits are formed in the coating, which can be readily observed with the unaided eye.

Observing an operating diesel with an experimental block and transparent windows makes it possible to visually estimate the zone of inception of cavitation bubbles, their approximate size, the direction of motion, and importantly, to establish that the areas of a surface where a small volume of bubbles are formed, whose lifetime is very short, are subjected to damage.

It was found that cavities (bubbles) emerge along the vertical axis of the external surface of a liner, at the site of the vibration antinode.

Bubbles entrained by the liquid flow, whose diameter is not less than 0.2-0.4 mm, are observable. The time they spend within the limits of visibility is about 1 second. In addition to these, smaller bubbles coalescing into larger bubbles up to 3 mm in diameter are observed; these larger bubbles separate due to lift action, float upwards, and are entrained by the liquid flow. Also observable are the cloudy regions consisting of large numbers of very fine bubbles.

When the idling rpm of Ch 15/18 diesel engines is increased, a gradual rise in the size and the numbers of bubbles grouping into larger bubbles is visible. Then they are entrained by the water flow. Bubbles smaller than 0.5 mm in diameter are not observed, just as is the case for the cloudy regions.

By increasing the diesel engine load from 0 to 100%, that is 1500 rpm, we observed a reduction in the bubble size due to the buildup in the intensity of liner vibrations.

Even at a 75% load, the bubbles decrease down to dimensions which make them virtually invisible and they can be tracked only as individual persistent cloudy regions. Using the high-speed SKS-1M-16 motion picture camera, the lifetime of the largest bubbles of the cloudy regions was established, 0.001-0.003 sec. The bubbles appear and disappear on the spot.

Finer bubbles cannot be observed in the cloudy regions without special telephoto and high-speed motion picture cameras, since their dimensions and lifetimes are very small. The high-speed camera used can provide filming at the speed of 800-1200 frames per second; this can record the buildup

of a bubble with a lifetime of 0.01 sec.

The use of a special coating and its damage show that small cavities, in the form of cloudy regions, are the most dangerous. Pits in light coatings form most often in their vicinity.

Visual observation of bubble growth confirms that cavitation erosion in diesel engines occurs most intensively at the highest vibration levels and corresponds to the maximum speed and load operating conditions of diesel engines, and a cooling temperature in the range 50-60° C with the pressure in the cooling system at 1-1.1 atmospheres.

Observation of the buildup of visible bubbles during the diesel engine starting and warming period shows that as a diesel engine warms up the number of bubbles becomes smaller. However, the bubbles forming in these regimes are larger in size and virtually always surface and are swept away by the water flow without disintegrating at their inception sites.

A block fitted with transparent windows makes it possible to visually observe the buildup of separate bubbles as the vibratory field of different cylinders is increased, which can be varied by changing the thermal gap between piston and liner and also by changing the gap in the lower seating shoulder between the liner and the block.

Observation results show that as the vibrational level is increased, cavity size becomes smaller and failure proceeds more intensively.

19. Estimation of Cavitation Damage in Diesel Engine Cylinder Liners

Cylinder liners fail in the zones of vibration and antinodes. The most intense damage lies on the surface of a liner perpendicular to the rocking plane of a connecting rod from the side force location. Therefore

in investigations to find the methods by which to reduce the intensity of cavitation damage in liners, the extent of damage must be estimated for surfaces at which it is most intense. An estimation of the extent of damage based on weight loss, related to the weight of the intact liner, is highly inaccurate owing to the great difference in the values of the weight loss and the weight of the intact liner, and also due to the weight losses associated with wear.

Figure 39. Arrangement of Zones of Maximum Cavitation Damage in a Cylinder Liner:

1 - Connecting rod rocking plane

2 - Direction along which side force P acts

3 - Zone of greatest to external surface of liner

4 - Specimen

More exact is the excised specimen method. A specimen with damage areas is cut out of the surface perpendicular to the connecting rod rocking plane at the side along which the maximum side forces acts, and a control sample free of cavitation damage is cut out of any part of the

undamaged surface, for example, from the area of point B (Figure 39). Specimens taken from liners of a 6 Ch 15/18 diesel are shown in Figure 40.

For the damage to liners from different diesel engines to be comparable, the ratio of the specimen area to the external area of the liner is assumed constant and equal to 0.025. On this basis, one can obtain the true extent of specimen area S_x for a liner of any diesel engine:

$$S_x = xy,$$

where x is the size of the specimen along the circumference (Figure 39);

y is the size of the specimen along the height of the liner.

Since $S_x/S_l = 0.025$, is assumed [l = liner], and $S_l = \pi D_{ou} l$ (S_l is the outer surface of the liner), then

$$S_x = 0.025 \pi D_{ou} l \text{ cm}^2.$$

Thus, the absolute extent of damage is determined from the difference in weights of identical-size specimens cut from damaged and undamaged liner surfaces.

Cases of cavitation damage to cylinder liners are observed in which a limited number of pits (only several) appear in the damaged surface, but they rapidly increase in depth and cause the liner to malfunction, by forming continuous flaws. In all cases the total weight loss of a specimen can be small, therefore here an estimation of the intensity of cavitation damage must be made by measuring the pit depth.

The extent of damage in liners depends on the operating time,

acceleration or vibrations, the cooling temperature, the liner material, the finish of the damaged surface, the pressure in the cooling system and several other factors. The level of vibrations in the operating time of the liner affects damage most strongly. Figure 40 shows the curves of damage intensity in time as a function of the dimensionless quantity S_c. S_c characterizes the acceleration of vibration motion of a surface. From Figure 41 we see that depending on the acceleration, the same weight loss of a liner $\triangle G$ can be obtained in different times, and the shorter the time, the greater the vibration acceleration. For a vibration acceleration of 100 g, a 1 gram failure can be obtained in 110 hours of operation, and for a 500 g acceleration, even in 60 hours.

a) b)

Figure 40. Specimens from Liners of a 6 Ch 15/18 Diesel Engine: a - After Service in the Diesel Engine b - Before Service

Figure 42 shows the damage to liners at different vibration accelerations. Analysis of these data shows that the damage curves constitute a family of parabolas passing through the origin of coordinates and which

can be described by the equation

$$\Delta G = q t^{l},$$

where t is the operating time of the liner after which damage is determined;

q is the parameter characterizing the acceleration of liner vibrations; and

l is the exponent of the power function, dependent on vibration acceleration.

In its final form, the expression for estimating the damage in cylinder liners as a function of vibration acceleration, under otherwise equal conditions, is as follows:

$$\Delta G = 5 \cdot 10^{-5} \Delta G_{[illegible]} ([illegible])^{[illegible]} S_c^{[illegible]} \qquad g, \qquad (30)$$

Here t is the diesel engine operating time in hours;

α [illegible] is the exponent for S_c in the equation, in which the negative term corrects it for low S_c values not exceeding 60.

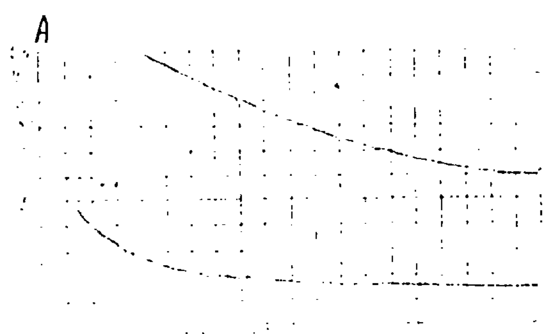

Figure 41. Dependence of Operating Time t Required to Produce the Same Extent of Damage for Different S_c:

1 - ΔG = 1 g   2 - ΔG = 0.1 g

KEY: A - t, hours

In estimating the extent of cavitation damage to liners one must allow for the kind of damage. Damage in cavitation is represented by cone-shaped pits with the apex directed downward in to the bulk of the metal. Experience has shown that if the pit depth is three-fourths of the thickness of the liner wall, cracks form in the liner extending through the damage craters and the diesel engine malfunctions. For example, for 6 Ch 15/18 diesel with 6 mm thick liners, a 52 gram weight loss of a liner specimen is the maximum. In this case the specific loss is 1.5 g/cm^2. At the same time, a specific loss of 0.08 g/cm^2 (absolute loss 3 g) is not dangerous since the pits have a negligible depth. Only clouded areas and opalescence colors are observed at the surface.

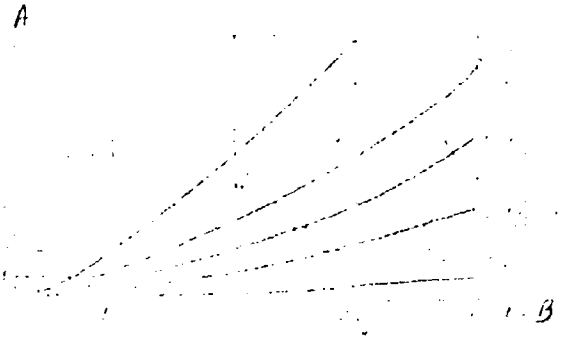

Figure 42. Cavitation Damage in Liners of Diesel Engines for Different Accelerations:

1 and 2 - Material specimen 3 - 5 - Diesel engine liners

KEY: A - ΔG, g
B - t, hours

The maximum allowable damage depends on the liner thickness and differs for different diesel engines. Figure 43 shows the coefficient ξ

characterizing the maximum allowable damage to cylinder liners of diesel engines as a function of wall thickness:

$$\xi = \frac{S}{\Delta G}, \tag{31}$$

where $S = S_x/S_0$ ($S_0 = 1$ cm^2, the area taken as a unit of damage);

$\Delta G = \Delta G_x/\Delta G_0$ (ΔG_x is the weight loss of a diesel engine cylinder liner; $\Delta G_0 = 10^{-3}$ kg, the weight loss taken as the zero threshold).

Where the case when only a few pits appear in liners subjected to cavitation damage, ξ must be determined with respect to the increase in pit depth.

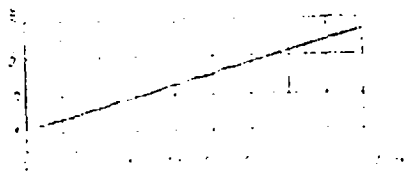

Fig. 43. Dependence of the coefficient ξ characterizing the maximum allowable damage to liners as a function of liner thickness h

CHAPTER FOUR

FACTORS AFFECTING THE INTENSITY OF CAVITATION DAMAGE IN DIESEL ENGINES

20: Intensity of Liner Vibrations and the Effect of Design Factors

The fundamental source of cavitation erosion in liners and blocks of diesel engines is the high-frequency vibrations of these cylinder liners caused by piston impact passing from one cylinder wall to the other near the top dead center as the sign of the side pressure force changes. Slap is caused by the presence of a gap between it and the cylinder liner. Thus, the smaller this gap the lower the impact energy of the piston against the cylinder wall. A significant reduction in the gap in the cylinder - piston group is a difficult task since a piston, allowing for thermal and mechanical strains arising as the load operating regime of a diesel engine is varied, must have a carefully profiled shape, that is, an oval, in cross section, and barrel-shaped, heightwise. A further decrease in the gap between the liner and the piston leads to scoring.

The size of this gap depends on the piston material (the coefficient of linear expansion), the level of diesel engine uprating, the design dimensions of the piston, its configuration, and so on.

The energy of the piston impact against the liner wall is determined by the velocity that the piston has in the transverse direction (slap) and by its mass. The piston velocity at the instant of encountering the liner wall will rise with increase in the gap in the piston-liner pair and with rise in the side pressure force (allowing for the gas and inertial forces acting on the piston).

The striking of a piston against its liner causes a "burst" of its vibrations with a wide spread of values. Analysis of oscillograms shows that the beginning of these intensified vibrations lags behind the instant of change in the sign of these side pressure forces in the piston mechanism by the time needed for the piston to travel within the gap limits from one cylinder wall to the other, and the recorded liner vibrations are caused by piston impact and not by strains produced by gaseous forces or other factors.

From an inspection of the oscillograms of liner vibrations we see that in most cases a liner vibrates together with the piston pressed against it. But in individual cases (but especially when the spread of vibration values is large), accelerations of vibrational motion prove to be so large that the inertial forces induced in the transverse direction exceed the force of the piston side pressure against the cylinder wall, resulting in the piston rebounding and then reimpacting against the cylinder wall. This can be seen from the breaks in the vibration peaks on oscillograms. During the period of these intensified vibrations, which constitute natural vibrations of the elastic wall of the liner with the piston pressed against it, which can be regarded as vibrations of an elastic rod with an attached concentrated mass, the accelerations of vibrational motion at a frequency in the range 900-2000 Hz. exceeds by tens of times the acceleration due to gravity, G. This vibrational process then is the main source of cavitation in a diesel engine.

As shown by experiments, the 25% increase in the gap leads to a 2.5 to 3.5 db increase in vibrations for a number of diesel engines, and a 50% gap increase leads to a 5 to 6 decibel increase. Tests

on a 4CH10.5/13 diesel engine showed that a 50% gap increased to an appreciable rise in vibrations in the high-frequency range.

An increase in the piston mass with the gap in the piston-liner pair and the side pressure forces kept constant leads to a rise in the energy of the impact and to a higher intensity of liner wall vibrations. Here one must take account of the fact that an increase in the piston mass leads to a rise in the inertial forces directed in the opposite direction of the gaseous forces, and to a decrease in the side pressure forces. This decrease in the side pressure forces leads to the velocity of piston transverse motion from one cylinder wall to another dropping off. To a large extent, this compensates for the increase in the piston mass in the resulting energy of the impact against the liner in the vicinity of TDC.

Table 12: Changes in Vibrations in a 1Ch8.5/11Diesel

1		4	5
2	3		
525	295	Втулка 6 Блок 7	115 114
525	305	Втулка 6 Блок 7	111 111
525	320	Втулка 6 Блок 7	114 112
525	340	Втулка 6 Блок 7	113 113

Key:

1. Piston weight in g.
2. Head
3. Trunk
4. Points at which vibration was measured, in db
5. Vibrational level of cylinder liners in db
6. Liner
7. Block

As experiments showed, an increase in piston weight by a factor of 1.5/2 does not cause an appreciable rise in the vibrations of liners and blocks in diesel engines. When experiments were conducted on diesel engines, the temperature regime, the gap in the moving members, combustion pressure, cycle roughness and several other parameters were kept constant. This made it possible to avoid the effect of extraneous factors on vibrations of diesel engine cylinder liners and block as the piston weight was varied. The pistons were made of different materials using the same drawings and identical thermal gap was maintained.

The nature of liner vibrations proved to be strongly affected by piston design and the distribution of its weight between parts situated above the axis of the piston pin and below it. This is because as the piston reverses vertical direction during the slap period, the impact against the liner is carried out by a corner of the piston. In this case, the vibrations intensify compared with those that occur if the piston strikes the liner simultaneously with the entire generatrix of its outer contour.

As studies showed, when the piston weight is redistributed between its head and skirt, the nature of liner vibrations is modified. Tests conducted on a 1Ch 8.5/11 diesel engine (Table 12) confirmed that minimum liner vibrations occur in the absence of canting of the piston relative to the piston pin axis. When the piston weight is redistributed relative to the pin axis, there is a change in the canting moment. Similarly, minimum vibrations are observed in a Model Ch 8.5/11 when the weight of the piston head is 525 g and the piston trunk weighs 395 g.

Thus, a variation in the ratio of weights of piston head to piston skirt leads to a significant change in vibrations, while the overall change in piston weight has a small effect on the intensity of liner vibrations.

Reducing the somersaulting action of a piston can be achieved also by increasing the piston length. Table 13 presents data on the intensity of vibrations on several models of engines as a function of the ratio of piston diameter to piston length.

Table 13: Effect of Piston Length on Range of Liner Vibrations

1	2		3	4	5
6	150	120	[illegible]	85	115
7	[illegible]	1,25	[illegible]	[illegible]	1,7
8	9	9	9	9	9

Key:

1. Diesel engine model
2. D6
3. Ch 10.5/13
4. Ch 8.5/11
5. D1548M
6. Piston diameter in mm.
7. Ratio of piston length to piston diameter
8. Range of intense diesel engine vibrations, Hz
9. To

From Table 13 we see that for a long piston (D1548M diesel engine) the vibrations of the engine become low-frequency as a result of the greater area of piston contact with the liner at the instant of slap.

The effect of increasing the length of the piston trunk on the intensity of diesel engine vibrations was tested on a Ch 8.5/11 diesel

engine which provided an indirect estimate of liner vibrations. Piston length was increased from 112mm (series-produced piston) to 130mm. As shown by studies, the minimum diesel engine vibrations were observed when the trunk length was increased by 9mm and were 114db. A further increase in the trunk length led to a rise in the intensity of vibrations. Vibrations reached a level of 120db when the piston length was 130cm [should be mm] as against 116db for a series-produced piston. This is because the increase above a certain limit (121mm) in the trunk length increases the moment canting the piston and causes a rise in the level of vibrations.

The canting of a piston during impact is also indicated by the change in the spectral composition of the vibrational level.

For a series-produced piston (112mm), the highest levels of vibrations are observed up to 2000 Hz, and when the piston length is 121mm - only up to 1500 Hz. As the frequency and amplitude of vibrations are reduced, the acceleration is likewise diminished, which leads to an abrupt reduction in cavitation damage.

The offset of a piston pin has some effect on reducing the vibrations of binders and blocks in diesel engines. Changes in vibrations for different piston pin offset values were tested on the diesel engines 1 Ch 8.5/11 and 1 Ch 10.5/13. A special piston was built in which the piston pin axis could be shifted relative to the piston axis by replacing inserts with excentric openings for the pin.

The shifting of the piston pin axis relative to the piston axis (offsetting of the piston pin axis) changes the side pressure forces. An additional moment appears tilting the piston. For the appropriate selection of the offset value, a reduction in the energy of impact of

the piston against the liner and a decrease in the intensity of liner vibrations can be achieved.

Table 14: Vibration Frequency as a Function of Liner Thickness

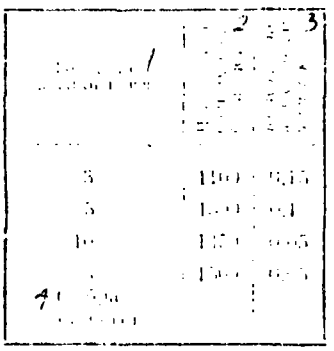

Key:

1. Liner thickness in mm.
2. Frequency of free vibrations Hz.
3. Vibrational speed in cm/sec
4. (Stiffness ribbing)

During the period of investigations, the offset value was varied within the limits from 0.5 to 6mm, and the overall vibrational level - by 3db.

To estimate the effect of cylinder liner stiffness on liner vibration, tests were made on cylinders of various thicknesses and on cylinders fabricated from different materials. Before the beginning of the acoustic tests of a diesel with different cylinder liners, the free-vibration frequencies of the cylinder liners were determined in static conditions. we know that the free-vibration frequency range changes with changes in structural stiffness. One must establish how the material and thickness of the cylinder liner affects its free vibrations.

An increase in the thickness of a cylinder liner made of the same material leads to a reduction in the intensity of its vibrations

(Table 14) in spite of an increase in the vibration frequency.

Tests in full-size conditions on operating diesel engines that were conducted on cylinder liners of various stiffness values confirmed the static test results. Vibrations of the cylinder liners decreased with increase in thickness. In approximate terms that can be assumed that a decrease in vibrations as the thickness of cylinder liners is increased obeys the following function:

$$L_2 = L_1 - 10 \lg \frac{H_2}{H_1} \quad \text{db} \ .$$

Here L_2 and L_1 are the vibrational levels for the tests and the rated cylinder thicknesses. H_2 and H_1 are the test and rated cylinder liner thicknesses.

From these data it follows that doubling the cylinder liner thickness reduces the diesel engine vibrations by an average of 3db (that is, by nearly half). At the same time, when the cylinder liner thickness is increased with a reduction in the total levels, the vibrations in the high-frequency spectral region become less.

A typical method of seating a liner in a cylinder block is the procedure in which the liner has in its upper section a shoulder and a guide zone, and in its lower section - a second support zone provided with rubber sealing rings.

Under otherwise equal conditions, the liner vibrations will be weaker, the shorter the span between the support zones and the tighter the seating of a liner in the block at the support zone. Naturally, a reduction in liner vibrations will be promoted by an increase in the number of support zones (if tight seating will be achieved between

them and the block, or when the gap is much smaller than the amplitude of the liner vibrations) and, as an extreme case, fitting the liner with screw-type support projections over its entire height.

Figure 44: Cavitation Damage in Specimens as a Function of the Gap Δh Between Them for Different Frequencies of Exciting Forces at Constant Acceleration:

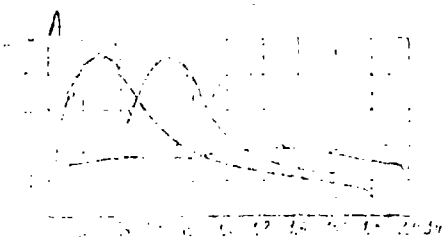

1 - 20 kHz 2- 10 kHz 3 - 5 kHz

Key: A - G, mg

Cavitation erosion in diesel engines is somewhat affected, with the liner vibration intensity kept constant, by the design of the water jacket, and above all by the thickness of the water layer surrounding the cylinder. Not only does the flow rate of the water depend on the distance between the walls of the liner and the block (the thickness of the water layer), but also the resilience of the layer. It is noted that the thinner (beyond some limit) the water layer in the water jacket, the less resilient it is. Cavitation erosion occurs more intensively in the narrow cavities for the same water flow rate not only within the cylinder but also within the blocks. This becomes especially evident at the locations of support zones if they have a gap sufficiently large that water passes through it.

The effect of the resilience of the water layer is associated with the fact as the water layer is made thinner, tensile and compressive stresses are produced, for smaller strains, which then give rise to the inception and collapse of cavitation bubbles.

Tests made on MEV showed (Figure 44) that the weight loss of aluminum specimens is markedly affected by the gap ΔH between vibrating and fixed (acting as a shield) specimens. Tests were conducted in tap water.

The damage intensity curves No. 1 and 2 plotted based on data of tests at 20 and 10 kHz have a well-defined maximum, however this occurs for different gaps between vibrating and fixed specimens.

S. P. Kozyrev [23] noted that the presence of a failure maximum is associated with the natural frequency of the cavitation bubbles, which on entering into resonance with the frequency of the exciting force, collapse more intensively and, as a consequence, more strongly damage the cooling surface. The corresponding diameters of the cavitation bubble can be determined from a formula derived by Sweet,

$$d = \frac{0{,}66}{f},$$

where d is the diameter of the cavitation void in cm, and

f is the frequency of the exciting force in kHz.

The diameters of cavitation bubbles capable of resonating as a function of excitation frequency will be as follows:

f in kHz...	2	5	7	8	10	12	15	20	22
d in mm ...	3.3	1.3	0.93	0.82	0.66	0.55	0.44	0.33	0.3

From these data we see that for vibrations of liners occurring at frequencies up to 2 kHz, evidently one must not expect a marked effect of resonance phenomena, since bubbles this large (diameters greater than 3.3mm for 2 kHz and below) have great lift and surface without collapsing. Therefore the effect of the thickness of the water layer in the jacket is associated mainly with changes in layer resilience. Moreover, even with the MSV it was noted that, beginning at excitation frequencies of 4.5 - 5kHz and below the damage values as a function of the gap between specimens levels off (Curve 3, Figure 44), since at this frequency the resonance cavitation bubbles are more than 1mm in diameter and surface.

In several cases, in studies made on the MSV the data on the effect of the gap between vibrating and fixed specimens do not agree with the data obtained in full-size diesel engine tests.

On the MSV the failure of the vibrating specimen (a liner analogue) increases with decrease in the distance to the fixed specimen (block analogue). The simulation failure of these tests is evidently associated with the following observations:

1) in MSV tests, the higher vibration frequency was directly above the intensity of the cavitation processes, therefore the resilience of the water layer played a secondary role; and

2) a flow of fluid from the vibrating specimen to the fixed specimen was arranged on the MSV, which altered the nature of the pressure distribution in the zone of the specimen compared with the actual cooling system where intense vibrations of liners caused a somewhat different distribution of acoustic pressure.

Figure 45: Liner of Diesel Engine with Cavitation Damage Along the Lower Zone

Figure 46: Appearance of Lower Zone of Liner

Figure 47: Damage to Block in Lower Zone

Intense cavitation damage in a number of diesel engines in narrow locations (in the areas of the seating shoulders) at times leads to cracks in liners and blocks.

Figure 45 shows the cylinder liner of a 6 Ch 15/18 diesel engine with intense cavitation pits along the lower seating zone, indicated with arrows. The cavitation pits, up to 1.5mm deep, are densely scattered over the surface in the area of the lower seating zone, where after 528 hours of diesel engine operation in a truck, a crack appeared in the liner and the diesel engine malfunctioned. Figure 46 shows a severely cavitated lower seating shoulder of the liner of a diesel engine from the SKL (German Democratic Republic) Diesel Plant having run for about 2000 hours with the gap at the shoulder of about 3mm. On another liner of this same diesel engine, the shoulder shows no discernable traces of cavitation damage since the gap was much smaller, 1.2mm. In these cases, the seating zones of the blocks also were attacked besides the attack in the liners.

Figure 47 shows with an arrow significant damage areas in the vicinity of the lower seating zone of the block of a 6 Ch 15/18 diesel engine.

It is shown by operating practice cavitation damage in the area of the upper seating shoulder can prove very dangerous. When a gap up to 1mm is present between the cylindrical sections of the liners and the blocks beneath the upper seating shoulder, intensive cavitation and damage can occur in the location of intense vibration, both in the liner and in the block.

21: Effect of Cooling System Design on the Cavitation Erosion of Liners and Blocks in Diesel Engines

Two systems of liquid cooling are used in diesels: flow type and closed type.

The flow system, fresh water or sea water, after cooling diesel engine parts, arrives at the overflow. Contrasted to this system, in the closed cooling system, water beyond the engine enters a heat exchanger where it is cooled (with water or air) and returned again to the engine.

In both the flow type and the closed cooling system, devices for temperature regulation can be provided so that the temperature of the water exiting from the engine for different load regimes varied only slightly. To do this, water is directed in two directions in the flow system from the thermostat (two-channel) installed at the outlet from the engine to the overflow end along a diversion pipe back to the water pump and to the engine. In the closed cooling system, the thermo-

stat directs the water also in two directions: to the heat-exchanger and back to the engine.

When a diesel engine is being operated at low loads, as the amount of heat given off into the water is reduced, the thermal regulation system that employs recycling most of the water passing through the engine back to the engine must maintain the required temperature level in the cooling system.

At the present time, cooling systems in use either have no temperature regulation system whatever, or else if present, they exhibit a degree of control nonuniformity so high that during the operating time at low loads engines prove to be supercooled.

A key disadvantage of the flow type system is the fact that when bilge(sea water) (marine installations) is used to cool a diesel engine, the temperature of the water flowing out of the engine must not exceed 50-55°C to avoid deposits of salt (scale) in the cooling system, that is, the temperature regime that is most disadvantageous from the standpoint of cavitation damage must be maintained. In the absence of a temperature regulating system, the temperature of the water at the inlet into a diesel engine fluctuates widely depending on the navigation conditions of the vessel and the time of the year, the diesel engine often operates supercooled and as a result gaps are increased and the level of liner vibrations rises.

Flowing water contains usually large numbers of cavitation nuclei in the form of bubbles of air and gas, and also in the form of solid suspended particles. All this makes the flow type cooling system unfavorable

with respect to cavitation erosion of cylinder liners and blocks. Moreover, when sea water is used in a flow type cooling system, all the water jackets of an engine are subjected to corrosive erosion.

Recently, the closed system of cooling is finding greater use in diesel engines of all types beginning with large crosshead, high-capacity engines down to small ones.

A system in which water is pumped from the water cooler into the cylinder jackets, and then arrives in the cylinder head and cavity of the exhaust manifold, and then back again into the cooler is the most widespread closed cooling system. The use of pure water with minimum alkalinity, acidity, and gas content in the system reduces the scale deposits and diminishes corrosion damage.

However, the closed system of cooling will be effective and justify itself in the control of cavitation erosion only if the cooling temperature regime is 85 - 90°C for a pressure in the system close to the atmospheric, 1.1 - 1.2 atm, and when the cooling temperature regime is 90 - 95°C for a pressure of about 2 atm.

This temperature regime must be maintained when the diesel is being operated in all regimes. But in actual conditions in many cases when diesel engines are operated at low loads, the temperature in the cooling system falls to 40 - 60°C, that is, down to a temperature that is the most unfavorable from the standpoint of build up of cavitation erosion processes.

The cooling system of the M50 marine diesel engines was modernized at the Dnepr Steamship Company for hydrofoil ships. The modernization of the cooling system consisted of 20 - 40% of the water pumped with a

water pump into the aft-jacket space and its bypass back to the intake connection of the water pump. This made it possible, first of all, to shorten the diesel engine warm up time and to raise the temperatures in the cooling system by 3 - 5°C for rated-power operation, which became 78 - 82°C after 900 hours of operation of a diesel engine with modernized cooling system; it was found that cavitation erosion to the cylinder liners and blocks of the engine was reduced compared with the damage over the same time interval, but with a series-built cooling system. After 900 hours of operation in series-built M50 diesel engines in the Dnepr Steamship Line, pits up to 2 - 2.5mm deep appeared on the cylinder liners, while with the modernized system damage was reduced.

Personnel at Northern River Steamship Line using 3D6 marine diesels also increased the temperature regime in the cooling system by modernizing it. The modernization of the cooling system consisted in bypassing 30 - 60% of the coolant water past the block into the jacket of the exhaust manifold. This measure was carried out by installing an additional 3/4"-section of piping from the water pump to the exhaust manifold cavity. As a result, it was possible to raise the temperature regime for 3D6 diesel engine cooling and, as a result, to prolong the service life of cylinder liners in the diesel engines from 2000 - 3000 hours to 4500 - 5000 hours.

The measures adopted by the steamship companies made it possible to raise the temperature of the cooling system (in all velocity and load regimes) and to reduce cavitation damage to liners and blocks in diesel engines. The same effect could have been achieved by improving the temperature regulation by increasing the proportion of water bypassed over

the cooler directly into the intake mainline of the water pump.

In evaluating the effect of the cooling system design on the cavitation damage, one must estimate the role of the water flow rate in the cooling cavities.

The flow rate in different diesel engines and at different points in a water cavity of the same diesel engine varies within the limits 0.2 - 1.5m/sec and only in some engines does it rise to 8m/sec at several points. As shown by the hydrodynamic theory of cavitation, this velocity is clearly insufficient for the initial stages of cavitation to build up. This was also confirmed by experiments in which water was pumped through the engine's forced feed cooling system in the absence of liner vibrations.

A study of combined effect of water flow rate and the vibratory field of a material specimen, using a MSV, showed that as the flow rate of the water is increased the damage at the same vibrational level rises. This can be accounted for by an increase in the flow rate v_w (w - water) of water layers with respect to each other and by a reduction in the rupture strength of water. The rupture of water and the implosion of cavitation bubbles occur, under otherwise equal conditions, with lower vibro-activity. When vibro-activity is increased, damage becomes more intense (Figure 48).

In some low-output diesel engines, the water pump capacity can be so high that the pressure drops in the water system at the locations of water inflow into the block will reach the level required for cavitation processes to occur. With the water pump capacity kept unchanged, this is also observed in downrated diesel engine models. The presence of liner

vibrations will promote the buildup of cavitation processes. Cavitation bubbles arise in the zone of minimum pressures at the areas of water supply narrowing, and on entering the increased pressure zone partially collapsing in the expanded cooling cavity, damaging the cooling surface both in the block and in the liner. The damage at these locations is eliminated by changing the cross-section and shape of the inlet and outlet water connections and by changing the angle of inlet and outlet inclination, that is, by reducing the pressure drop in the nearest cross section of the water-inlet and water-outlet channels.

Figure 48: Dependence of Cavitation Damage to Specimens on the Flow Rate of the Fluid and the Vibratory Field.

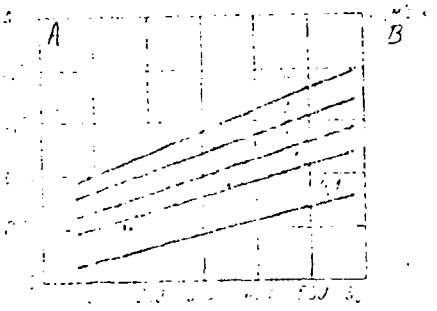

Key: A: ΔG, g
B: v_w, m/sec

72: Effect of Diesel Engine Operating Regime

The diesel engine operating regime affects the intensity of vibrations of cylinder liners by way of changes (in accordance with the diesel engine operating regime) in the clearances in the piston-cylinder group, and by changes in the side pressure forces. Increasing the rpm for a specific diesel engine is reflected in a change in the side pressure forces owing

to a rise in the inertia component (the overall side pressure force becomes smaller). With an increase in rpm per unit diesel engine operating time, the number of piston impacts against the cylinder wall rises and so do the losses of intense cylinder liner vibrations, leading to cavitation erosion.

A rise in the side pressure force as a function of the extent of change in rpm can play either the principle or secondary role. The quality of temperature regulation of the engine affects the intensity of cavitation erosion when the load regime is increased. If, for a reduced load the temperature of the water in the cooling system is sharply lowered, then as the load is increased, the temperature regime proves to be more optimal and the cavitation erosion becomes less. Experiments showed that in model Ch 10.5/13 diesel engines (with aluminum pistons) a rise in the load is accompanied by a reduction in cavitation damage, but in model Ch 15/18 diesel engines, in contrast, by greater damage.

An increase in the rpm in all cases must lead to greater damage per unit diesel operating time.

Figure 49 presents a nomogram for estimating the vibro-activity of diesel support flanges. The level of main-frequency and high-frequency caused by operation of the piston-cylinder group and transmitted from the diesel engine block to the support flange is determined with the nomogram at the point at which the lines of power and diesel engine rpm intersect with the inclined line characterizing the vibrations of the diesel engine block. The vibrations are read off upward.

Figure 49: Nomogram for Calculating the Vibration of Diesel Engine Bedplate.

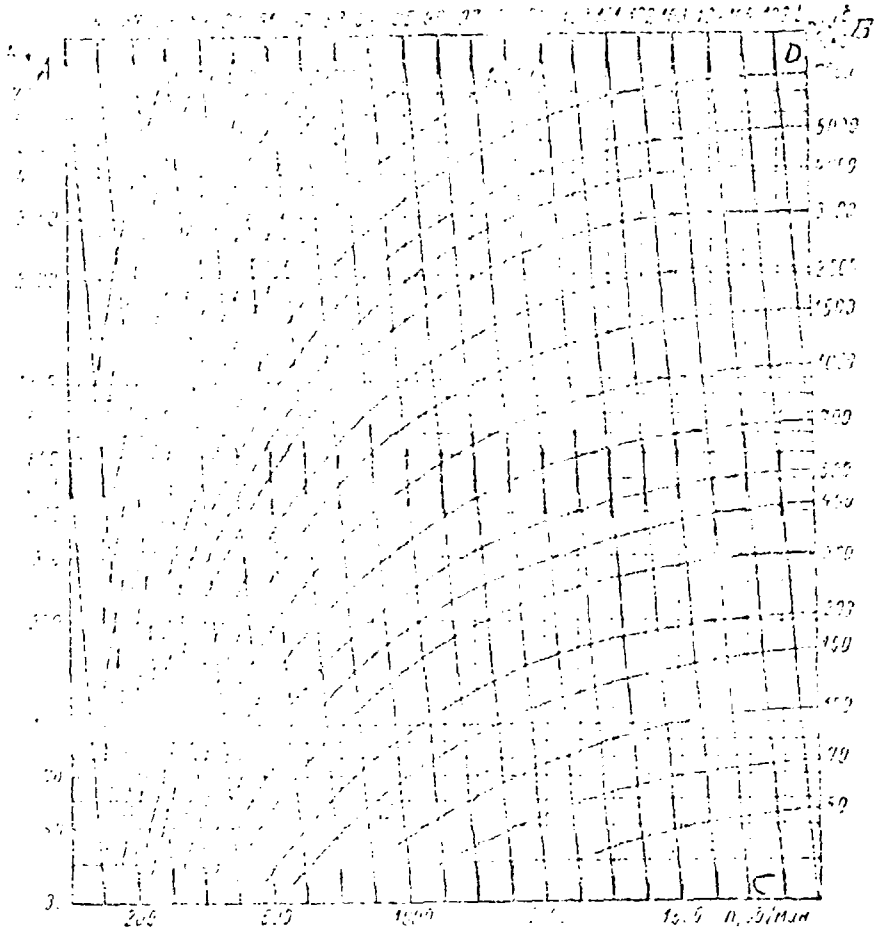

Key A: N_e, hp
B: L_v, db
C: n, rpm
D: G, kg

From the nomogram we see that the total level of diesel engine vibration increases with an increase in the rpm, and on the average this total rises by 1 db per each 100 rpm for the high-speed diesel engines. Vibrations increase by 0.4 db for this case, with a two-fold rise in power.

Figure 50: Vibration Spectra of the 6 Ch 15/18 Diesel Engine Block

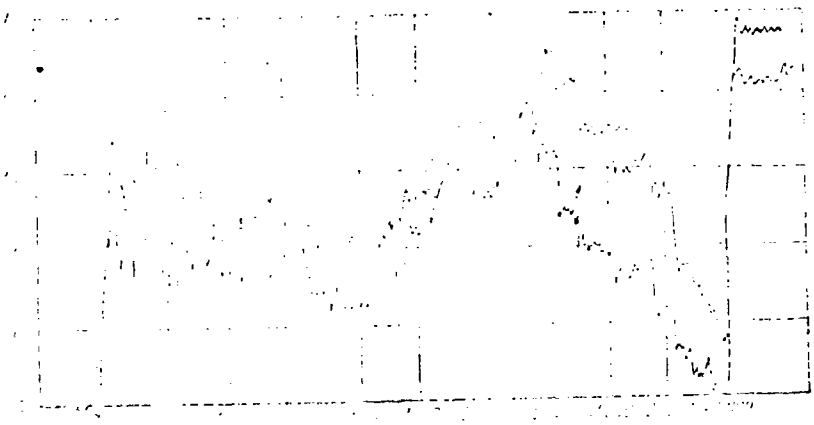

Figure 50 shows the vibration spectra of a 6 Ch 15/18 diesel engine block. Curve 1 characterizes the vibration spectrum at 1000 rpm with a 10% load, and Curve 2 - the spectrum at 1500 rpm with a 100% load. Vibrations of liners and blocks increase as the cooling temperature is lowered.

23: Effect of Properties of Coolant Liquid on the Intensity of Cavitation Damage

It was experimentally observed that the frequency of turnover of coolant water in a diesel or water in which tests are conducted on a MSV affects damage intensity.

When long-term experiments were conducted for a number of hours in the same water, damage occurred somewhat slower. The experiments conducted in which water was periodically changed show that cavitation damage intensifies with respect to experiments conducted in the same water.

The buildup in cavitation damage in replaced water can be accounted for by the presence in it of a larger amount of dissolved air than in the water from which dissolved gases and air have already evolved.

Figure 51: Effect of Frequency of Water Replacement on the Failure of a Cast-iron Specimen Tested on a 18.5 kHz MSV (S_c=1370, Surface Finish ▽3):

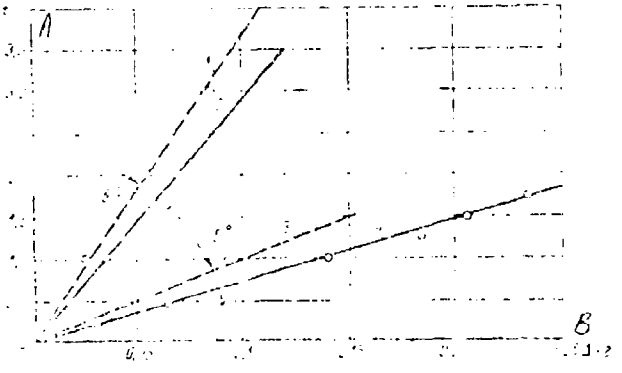

1 - and 3 - Water is not changed
2 - and 4 - Water is changed
1 - and 2 - T=15°C
3 - and 4 - T=65°C

Key: A: t, hours
B: ΔG, g

Air dissolved in water reduces the strength of water, which then leads, for the same vibration amplitudes and frequencies, to the more facile formation of vapor-gas bubbles. Conversely, a sharp rise in the number of air bubbles in water leads to an increase in its resilience and hampers the collapse of cavitation bubbles.

Prior treatment of water when it is warmed and sound-irradiated reduces the intensity of cavitation damage.

Figure 51 shows the change in the weight losses of specimens as a function of test duration for different temperatures, in which water was replaced and in which water was unchanged during the experiments. The curves in this figure show that the damage intensity depends on temperature.

For experiments in water whose temperature was kept at 15- and 65°C, water replacement was shown to have an effect. It was found that the slope of the curve characterizing damage when water was changed, compared to curves obtained in experiments using the same water is 5° higher and remains unchanged for different water temperatures. On this basis the intensification of damage can be determined for cases in which water was changed.

From Figure 52 we see that the build up in damage ΔG is the difference

$$\Delta G = G'_1 - G' = G' \left(\frac{\quad}{\quad} - 1 \right),$$

where G'_1 and G' are the damage intensities in replaced and unreplaced water.

Assuming that $\alpha = \beta + 5^\circ$, we get

$$\Delta G = G' \left(\frac{\quad}{\quad} - 1 \right).$$

The ratio

$$\left[\frac{\quad}{\quad} - 1 \right]$$

for a given coolant water temperature remains constant and can be taken as the coefficient k_1. Then an increase in the intensity of damage to a surface for the same duration, under otherwise equal conditions,

expressed in grams, will be as follows for the case of periodic water replacement:

$$\Delta G = k_1 G_1.$$

Thus, the coefficient k_1 is a function of the coolant liquid temperature since the damage at different temperatures differs (the slope of the curves is different) and, therefore, the slope data of these curves is also different.

The total weight loss for damage in replaced water is found as the sum

$$G'_1 = G' + k_1 G' = G' (1 + k_1).$$

Figure 52: Diagram for Calculating Damage Increase

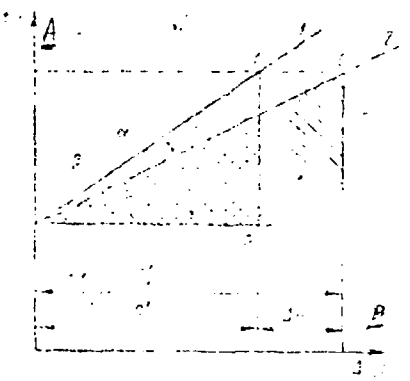

1 - Water unchanged 2 - Water changed

Key A: key, hours
B: ΔG, g

The slopes of the damage curves for different temperatures were taken from materials of the preceding sections of this book. Th

coefficients calculated based on the experiments conducted are listed in Table 15.

From these data it follows that in the temperature regimes corresponding to the regimes of diesel engines with the flow-type cooling system (50-60°C), processes of cavitation damage intensify by 20 - 23%.

The highest intensification of cavitation occurs at low temperatures corresponding to starting regimes. It is typical to note that in the high temperature range, 85 - 90°C, the process slows down at atmospheric pressure and is equated to the process occuring in water that has lost its dissolved air.

Table 15: Coefficient k_1

[1]							
Угол β [2]	[illegible]	[illegible]	[illegible]	[illegible]	15	16	[illegible]
k_1	[illegible]	[illegible]	[illegible]	[illegible]	[illegible]	[illegible]	[illegible]
[1]	[illegible]	[illegible]	55	57	60	65	68
Угол β [2]	[illegible]	[illegible]	21°30'	22°15'	23	25	25°45'
k_1	0,3	[illegible]	0,27	0,26	0,25	0,24	0,23
[1]	[illegible]	[illegible]	[illegible]	[illegible]	85	[illegible]	[illegible]
Угол β [2]	[illegible]	[illegible]	[illegible]	31°15'	34°	[illegible]	41°30'
k_1	[illegible]	[illegible]	[illegible]	[illegible]	[illegible]	[illegible]	[illegible]

Key: 1. Temperature of water in °C
2. Angle β

The effect of the water temperature on cavitation damage is caused mainly by changes in the saturated vapor pressure.

It bears noting that oxygen is the most corrosive component affecting a buildup in damage. Figure 53 shows the dependence of damage on

purging of water with various gases. The greatest damage results when water is swept with oxygen (Curve 1). This damage is much more intense than damage in tap water (Curve 2). Sweeping water with gases that do not intensify the oxidation of N_2 and CO_2 leads, conversely, to a weakening of cavitation damage.

In those cases when the material damaged by cavitation is subjected to oxidation (for example alloy steel) even sweeping water with oxygen reduces the cavitation intensity (Figure 54). Here the presence of gases in water increases its damping properties and compressibility. Figure 55 shows the rate of damage for steel 60 as a function of the frequency of specimen vibrations. The effect of the presence of oxygen in water begins to become evident at the frequency 2.5 - 3 kHz, that is, precisely in the frequency range at which oxidation processes begin to become evident in cavitation damage. Generally only mechanical factors affect damage in the lower range of vibration frequencies.

If a material is weakly affected by oxidation (Figure 56), the presence of oxygen in water is equivalent to the presence of any other gas in water and does not intensify the damage process even in the high-frequency range, 10 - 20 kHz.

It is useful to examine in closer detail the effect that oxygen dissolved in water has on the damage suffered by materials used in diesel engine building.

Verification of the effect that the oxygen content has on cavitation damage was conducted on aluminum and cast-iron specimens 30mm in diameter on a MSV in tap water, distilled water and also in high-purity water (high-purity water is distilled water purified in

a KI-5 ion-exchange filter, ensuring total removal of oxygen from water). The specimens were tested in a hermetically sealed bath with steady water replacement in the bath every 15 minutes. The specimens were weighed every hour of operation. The water temperature was kept constant in the range of 18 - 20°C. During the investigation, a regular analysis was made of water for oxygen content, (Table 16).

Figure 55: Damage to Steel 60 in Water Saturated With Various Gases (f=19kHz, A=0.075mm, p=1 atm, and Gas Volume Flow 50 ml/min)

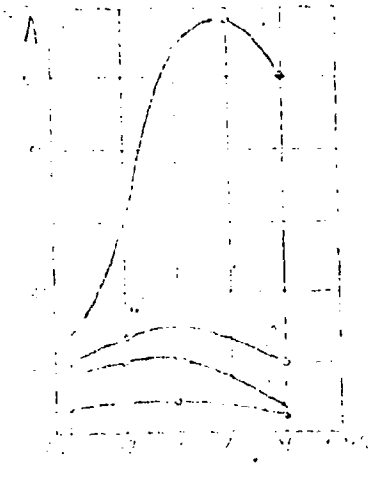

1 - O_2 2 - Without gas sweeping 3 - N_2 4 - CO_2

Key: A: Δg, mg/hr

Figure 54: Damage to the Steel EI 12 CrNi183 in Water Saturated with Gases (f = 19 kHz, A = 0.025 mm, p = 1 atm, and Gas Volume Flow 50 ml/min):

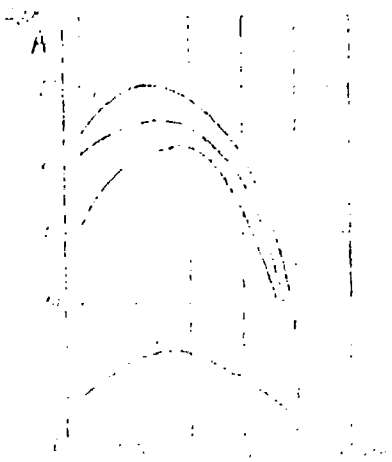

1 - Without gas sweeping 2 - N_2 3 - O_2 4 - CO_2

Key: A: Δg, mg/hr

Figure 55: Effect of Gas Content in Water on the Damage to Steel 60 as a Function of the Vibration Frequency (A = 0.075 mm, p = 1 atm, t = 55°C, and Gas Volume Flow 50 ml/min:

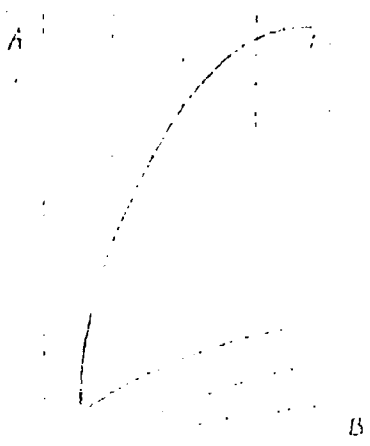

1 - O_2 2 - Without gas sweeping 3 - N_2 4 - CO_2

Key A: Δg, mg/hr
B: f, kHz

Figure 56: Effect of Gas Content in Water on the Damage to the Steel Kh 12 GrNi188 as a Function of Vibration Frequency (A = 0.025mm, p = 1 atm, t = 55°C, and Gas Volume Flow 50 ml/min):

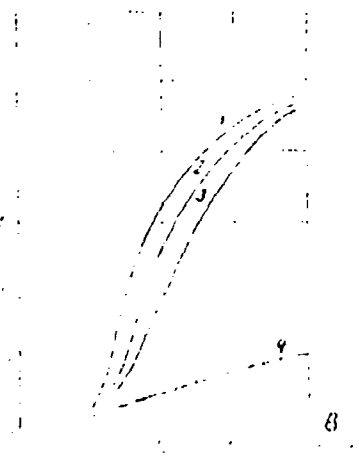

1 - Without gas sweeping 2 - N_2 3 - O_2 4 - CO_2

Key A: Δ_{γ}, mg/hr
B: f, kHz

Figure 57, a and b shows the intensity of cavitation damage to aluminum and cast iron as a function of the oxygen content in water. Tests showed that the gas saturation of water has different effects on the intensity of cavitation damage of cast iron and aluminum.

Purifying water of oxygen makes it possible to significantly reduce cavitation damage to cast iron specimens. In tap water the damage was approximately 13- 17 mg/hour, while in distilled water it was 5 - 6 mg/hour and in high-purity water, 3 - 4 mg/hour. The nature of the erosion damage to a sample surface also varied. The surface of a sample tested in tap water was coated with pits up to 1mm in diameter and 0.6 mm in

depth, and with a uniform layer of corrosion products. The corrosion products were completely absent on the surface of the specimen tested in high-purity water. The erosion pits were not more than 0.2mm in diameter, that is, 5 times smaller than in tap water, and at a depth of 0.15 mm. These results correspond to the data presented in the study [3]. However, in this study no consideration was given to the corrosion factor, which morphically becomes manifest when cast iron was tested in high-purity water. Steel is not coated with corrosion products in this kind of water and its weight loss is smaller than in tap water.

Figure 57: Damage to Specimens in Water: a - Ch 24 - 44 Cast Iron; b - AL4 (Aluminum Alloy)

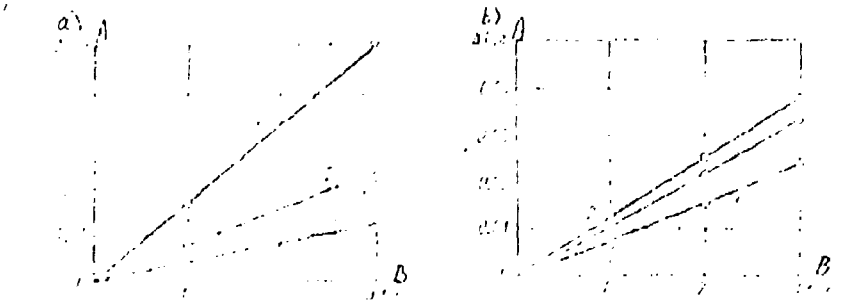

1 - Tap water 2 - Distilled water 3 - High-purity water

Key A: ΔG, g
B: τ, hours

Experiments showed that the effect of the gas saturation of liquid on erosion damage cannot be considered apart from chemical activity and the corrosion resistance of a material. This is confirmed by the fact that when considerable amounts of gas are present in a liquid, the force of the hydraulic impact arising from the implosion of cavitation bubbles

decreases, that is, the gas contained in the liquid and in bubbles has a damping action on the collapse of the bubble and does not permit it to completely break down. This is most characteristic for aluminum alloys. Tests of aluminum specimens in distilled water and in high-purity water form cavities in the metal 1½ to 2 times deeper than in tap water containing large gas content.

Table 16: Gas Content in Water

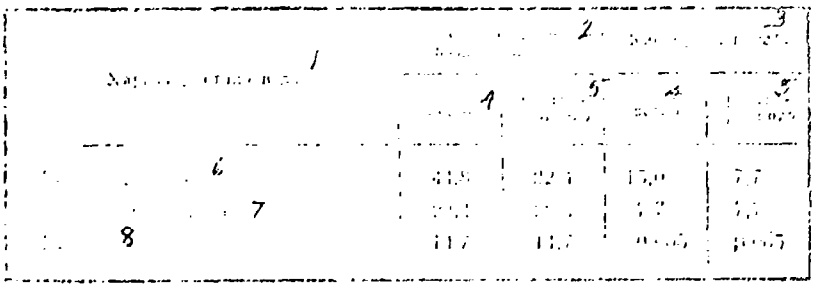

Key:

1. Water characteristics
2. Air content in mg/l
3. Oxygen content in mg/l
4. Total
5. Dissolved
6. Tap water
7. Distilled water
8. High-purity water

It must be noted that damage to aluminum in distilled water and in high-purity water also differs compared to each other, although to a lesser extent than this damage differs in tap water. Weight losses and dimensional changes in pitting damage in high-purity water proved to be somewhat greater and more localized. This indicates the predominance of mechanical factors of attack in this situation. Mechanical damage is somewhat less in distilled water, however, here the chemical

processes occur more actively, where the oxide film in distilled water proves to be twice as large in area than in high-purity water.

Cast iron is a stronger material and at the same time has a lower corrosion resistance. During tests made in high-purity water, the cavitation of cast iron proved to be four times less than in tap water. When a vapor-gas bubble collapses, the air contained in it is heated to a high temperature. The presence of high temperature and high oxygen content in water (the air dissolved in the water is somewhat richer in oxygen than atmospheric air) promotes energetic oxidation processes during cavitation.

In the closure and collapse of cavities formed in high-purity water, the strength of the hydraulic impacts is commensurable with the strength of cast iron, 85 kg/mm^2. The closure of vapor-gas bubbles formed during cavitation in tap water reduces the force of the hydraulic impact which are commensurable only with the strength of aluminum 15 - 20 kg/mm^2.

A study of the effect that the gas saturation of liquid has on cavitation erosion during accelerated tests on magnetostrictive vibrators suggested preliminary conclusions on the usefulness of conducting full-size tests on diesel engines using degassing of water for engine cooling systems made of different construction materials.

The viscosity of the coolant strongly affects all physicochemical processes occuring in it. First of all, the compressibility of the fluid and forces of interaction of the molecules in the medium change. All these quantities affect cavitation and cavitation damage.

Let us consider the effect that the viscosity of the medium has on cavitation damage only with respect to the damage to the slip bearings lubricated with oils of different viscosities. Changing the viscosity of a fluid in diesel engine cooling systems by using anti-freezes and other fluids more viscous than water is not justified.

Figure 58 shows a curve characterizing the damage to Babbitt resulting from the viscosity of oil; oil viscoscity is regulated by temperature. With an increase in viscosity, the damage becomes less, since it is difficult to rupture the fluid at high viscosities.

A study of the effect that the viscosity of a medium has on cavitation damage to different bearing materials (A92 aluminum alloy, lead bronze, and Bk-2 Babbitt) shows that aluminum alloy proved to be the most resistant material to cavitation damage in oil. Data characterizing damage in terms of the cavitation pit depth in different materials in M12B oil at 60°C with a viscosity of 44.7 centistokes in 1.5 - hour tests on a MSV were as follows: Bk-2 Babbitt was damaged to a depth of 0.6mm during this time, lead bronze - to a depth of 0.2mm, and aluminum alloy - only to a depth of 0.09mm.

The viscosity decreases and damage intensifies with increase in the temperature of a medium. Thus, when the temperature is raised from 60 - 90°C, the intensity in damage increases roughly by twofold. The temperature dependence of oil viscosity is shown in Table 17.

24: Preliminary Evaluation of Factors Determining the Overall Damage in Diesel Engine Cavitation

Experimental studies conducted in the TsNIDI, [Central Scientific

Research Diesel Institute] and a generalization of research studies [15, 21, 35] show that cavitation damage to the surfaces of liners and blocks swept by coolant water in most cases results from the combined action of mechanical and electro-chemical factors.

Figure 58: Cavitation Damage of Babbitt as a Function of Oil Viscosity:

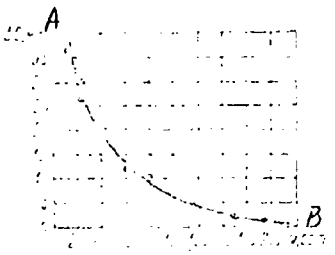

△ M14V oil □ MS-20 oil ● DP-11 oil

Key: A: ΔG, mg
B: Centistokes

Table 17: Kinematic Viscosity of Oils in Centistokes at Various Temperatures

Марка масла 1	Температура в °С 2			
	0	20	50	100
3 ДП-11	15	25	46	135
4 МС-20	27,5	35,1	61	165
5 М14В	18,5	34,5	60,0	151
6 М12Б	15	27	45	108

Key: 1. Oil grade
2. Temperature in degrees C.
3. DP-11 oil
4. MS-20 oil
5. M14V
6. M12B

Figure 59 shows the overall specimen damage curve, plotted in coordinates of weight loss and frequency, with the vibration acceleration kept constant. Also plotted in this figure are approximate data on the components of overall damage, mechanical and electrochemical factors.

At point A' in Curve 2, the damage was obtained on a magnetostrictive vibrator, and at point A" in Curve 3 - the weight loss was for the same specimen as at point A' but after the specimen had been cleaned free of corrosion products in an oil bath with an ultrasonic device.

The damage at point B, C, and D in Curve 1 were obtained with a magnetostrictive vibrator. Washing the specimens in an oil bath did not produce decrements to the weight loss.

Figure 59: Specimen Damage

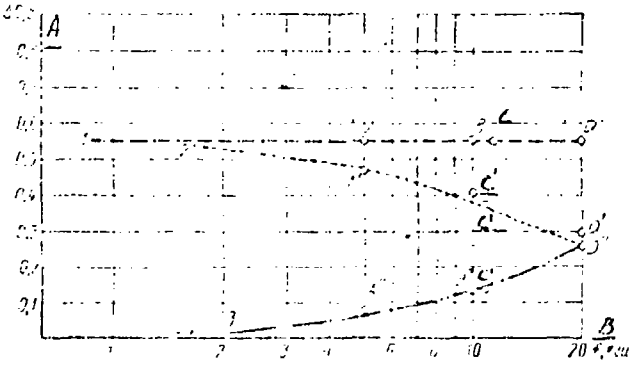

1 - Total damage 2 - Due to mechanical forces 3 - Due to electrochemical processes

Key: A: ΔG, g
B: f, kHz

At the point B', C', and D' the weight values were obtained by weighing dried remains of metal particles precipitating in the water

during the specimen damage process, and at points B", C", and D" - by filtering the corrosion products from the water. Particles precipitating were not taken into account. In plotting the curves, no consideration was given, either, to the fact that the electrochemical processes promote more intense mechanical damage. Therefore these data must be regarded as approximate.

From preliminary data (Figure 59), it follows that in the region up to 2000 - 3000 Hz, the chief factor in the overall damage is mechanical, that is, damage occurs mainly due to the mechanical separation of metal particles under the effect of the shockwave formed during the implosion of the cavity. In this vibration frequency range the cavitation cavities formed due to the separation of the liquid are relatively large and attain a radius of a tenth of a millimeter. Upon collapse of a cavity of large initial volume, very high pressures build up in it capable of breaking apart metal particles. The cyclicity of cavity formation is directly proportional to the vibration frequency and is relatively low. Here the high temperatures building up in the cavity, in turn, being responsible for electrochemical processes, are able to be sharply reduced owing to heat removal into the ambient medium considering the low cyclicity of the process and the relatively small number of large cavities. Therefore, even though the electrochemical process is observed in the vibration frequency range up to 1000 - 3000 Hz it does not have an appreciable effect.

Upon inspection of the liners of several diesel engines which vibrated within the limits 1000 - 3000 Hz, it was noted that after 300 and 500 hours of operation an even thin coating of corrosion products

appeared on their surfaces and only scattered points in the damaged surface had damage areas relatively free of corrosion products.

Thus, an apparent contradiction is in effect. Initially the studies stated that in this frequency range the electrochemical factor plays a secondary role in failure. On the other hand, inspection of liners and blocks of diesel engines indicates the clear presence of corrosion products.

The electrochemical process does not play a substantial role in damage to cylinder liners and blocks either in a gravimetric sense, or by forming deep pits. Mechanical damage in this range of vibrations many times exceeds electrochemical damage. But the presence of an even layer of corrosion products is due only to the fact that here there is no cleaning of the surface free of corrosion products by means of acoustic vibrations. The effect of acoustic vibrations on surface cleaning shows up in the higher frequency range.

Fractionation of cavitation cavities occurs in the range of high vibration frequencies, 5000 - 20,000 Hz with voids produced in the liquid. As shown by high-speed motion picture photography and visual observation, cavitation cavities become very tiny and their initial diameter is only thousandths and millionths of a millimeter which is many times smaller than the diameter of cavities in low-frequency vibrations. This phenomenon (fragmentation of cavitation cavities) is due to the emulsifying of liquids when exposed to ultrasonic vibrations. Here the number of vapor-gas cavitation cavities is very large and they are observed in the form of clouded areas in the vicinity of the vibrating surface. Individual cavities cannot be seen and photographed without

high magnification. As a result of the very low initial volume of the cavities, when they implode lower pressures build up in them than the pressures which are attained in the implosion of large cavities in low-frequency vibrations, and therefore, their kinetic energy is less.

The hydrodynamic theory enables us to estimate, to the first approximation, the kinetic energy T_r in the implosion of a cavity in terms of its initial diameter

$$T_r = \frac{4}{3}\pi\rho r_0^3,$$

where r_0 is the initial greatest radius of the cavity.

Thus, in the collapse of a small-volume cavity the impact force is less. Because a large number of cavities implode in a limited volume of the liquid adjoining the surface of the vibrating part the removal of the heat given off in cavity implosion is hindered. The temperature of the medium in this volume rises. The hydraulic impacts induced during the closure of each of the cavities at the microsurfaces can form micro-couples with very low internal resistance. As a result, an intense electrochemical process of the erosion of the part can occur, which based on the data in brackets [17, 59] is aggravated by the facile damage to the oxide film by the mechanical action of the forces induced in the implosion of cavities when the surface is undergoing high-frequency vibrations.

Thus, in high-frequency vibrations, together with mechanical erosion in the overall process of cavitation damage, electrical erosion can be more strongly evident.

The absence of corrosion products on the damaged surfaces of parts (in particular in diesel engines) subjected to high-frequency vibrations

is accounted for by the fact the corrosion products are cleaned off the surfaces into solutions upon exposure to high-frequency vibration. The corrosion products can be separated from the water by filtration.

Based on the data given in [30], the temperature of gas within a cavity T_g max can reach very high values and is determined by the following expression:

$$T_{g\,\max} = T_0 \left[1 + (\gamma - 1) \frac{P_0}{P_e}\right].$$

[e = end]

Here T_0 is the initial temperature;

γ is the index of the cavity compression adiabat;

P_0 and P_e represent the pressure at the beginning and the end of compression.

Since an exact measurement of temperatures in the microvolumes of water thus far cannot be achieved owing to the high-frequency nature of the process and its instability, it is very difficult to estimate the true temperatures during the closure of cavitation cavities.

However, indirect observation show that the temperatures developing in microvolumes are 700°C and higher. This can be estimated by the flashes of powder particles introduced into a cavitating volume of water (the powder ignites) and by the opalescence colors which accompany the initial stage of damage. The opalescence colors are clearly discernable in diesel engine blocks made of aluminum and cast iron, and also for steel and chrome-plated steel liners. Further investigations will doubtless represent the pattern of damage in various diesel engines with

different frequency-amplitude characteristics, more exactly, which in turn will determine well-defined ways of protecting diesel engines against cavitation damage.

CHAPTER FIVE

METHODS OF REDUCING CAVITATION PROCESSES IN DIESEL ENGINES

25: Design Methods of Decreasing Vibrations in Diesel Engine Cylinder Liners

In diesel engine design, special attention must be given to eliminating vibrations in cylinder liners or decreasing their intensity to allowable limits (18 - 20g).

It is always more rational to eliminate the sources leading to cavitation processes in diesel engines than to find ways of controlling their aftereffects.

Let us examine what then are the main design procedures for reducing cylinder liner vibrations.

The most effective means of reducing the energy of piston impact against the cylinder wall is to decrease the gap between the piston and the cylinder liner.

In estimating the required gap one must consider that the diesel engine operates in various load and velocity regimes, and when they undergo changes in piston temperature and diameter change. To insure the operation of the cylinder-piston group with minimum gaps in all regimes, the preference (as far as possible) must be given to materials with low coefficients of linear expansion, and also for pistons made of light alloy, - aluminum alloys with increased silicon content (AL26). These alloys,

exhibiting good strength properties are suitable for chill-casting of pistons and have much lower coefficients of linear expansion compared with the ordinarily used forged AK 4 aluminum alloy.

So if one considers that the temperature of the piston trunk when the engine is being operated at full power is 120°C, for an initial diameter of 150mm (that is 20°C), a piston made of AK 4 alloy, depending on load, will vary by 0.39mm, while a piston made of Al 26 alloy will vary only 0.27mm.

In building engines of the same type in modifications with different operating levels, cavitation erosion in cylinder liners can be reduced by manufacturing several groups of pistons (on the same production line) differing in diameter to prevent installing a piston of the smallest diameter in the low-uprated modification.

Composite pistons with cast-iron trunks are used for highly uprated diesel engines of the locomotive class. Cast-iron and steel pistons are also used for low-speed and moderate-speed diesel engines. Pistons made of these materials change little in diameter when heated. Therefore, the adjustment (cold) in their use can be appreciably less than for aluminum alloy pistons.

Thus, cases of cavitation damage in cylinder liners in diesel engines with steel and cast-iron pistons are encountered incomparably less often than in diesels with aluminum pistons.

To determine the required thermal gap between a piston and the cylinder liner, one must have experimental data on the piston temperature and the different zones along its height and also about the temperature of the cylinder liner when the diesel engine is operating at maximum

power. The thermal deformations of the liner and corresponding piston zones can be calculated based on these temperatures and the preliminary values of the minimum allowable clearances can be determined. These values must be corrected with allowance for the non-uniformity (circlewise) of piston thermal deformations, especially in the zone of the piston pin bosses. Additionally, here the deformation of the piston leading to its ovalization when acted on by the gas pressure at the piston head and the side pressure against the cylinder wall is taken into account.

The ovalization of the piston from the above-enumerated factors occurs in the same direction (the major axis of the oval is directed along the axis of the piston pin). The piston expands unevenly in the various zones along its height owing to the different temperatures and different distribution of the metal over the periphery, therefore the initial optimal shape of a cold piston is quite complicated.

In its cross section a piston is oval, and the required size of the oval varies with height. But the generatrix of the piston is a curved line. The piston must be barrel-shaped, with a greater diameter in the lower and a smaller diameter in the upper section. Owing to the complexity of fabricating pistons of this design, it is replaced with a simpler design. In particular, the external contour of a piston is machined according to several (for example, four) conical surfaces.

The final finishing of the external piston contour is carried out experimentally in the test compartment or the test-equipped engine. Here the piston is installed initially with unacceptably small clearances, and then after brief operation in the compartment or the engine the locations where rub marks begin are lowered. Thus gradually after several

dismantlings, the piston is given the optimal shape which is subsequently measured and replaced with an approximate but more technologically feasible shape. All this makes it possible to appreciably reduce the thermal gap and to sharply diminish liner vibrations (in some cases by 5 - 15db).

In piston designing, one must also allow for the effect of its canting during slap on liner vibrations, and here it is useful to employ long pistons (about 1.4 cylinder diameters in length). Shorter pistons will have to be made for light high-speed diesel engines, however even here it is necessary that the piston length not be less than its diameter.

In the case of the long piston not only is rocking of the piston during slap reduced, but the weight is rationally distributed between the head and the trunk.

The offset of the piston pin relative to the piston axis must be made small, within the limits 0.2 - 1.5mm (for a 105mm diameter piston) toward the crankshaft rotation side. For an offset value this small, the danger arises of installing the piston with the engine dismantled with a 180° revolution, (that is, with the offset at the reverse side). This factor as well as the technological complication of piston manufacture led to the fact that usually the piston pin axis is not offset.

The vibration of diesel engine cylinder liners can be achieved also by the damping action of an oil layer. The damping oil layer can be produced in different ways. When oil-scraper rings are present in the lower section of the piston and over the piston pin, the lower oil-scraper

beveled ring is rotated, making it an oil-thrower ring. In this case, an oil film is retained on the piston surface between the upper oil-scraper and the lower oil-thrower rings. Oil-retaining grooves can be machined in the piston trunk. A test of the effectiveness of these grooves in the diesel engine 1 Ch 8.5/11 and 1 Ch 25/34, where the grooves were 0.7mm deep and 2mm wide in the first diesel engine, and 4mm wide in the second, showed that in the cases tested the liner vibration level was reduced by 2 - 4db.

The oil layer can be formed also by installing nozzles feeding oil onto the cylinder surface. When this is done, the oil-scraper rings must be left on the piston only above the piston pin axis. This was carried out, in particular, on the D1548 diesel engine built by the MAN Company. A test of this measure on the one cylinder experimental diesel engines Ch 12/14 and Ch 18/20 showed that liner vibration was reduced by 3 - 5db. However, the oil consumption in deposits rose by 5 - 10%.

Reducing cavitation damage in designing cylinder liners and blocks can be achieved by increasing the stiffness of the liner through making it thicker and by reducing the height of its unsupported section, and also by tight seating of the liner in the block.

The effect of greater liner thickness shows up most strongly in light high-speed diesels in which thin-wall liners are commonly used. Here, in designing a new engine the thickness of the liner walls is easily increased. Besides adding to the stiffness of the liner, which promotes a reduction in the vibration amplitude and in the accelerations (in spite of some increase in frequency), when the liner wall thickness is increased, the liner will vibrate with a smaller number of antinodes in the liner

cross section. For example, increasing the liner thickness in the experimental Ch 15/18 diesel engine from 6 to 12 mm led to a reduction in the vibration acceleration from 40g to 14g. The vibration spectra are shown in Figure 60. The overall vibration level L of a thinner liner was 122 db, and for a thicker liner - 113db.

Figure 60: Spectra of Liner Vibrations Recorded Based on Accelerations:

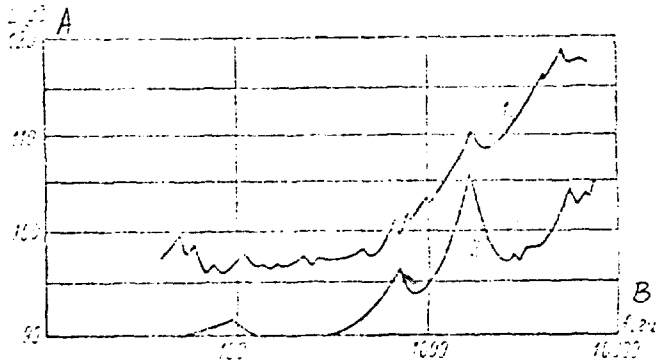

1 - 6mm thickness L = 122 db, W = 40g. 2 - 12mm thickness L = 113 db, W = 14g.

Key: A; L, db
B: f, Hz

Thus in this case increasing the liner thickness by twofold (in spite of an increase in the distance between supports of 60mm) led to nearly a threefold reduction in vibrations and removed them from the danger zone with respect to cavitation damage.

After 1200 hours of stand tests, no significant damage was detected on the liners and blocks of the experimental diesel engine. A bakelite coating on the inner cavity of the block was well preserved, and traces of the initial stage of cavitation damage was observed over the surface of liners only in the zones at which the maximum side pressure forces were

active. (Figure 61). Incipient foci of cavitation pits (arrow A) did not exceed in size tenths of a millimeter and had practically no depth.

A considerable reduction in liner vibrations can be achieved by reducing the height of its unsupported section. Here the following circumstances must be taken into account.

1. For a rigid thick-walled liner, shortening the diesel engine piston stroke (reducing the ratio of piston stroke to piston diameter) promotes a reduction in the length of the liner and a shortening of the height of its unsupported section. The height of the water jacket must be at a minimum owing to the need to insure normal cooling of the cylinder-piston parts.

2. Supplementary intermediate supports can be introduced in long-stroke diesel engines. Studies on Ch 15/18 engines made it possible to find how effective the use of three support cylinder liners is.

Table 18 shows the vibration levels of series-built three-support liners of 12 Ch M 15/18 diesel engines.

Introducing the third support means a 10 db reduction in vibrations. Photographs of three support liners are shown in Figure 62. The intermediate support of the liner is mounted on projections in the diesel engine block, which are made in the form of teeth to admit coolant water (Figure 63). The gap when the liner is installed in the block must not exceed 0.1 - 0.2mm, since with a greater gap the detainment (stop) of the liner on the block cannot be insured as the diesel engine warms up. The location of the support must be selected by calculation and must lie in the location of maximum vibration amplitude. If the materials used in

Figure 61: Magnification of Liner Section

Figure 62: Liner with Third Intermediate Support

Figure 63: Diesel Engine Block with Intermediate Support, of TM3 Design

making the block and the liners of the diesel engine are dissimilar in thermal conductivity (block made of silumin, and liner made of steel), then a tread ring of aluminum in the heated state with a large interference must be installed at the third intermediate liner shoulder; the ring rests on the support of the silumin block. This is necessary to provide a tight fit at the third liner support on the silumin block as the diesel engine warms up.

A considerable reduction in vibration by using intermediate supports make it possible to sharply reduce cavitation damage. Tests of diesel engines with liners using intermediate supports showed that after two and one half hours of operation, the liners and block had no traces of cavitation damage. Series-built liners and blocks cavitated by 1.5 - 2mm in depth during this time interval.

Some foreign companies also use multi-support cylinder liners. For example, the multi-support seating of liners in the block is employed by the NOCHAB Polar Company in a four-stroke 1800 hp diesel engine, 750 rpm.

Even more effective is the design of a liner supported on the block over the entire length. In 12 Ch N 18/20 diesel engines (Figure 64) this is achieved by fitting the liner with threaded ribs which then rest on the block. These liners installed on 12 Ch M 18/20 diesel engines are not subject to cavitation damage.

The proper selection of seating at the location of the liner supports is vital in increasing the stiffness of liner installation in a block and reducing liner vibrations. The seating of the liner with interference

leads to formation of an hour-glass shape in the working surface and can cause piston scoring. An excessive gap (close to the spread of the liner vibrations in magnitude) will not prevent the liner from vibrating. The type of the seating in each individual case must be determined with allowance for the working temperatures of the liner and the block and their materials.

Figure 64: Monoblock Construction

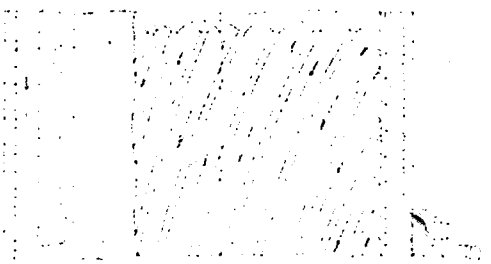

Table 18: Liner Vibration Levels

1	2	Втулки 3	
		4	5
6	0	119	108
	50	120	110
	100	122	112
7	0	117	107
	50	120	109
	100	121	110

Key: 1. Nature of vibration
2. Diesel engine load in per cent
3. Liners
4. Series-built, two-support liner (1500 rpm)
5. Experimental three-support liner (1600 rpm)
6. Vibrations in middle of liner span, in db
7. Vibrations at lower seating shoulder of liner, in db

26: Reducing Cavitation Damage in Blocks and Liners of Diesel Engines By Modifying the Properties of the Coolant Liquid

A change of the gas content in water and its resilience strongly affects processes of cavitation damage. Accordingly, let us examine the question of whether it is possible to reduce cavitation damage in diesel engine cooling systems by increasing the resilience of the water and by giving it anti-corrosion properties by means of adding special additives to it. This must be done in those cases when in designing the diesel engine not enough attention was given to reducing the liner vibrations, increasing the resistance of liners and blocks against cavitation erosion, and when the selection of the optimal temperature regime in the cooling system did not lead to elimination of the cavitation damage.

Using additives for the coolant water involves several operating inconveniences, for example, some additives are toxic. Moreover, as the diesel engine is operated, the additives become used up, therefore, it is required to monitor their concentration in the water and periodically replenish them.

The use of additives providing a protective film on the surfaces of liners and blocks by means of their practically complete precipitation from the water is not reasonable, since the protective layer rapidly breaks down by the action of the high-frequency vibratory field and no appreciable protection against cavitation damage occurs.

Problems of protecting against cavitation by using additives have been studies relatively recently. The papers [3, 9] present data on laboratory tests of various additives using magnetostrictive vibrators as well as full-scale tests on marine diesel engines.

In the laboratory tests of individual additives on MSV, using a three-hour program, the following data were obtained:

Type of Additive	Specimen Weight Loss in mg/hour
Tap water	110
Chromates	62
AM emulsion	49
VNII - NP-117	35
Emulsoid KS	13
INK-S	46

Laboratory tests of various additives to be used in water showed that the best result in the short-term protection of the surfaces of specimens of various materials against cavitation damage are shown by the additive KS (Urals Polytechnic Institute) and VNII - NP 117.

However, short-term laboratory tests on magnetostrictive vibrators did not make it possible to take account of a factor as important as the time during which the additives acts, that is, its serviceability. Therefore, these tests are meaningful only for a preliminary estimate of how effective a given additive is. Based on laboratory tests, the additive can be recommended only for long-term full-scale tests on diesel engines. Materials from tests made from aluminum and cast-iron specimens in water containing these additives are shown in Figures 65 and 66.

Relatively good results from laboratory tests were also shown by the Shell Dromus additive, and the Dikul 1 and Dikul 5 additives, of British manufacture.

It must be noted that even for accelerated laboratories, the effectiveness of the given additive will depend on the amplitude-

frequency characteristic of the vibratory field of the stack, that is, on the vibrational acceleration, since the process of cavity growth and collapse, as well as cavity size and cavity number are associated with the vibrational acceleration. This, in turn, affects changes in the ratio of mechanical and electrochemical factors in the overall damage process. Therefore even results of laboratory tests conducted in different vibration frequency ranges and at different amplitudes may not agree. Figure 67 shows the specimen damage curves obtained when the vibration amplitude was varied using different additives. The rate of increase in damage for different additives is not identical, and depends on the vibration temperature, and therefore, neither is the effective production in different ranges of vibration amplitude the same.

Figure 65: Damage of Specimens in Water Containing KS
Additive: a - Steel 10, b - Gray Cast-iron,
c - copper

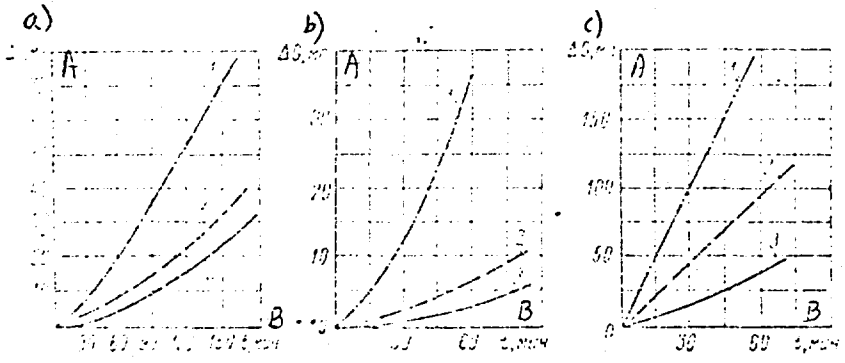

1 - Water 2 - Water and 0.01% KS 3 - Water and 0.1% KS

Key: A: ΔG, mg
B: t, min

Figure 68 presents curves showing the protection of specimens when additives are added to the water, compared to damage incurred in tap water.

Figure 66: Specimen Damage: a - AL 4 Specimen

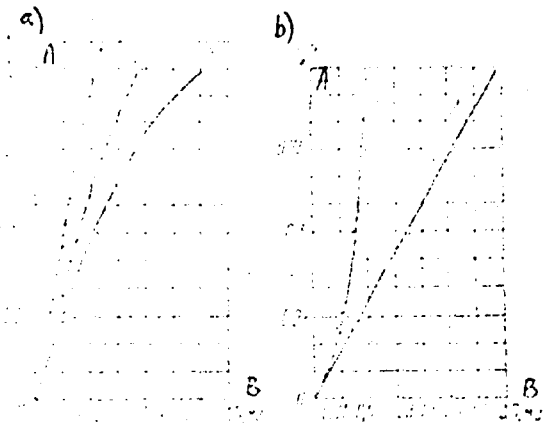

1 - In water containing VNII - NI-117 2 - In water containing Shell Dromus additive

3 - In water containing no additives

b - Cast-iron specimens:

1 - In water containing VNII NP-117 2 - In water containing no additives

Key: A: t, hr
B: ΔG, mg

Figure 67: Effect of Additive on Damage (f = 6.2 kHz, t = 55°C, p = 1atm):

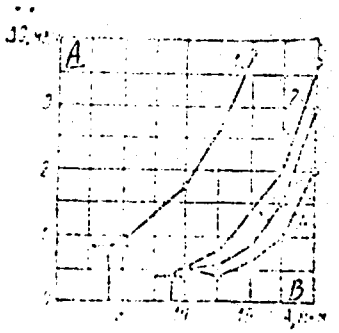

1 - Distilled water containing no additives
2 - Water + 6g/l of baratt-nitrate
3 - Water + 2.5 g/l $K_2Cr_2O_7$
4 - Water + 1% oil

Key: A: ΔG, mg/hr
B: A, microns

Figure 68: Protection of Specimens Using Various Additives:

1 - KS emulsoid 2 - Akvia-Glar 3 - VNII Rp-117
4 - INK - 8 5 - $K_2Cr_2O_7$

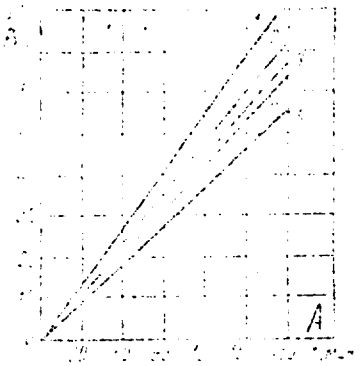

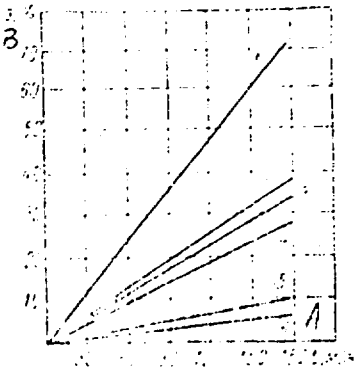

Key: A: t, min
B: Protection, %

Figure 69: Protection of Specimens in Water Containing Additives:

1 - VNII NP-117 2 - KS emulsoid 3 - Shell Dromus
4 - INK - 8 5 - $K_2Cr_2O_7$ 6 - $K_2Cr_2O_7$ + $NaNO_2$

Key: A: t, min
B: Protection, %

These tests were conducted with a vibration amplitude of 30 - 36 microns at a vibration frequency of 8000 Hz.

Figure 69 presents the curves on the extent of protection for specimens when the amplitude vibration was 60 - 65 microns and the vibration frequency was 8000 Hz. These curves were recorded at considerably higher accelerations than the curves in Figure 68. Therefore the degree of protection using various additives is not the same in both cases.

Conducting full-size tests of additives on operating diesel engines provides the final evaluation of the efficiency of a particular additive.

For example, the KS additive cannot remain in aqueous solution for a long time, precipitates, and when diesel engine liners and blocks undergo high-frequency vibrations is stripped off their surfaces.

After 500 hours of testing, opening up the water jackets of a Ch 15/18 diesel showed that the cast-iron jacket of the blocks made of Ch 15/32 cast-iron and tested with a 0.1% KS additive concentration, had pittings over their entire surfaces to a depth of 0.3 - 0.5mm, that is, the same kinds of pittings as in the series-built engine operated without the additive. Damage was observed also in the cylinder liners. Similar results were obtained from testing KS emulsoid in other diesel engine models as well.

Tests were conducted also on other kinds of additives on diesel engines of domestic and foreign manufacture. First of all, we must mention the additive VNII NP-117 and Shell Dromus S additive. The best result in eliminating damage effects in surfaces of cast iron, steel and aluminum alloys swept by water was shown by the additive VNII NP-117 in low-speed and moderate-speed diesel engines with low vibro-activity, of models DN 23/30, D 30/50, D 43/61, and from SKL Plant (GDR). Figure 70 shows liners of the 4 Ch 17.5/24 diesel engine from the SKL Plant having served 2000 hours in diesel engines with 0.5% VNII NP-117 additive and Figure 71 shows liners after 2000 hours of operating the diesel engine without use of an additive. The liners of a diesel engine that had operated with an additive are completely clean and not affected by cavitation or corrosion.

The VNII NP-117 additive dissolves readily in water and forms a stable highly dispersed emulsion of the oil-water type, increasing the

damping properties of the water. At the present time, several diesel-building plants have recommended this additive for commercial use and production and are adding it in the amounts of about 1% of the volume of coolant.

In those cases when electrochemical processes predominate in the cooling systems of diesel engines, a potassium bichromate additive has proven itself. This additive gives good results in protecting cylinder liners and blocks of high-speed light diesel engines of models Ch 10.5/13, Ch 15/18, and Ch 18/20, exhibiting high-frequency intense vibrations, against cavitation damage. In these types of diesel engines, evidently electrochemical processes also play a significant role in the overall damage incurred from cavitation. The potassium bichromate type of additive is a mixture of potassium bichromate $K_2Cr_2O_7$ and technical sodium nitrate $NaNO_2$ in a 1:1 ratio. The additive is introduced into the cooling system in the amount of 0.5% of the weight of the water in the system. The time by which a next addition of the additive is made is determined from the change in the color of the water in the system of the inner circuit from orange-yellow to yellowish-greenish to green. When the potassium bichromate - nitrate additive is used, relatively good protection of liners against damage is provided. A full-size test of the effectiveness of this additive in Ch 15/18 diesel engines was carried out in many steamship lines with a large number of engines.

Thus, based on the data of the Leningrad Institute of Water Transportation, the additive was tested in the 1959 navigation season in 44 engines in the Gor'kiy Steamship Line and 32 engines of the

Northwest River Steamship Line. The dismantling of ten Ch 15/18 engines, which had served with the additive from 2300 to 4700 hours showed that when this additive is in regular use, damage to liners and blocks of diesel engines is considerably reduced. When there is an extended interruption in additive use, the damage process occurs with its usual intensity.

Figure 70: Liner After 2000 Hours of Operation With 0.5% VNII NP-117 Additive

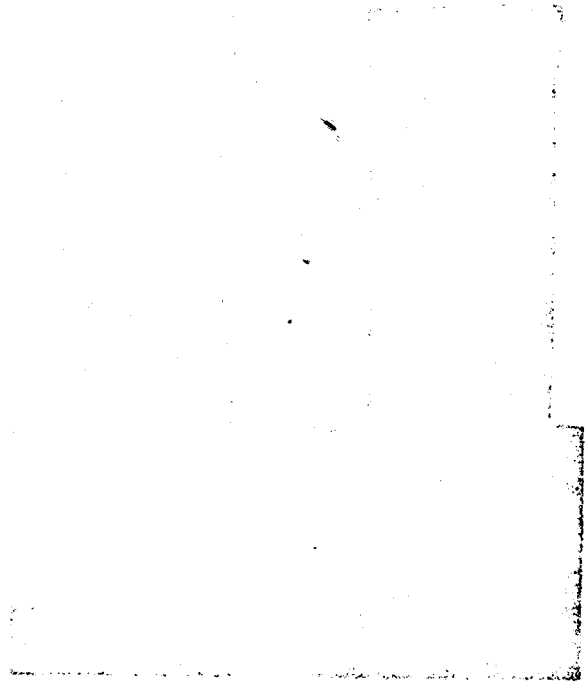

The mean consumption of the potassium bichromate - nitrate additive per 1000 hours of operation for the 3D6 engines is about 700g. The additive of this type has also proven itself in Ch 18/20 diesel engines without monoblock.

Figure 72 shows a section of the block of a Ch 18/20 diesel engine that has been run for 500 hours with the KS additive. Damage areas in

the form of gleaming patches of internal surface are clearly visible in the block. When the engine was operated with the potassium bichromate additive, the initial stages of cavitation damage to the block appeared only after 1000 hours. Figure 73 shows the cylinder liners of the 12 Ch N 18/20 diesel engine after 500 hours of operation with the potassium bichromate additive. The liners had no traces of damage to the porous chromium layer. A disadvantage of this additive is its toxicity, and when it is present in very slightly higher amounts than the specified norms for protection against cavitation damage, erosion is intensified.

Figure 71: Liner After 2000 Hours of Operation Without Additive

Figure 72: Block Damage

Figure 73: Cylinder Liners of Diesel Engine After 500 Hours of Operation with Potassium Bichromate Additive

Figure 74: Effect of Additives on Cavitation Damage to Cast-iron As A Function of Additive Concentration in Water:

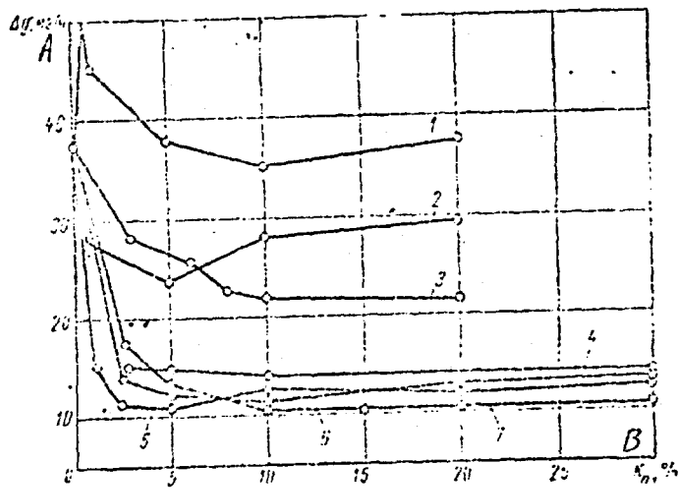

1 - $NaNO_2$ 2 - Potassium Bichromate 3 - Barrate-nitrate
4 - Organic inhibitor 5 - Emulsion of Oil No 1 6 - Emulsion of Oil No 2
7 - Emulsion of Oil No 3

Key: A: Δg, mg/hr
B: K_{add} [add = additive]

Laboratory tests on MSV make it possible to select the additive concentration K_{add}. Figure 74 shows the curves of specimen damage rates as a function of the additive concentration with respect to the volume of water used. These data show that the maximum percentage of the additive in the water that still affords an effective protection against damage does not exceed 2.5%. The optimal concentration is 1 - 1.5%. However, the use of additives is desirable only in running diesel engines.

Using even the most efficient additives in coolant water is an extreme measure in controlling cavitation-erosion damage of newly designed diesel engines. The most radical and advantageous methods must be viewed only as design-technological measures to control the cavitation-corrosion processes.

Of those tested, the additive VNII NP-117 and potassium bichromate can be recommended.

27: Reducing Corrosion Damage By Building Rational Cooling Systems

Use of closed cooling systems is preferential for diesel engines of all models from the standpoint of reducing the cavitation damage to liners and blocks, for the following reasons:

1) In a closed cooling system the optimal temperature regime and the required pressure, for example, 80-85°C at a pressure of 1 - 1.2 atm, or 90-95°C at higher pressures, can be maintained;

2) The use of the same water for a long time in the system reduces the gas content and diminishes cavitation intensity. Only with a closed cooling system can additives for water be used to reduce cavitation damage;

3) It is no longer necessary in marine conditions, to use bilge sea water in cooling an engine, which causes severe corrosion and leads

to large salt deposits in the extra-jacket spaces;

4) The system of temperature regulation in which rapid buildup of the diesel engine after starting is maintained is achieved more easily with a closed cooling system than in a flow-through type. For operation in all load and velocity regimes, the water temperature is near-optimal.

In designing the cooling system, one must take account of the following factors.

1) The width of the water cavity must be not less than 10mm to avoid intensifying cavitation. Here consideration is given to the fact that when the distances between the vibrating liner and the block are small, damage to the block walls is intensified.

2) To prevent abrupt changes in flow rate and pressure, there must be no local constriction in the water jacket. Selection of the water jacket dimensions with which abrupt changes in pressure and flow rate are absent can be done by the electrodynamic analogy method. In this case, the elements of the water cavity of the engine (block section and liner) made of wax or stearin are placed in a bath containing an aqueous solution of copper sulfate. Using a moving rod one determines the electrical voltages at different points of the model. The constant-voltage lines correspond to the constant-flow rate lines. The flow rate of the water in the jacket must not be greater than 2m per second.

3) The sites of water inflow into the jacket and water outflow must not have pressure drops so abrupt that hydrodynamic cavitation can be induced. Therefore the flow rate in the inflow pipes and ducts must not be more than 5m/sec. Preference must be given to the tangential inflow of water to the cylinder liners (although in most cases this does

not play a decisive role).

4) The support zones of cylinder liner and block must be designed so that water does not enter the gap between the liner and the block. Here it is necessary to insure the highest possible stiffness of both liner and cylinder block.

5) The capacity of the fresh water pump must be selected so that the drop in the temperatures of the water flowing into the engine and the exiting water must not exceed 7 - 10°C. Only in this case can the optimal water temperature means be maintained in the region of the cylinder liners to reduce cavitation damage. The system of temperature regulation must include a 2-valve thermostat and exhibit low regulatory non-uniformity.

6) The heat exchanger for cooling the fresh water must exhibit resistance to corrosion that may be caused by sea water. Flowing sea water enters the heat exchanger in a self-suction water pump made of anticorrosive materials.

7) The cooled surfaces must be as smooth as possible.

Dissimilar materials forming pairs must be voided. The cooling system must be provided with a filter to trap contaminants and corrosion products and to insure complete drainage of the coolant fluid when the system is emptied.

CHAPTER SIX

METHODS OF INCREASING CAVITATION RESISTANCE OF LINERS AND BLOCK SURFACES

28: Requirements of Metals Used in Diesel Engine Liners and Blocks

Selection of the material used in liners subjected to cavitation erosion must make allowance for the mechanism of metal damage during cavitation. In its initial stage, damage is expressed in the formation of opalescence colors on the metal followed by formation of micro-relief. The macroscopic damage pattern consists of a cluster of individual deep pits, grooves, gouging of metal particles and so on. The nature of damage to parts in cavitation differs and is determined by the characteristic of the vibratory field of the diesel engine (vibration frequency and amplitude), the flow rate, and the nature and structure of the alloy.

The area of damage on individual surfaces extends from fractions of a millimeter to hundreds of square centimeters. The process lasts from several minutes to thousands of hours. This is associated with the intensity of the diesel engine vibratory field. Metallographic examination shows that in steels the initial damage foci arise primarily at the ferrite-perlite interface, and then spread into the ferrite. With time, this leads to chipping out of metal particles. An examination of the damage foci occurring when cavitation due to vibration at frequencies up to 3000 Hz occurs showed a 20 - 30% local increase in micro-hardness. The nature of the damage depends on the character of the metal. For example, damage to armco iron occurs locally, by forming deep pits,

while damage to metals such as aluminum and copper occurs initially due to depression of the metal, followed by the formation of funnel-shaped pits.

Cavitation caused by high-frequency vibrations forms damage areas in which metal fusion is observed. Macroscopic analysis of these damaged areas indicate that during cavitation temperature also plays a certain role, therefore, the edges of pits in microvolumes are melted. From the initial stages of damage with the formation opalescence colors and by the melting of pit edges in a given material, one can indirectly estimate the temperatures in the microvolumes. In all probability they are high and are in the hundreds of degrees. Damage foci appear especially distinctly when tests are made of materials on MSV.

Cavitation damage to surfaces occurs gradually, initially there is first a change in the microrelief, and then greater damage sets in, characterized by the formation of clusters of deep pits.

Traces of plastic deformation manifested in slip lines are observed in the metal layers lying at the damaged surface areas, and manifested in fine structure in iron, in individual grains. Plastic deformation at the structure of cavities in copper occurs somewhat differently. Crystal-like structures form in copper. Deformation of the surface beneath the damaged metal is in the form of viscous flow. Extension of the deformation is uneven. In some grains severe form modification occurs, while in others there is a nearly complete absence of traces of deformation.

The presence of high temperatures in microvolumes in a damage area when high-frequency cavitation is underway causes thermal and electro-

chemical damage, which is aggregated with the mechanical damage. Because of this, the overall damage process in a surface is accelerated.

Thus, the mechanism of metal damage in cavitation is highly complex and depends on numerous factors. First of all, they must be regarded as including the intensity and frequency of surface vibrations, pressure in the medium, and the properties of the surface being damaged. Materials subject to cavitation erosion must exhibit the following main properties: high surface hardness, which can be attained also by using a protective coating, uniformity of structure, heat resistance, and corrosion resistance.

29: Role of Machining Finish

The machining finish of a surface significantly affects the intensity of surface damage in the same time interval. We know that a rough surface is damaged more intensely due to the accumulation in scratched depressions of vapor-gas nuclei which intensify the cavitation process. Discontinuity produced in a fluid is facilitated when vapor and gaseous cavitation nuclei adhering to the surface of a solid are present.

However, it is assumed that the intensification of cavitation and cavitation damage on a rougher surface is caused by the the presence of turbulence in the liquid owing to the presence of lands. This increases the rupture stresses in water and promotes more favorable conditions for the formation of cavitation cavities under otherwise equal conditions.

During the investigation tests were made of cast iron, steel, and aluminum specimens on a a magnetostrictive vibrator (Figure 75). In all cases the weight loss (damage intensity) for the same time interval

increased if the machined surface finish was degraded. However, the intensity of damage for different materials differs and is characterized by the hardness of the given material and the structure. For example, AL4 aluminum, when the surface roughness is increased from ▽7 to ▽3 over the same time interval, the intensity of damage based on weight rose by roughly 1.5 - 1.6 times, for cast iron - by 2 - 2.3 times, and for steel - it increased by 2.3 - 2.5 times. Therefore, the greatest effect of surface finish on damage is observed in steel, and the least - in aluminum when the rating is made on a basis of weight loss.

In estimating damage volumetrically the opposite situation is found. The greatest volume is lost by aluminum, and the least - by steel. This factor must play a definite role in selection of materials for each specific part subject to cavitation erosion, since an aluminum alloy can have deeper damage pits than steel or cast iron with a lower weight loss.

It must be noted that the better a surface is machined, the less intense is the damage in the initial period. This is readily seen in a plot of the damage to a surface with ▽9 of a cast-iron specimen (Figure 76). Conversely, a rougher surface is damaged more intensively in the initial period, and then the rate of damage decreases, which can be seen from the test data in Figure 76.

The variation in the rates of damage in the initial and subsequent periods for a well-machined surface is accounted for by the fact that until its surface roughness is increased by damage, it is damaged more slowly; in contrast, a rougher specimen, on being intensively damaged in the initial period, has its surface smoothed resulting in the damage rate then slowing down.

Figure 75: Damage to Specimens with Different Machined Finish Tested on a 11.8 kHz MSV (A = 0.008 mm):

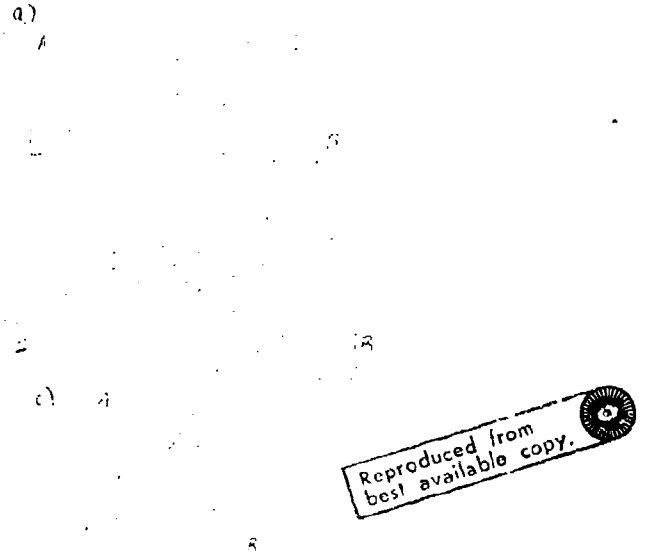

a - AL4 b - Gray cast-iron c - 38KhMYuA Steel

Key: A: t, hr
B: $\triangle G$, g

Figure 76: Damage to a Cast-iron Specimen (f = 11.8 kHz, A = 0.008 mm)

Key: A: t, min
B: $\triangle G$, g

It must be noted that the time interval after which a change occurs in the damage rate either toward a higher or toward a lower value depends entirely on the intensity of the vibratory field.

For accelerations of 50 - 60g, this interval is hundreds of hours, and for accelerations of hundreds and thousands of g's - it is in the minutes.

Thus, studies with specimens having different machined surface finishes show that increasing the surface machined finish in any case leads to a reduction in cavitation damage, especially in the initial period.

30: Damping Coatings

To eliminate cavitation damage to the cooling surfaces of series-built diesel engines, basically two types of coatings can be recommended. The first type of coating includes all damping coatings attenuating the vibratory field of the liner or block of the diesel engine and eliminating the phenomena of cavity formation and collapse, and the second type of coating includes all hard and refractory coatings which cannot eliminate the effects of cavitation and bubble collapse, but which, due to their hardness and refractoriness, protect the surface against the action of pressures, temperatures, and electrochemical processes induced in the collapse of cavities.

Any materials exhibiting relatively high coefficients of internal friction can be used as damping coatings. One must only consider the fact that the suitability in diesel engine building of a given coating

depends on the thickness of the damping layer applied. If the coating will exhibit good damping properties only for thicknesses of several millimeters it will not be useful, since in this case the passages for the coolant liquid will be significantly constricted.

To establish the type of coating exhibiting the best damping properties for minimum thicknesses, numerous tests were made on specimens using magnetostrictive vibrators. Varnishes, epoxide and polyester resins with fillers, elastomers and Nairit coatings were used as damping coatings. The test results showed that varnishes, epoxide resins and polyester resins and GEN elastomer, even though exhibiting damping properties, still owing to their high brittleness do not protect the surface against cavitation damage. In view of their brittleness, they do not remain on the surface for a long time, but crack and scale off. These coatings on diesel engines with moderate vibro-activity of 20 - 25g protect the surfaces only for 30 - 70 hours. This brief protection is meaningless in practice.

The Nairit type of coating is stronger. Results of tests made on MSV and in diesel engines showed that they exhibited several advantages in protecting cooling surfaces against damage. Figure 77 shows the breakdown time curves for coatings deposited on a cast-iron specimen in relation to coating thickness b. Curve 1 characterized the breakdown of a coating on a 12kHz MSV with a vibration amplitude of 10 microns for S_c = 5100, and Curve 2 shows the breakdown of a coating tested on a 19kHz MSV with a vibration amplitude of 5 microns for S_c = 8000. From these curves it follows that the coating breakdown sets in more rapidly, the higher acceleration of the surface vibrations.

Results of tests made on MSV established that the service time of the specimen before coating breakdown depends on parameters such as the coating thickness, vibration acceleration, and the material of the specimen on which the coating was deposited.

Figure 77: Damage of Coated Specimens Tested on a MSV

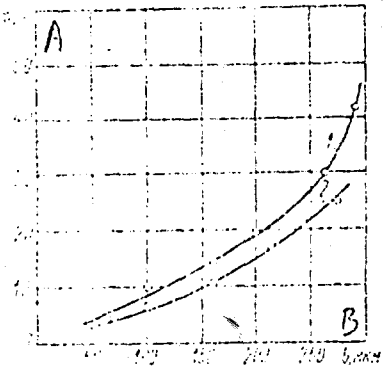

Key: A: t, hr
B: b, microns

Failure pits appeared on the coatings of limited thickness, 50 - 60 microns, in 4 - 5 hours of service. The initial failure in thicker coatings of 200 - 500 microns set in after 25 - 30 hours of service.

More intense damage to coatings occurs when tests were made on MSV producing higher accelerations. Thus, the damage to a 200 - micron Nairit coating on a steel specimen tested with a 12kHz MSV with a vibration amplitude of 10 microns and with S_c = 5100 occurred in 23 hours. The same damage, but on a 19kHz MSV with a 5 micron amplitude and S_c = 8000 occurred in 17 hours, that is, the higher the acceleration of the vibrational motion of the specimen the more rapidly the breakdown and damage to the coating sets in.

Using the data of the time scale factor characterizing the dependence of damage on the acceleration of the vibrational motion of a surface, one can determine how much time a given coating deposit on the external surface of a diesel engine cylinder liner will elapse before breakdown, if the diesel engine liner exhibits a vibratory field characterized by S_{c_x}. Such reconversions were made and are plotted in curves in Figure 78 for a Nairit coating deposited on steel and cast-iron cylinder liners of various diesel engines. Coating a steel liner with Nairit, for the same coating thicknesses and vibration accelerations, lengthened the service time longer than coating of a cast-iron liner. This evidently is associated with several poorer adhesive properties of the coating with respect to cast iron. A 300 micron coating, with $S_c = 10$, will function before breakdown for 1580 hours on a steel liner, and for 1000 hours on a cast-iron liner, with the very same acceleration. These data show that in diesel engines of increased vibro-activity ($S_c > 20$), the operating time of a coating is sharply reduced. For example, in a diesel engine with cast-iron linings in which the vibrational level $S_c > 60$, a 300 micron coating will prolong the surface life of the liner by no more than 400 hours.

Full-scale tests of a Nairit coating were made on Ch 10.5/13 and Ch 15/18 diesel engines. To accelerate the breakdown count the vibrational fields of the diesel engines were intensified by increasing the thermal gap between the piston and the liner by 0.2 - 0.3mm. For a 0.6mm gap, the vibrations of cast-iron liners in a Ch 10.5/13 diesel engine amounted to 140 g and coating breakdown was achieved in 130 - 150 hours of operating, that is, the service life of the coating was checked by accelerated

methods. Full-size tests of Nairit coatings on diesel engines agree well with the data of accelerated tests on MSV.

Figure 78: Service Time of a Nairit Coating of Various Thickness b on Steel Liners with Different Vibrational Levels

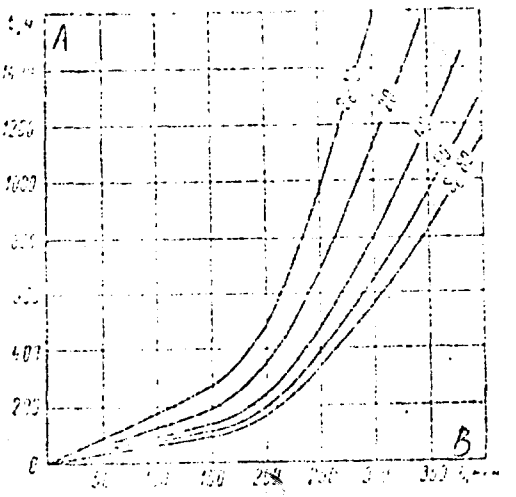

Key: A: t, hr
B: b, microns

In the tests the effect of coatings on the internal surface of the liner, the surface facing the combustion chamber (Figure 79), was established. From Figure 79 we see that in the area of the combustion chamber (the TC area), the liner temperature rises by 8°C for a 100% load, (Curve 1 and 1'). Measured downward, the liner temperature increases by 20°C and did not exceed 130°C, which is wholly acceptable. The possibility of using coatings with low thermal conductivity must be decided for each specific case in relation to the initial temperature condition of the engine when operating at full load.

Nairit coatings will prolong the life of diesel engine cylinder liners. Calculated data on coating service life are in agreement with experiments.

The type of coating of cylinder liners or blocks of diesel engines must be selected in relation to the vibratory field of the diesel engine determined from tests of coatings made on MSV using material specimens.

Thus, any coatings can be preliminarily tested on MSV and recalculated for the operating conditions of cylinder liners in diesel engines.

Rubberizing compositions of the NT Nairit consist of 50 - 70% solutions of rubber mixture of liquid Nairit (low-molecular chloroprene rubbers of different types) in a solvent. The solvent includes 76% solvent naphtha, 19% turpentine and 50% butanol. Damping anticavitation coatings consisting of liquid Nairit exhibiting the consistency of enamel paint, can be applied on liners with brush, sprayer, and immersion of parts. When painting with a brush, a layer of 150 - 200 microns is applied in each stroke. The properties of liquid Nairits, methods of preparing parts for coating, and the coating itself are described in this study [5] and do not require a detailed presentation. An advantage of this method of coating is the fact that it can be used in service in the repair of diesel engines and can be applied even on liners and blocks where partial cavitation damage has already occurred.

31: Solid Coatings

Since the mechanical factor is fundamental in cavitation damage to cooling surfaces of liners and blocks in diesel engines, that is, damage

Figure 79: Dependence of Temperature at Different Liner Points in a Diesel Engine on Load

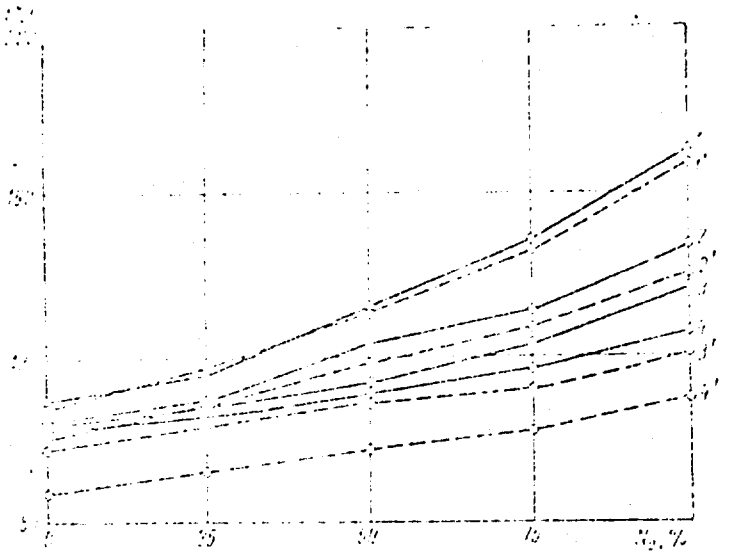

1 - Upper ring t, °C 2 - 30mm from the TDC 3 - 60mm from the TDC

4 - in the area of the BDC (bottom dead center)

Figure 80: Increase in the Surface Life of a Liner When Hard Chromium is Deposited on its Surface

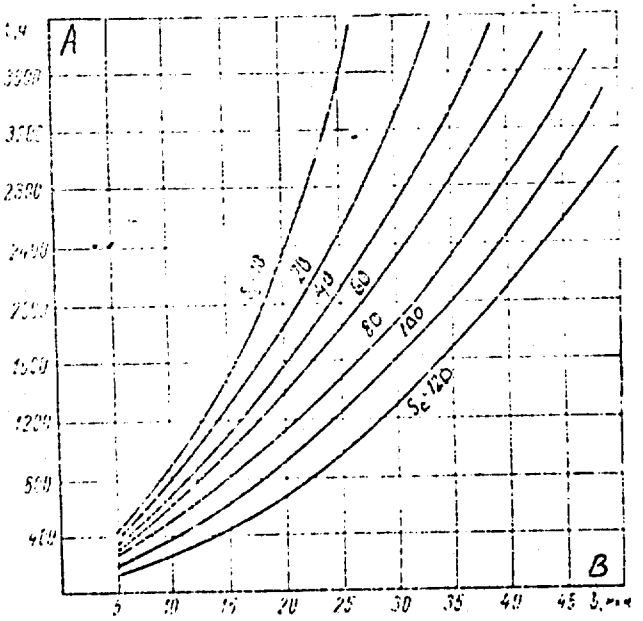

Key: A: t, hours
B: b, microns

CHAPTER SEVEN

CALCULATION OF CAVITATION DAMAGE TO DIESEL ENGINE CYLINDER LINERS

32: Determination of Liner Vibration Accelerations

Based on the data of theoretical and experimental studies, an approximate method of calculating the accelerations of liner vibrations, and liner cavitation damage, in which the absolute weight losses and the maximum operating time of liners before replacement because of cavitation damage to surfaces swept by water are determined.

To define the maximum time of surface liners, it appears necessary to determine several intermediate parameters, which must be regarded as including first of all the free-vibration frequency, the amplitude of liner vibrations at a given frequency, vibration acceleration, and absolute weight loss. One must calculate the free-vibration frequency to calculate liner accelerations. In calculating free vibrations, it is provisionally assumed that a liner vibrates without the piston pressed against it by the side pressure forces. The calculation is made in the following order for the specified quantities: n_1 is the number of cylinder waves (1, 2, 3, ...); m is the number of axial half-waves (1, 2, ...); a is the mean liner radius; l is the liner length; h is the liner thickness; σ is Poisson's ratio; ρ is the density of the liner material; E is Young's modules; and g is the acceleration due to gravity.

The coefficient λ of the axial wave length and the quantity b are determined:

$$\lambda = \frac{\pi a}{l} m \quad \text{and} \quad \beta = \frac{h^2}{12a^2}.$$

The frequency coefficients K_o, K_1 and K_2 are found from the calculated values of λ and β:

$$K_0 = \frac{1}{2}(1-\sigma)^2 (1+\sigma)\lambda^4 + \frac{1}{2}(1-\sigma) \times$$
$$\times \beta \left[(\lambda^2 + n_1^2)^4 - 8\lambda^2 n_1^4 - 2n_1^8 + n_1^4\right];$$
$$K_1 = -\frac{1}{2}(1-\sigma)(\lambda^2 + n_1^2)^2 + \frac{1}{2}(3-\sigma-2\sigma^2)\lambda^2 +$$
$$+ \frac{1}{2}(1-\sigma) n_1^2 - \frac{1}{2}(3-\sigma)\beta(\lambda^2 + n_1^2)^3;$$
$$K_2 = 1 + \frac{1}{2}(3-\sigma)(\lambda^2 + n_1^2).$$

Then, one determines Δ

$$\Delta = \frac{K_0}{K_1} - \frac{K_2}{K_1}\left(\frac{K_0}{K_1}\right)^2,$$

then the free-vibration frequency of the cylinder liner is calculated:

$$f_{fr} = \frac{1}{2\pi a}\sqrt{\frac{E}{\rho(1-\sigma^2)}}.$$

The frequencies of free vibrations are determined for the following cases:

$$n_1 = 2; \quad n_1 = 3; \quad n_1 = 2;$$
$$m = 1; \quad m = 1; \quad m = 2.$$

The amplitude of the liner vibrations is determined as the difference between the amplitude A_{max} for dynamic exposure to side forces P_{max} and the amplitude of the static deflection of the cylinder liner A_{st} in the static application of side forces P of maximum value:

$$A = A_{max} - A_{st}$$

The static deflection is found from the expression

$$A_{st} = P_{max} / K_{red},$$

where $K_{red} = \omega^2 M_{red}$ is the reduced stiffness [red = reduced].

The reduced mass of the liner is determined by the following formula:

$$M_{red} = \frac{\pi c_1 h_p}{2} = \frac{1}{\sin \frac{\pi c_1}{l}}.$$

Here $c_1 = c_o + 0.067$ H, the distance from the upper edge of the cylinder liner to the point corresponding to the position of the piston pin for a 30° crank angle (it is assumed that here the maximum side forces will be operative); c_o is the distance between the upper edge of the cylinder liner and the piston pin axis when the piston is in the TDC; and H is the piston stroke.

The maximum side force is determined with the expression:

$$P_{max} = 2,7 \lambda' P_e F_p \qquad [p = \text{piston}]$$

where $\lambda' = R/L$ is the ratio of the crank radius to the connecting rod length of the diesel engine;

P_e is the mean effective pressure;

F_p is the piston area.

The dynamic displacement of the liner A_{max} is found from the expression

$$A_{max} = A_{st} k'_1.$$

Here, $k'_1 =$ [illegible] is the period of liner vibrations determined from the calculated vibration frequency f_{fr}; T is the rise time for the load of the side pressure force, from zero to P_{max} determined from the plot of the forces or taken to be the time when the crankshaft rotates by the angle φ, that is, $T = \varphi / 6n$ sec.

In the calculations it is convenient to assume $\varphi = 15 - 30^{\circ}$ CA [CA = crank angle], since here the maximum side force P_{max} in the direction of the piston against the liner will be operative.

Therefore, the amplitude we seek will be

$$A = A_{st} (k'_1 - 1).$$

Inserting the values of A_{st} and k'_1, let us write the final equation for the vibration amplitude in the form:

$$A = 5{,}1 \frac{\lambda' p_e F_p \tau}{\omega^2 a l h \rho T} \sin^2 \frac{\pi a c_1}{l}.$$

In this expression, λ'_1, p_e, F_p, a, l, h, ρ, and m are specified by the design and the calculation, while the values of τ, T, and c_1 are calculated.

The acceleration of the vibrational motion W_{cal} of cylinder liners is calculated based on calculations of the vibration frequency and amplitude, using the following expression:

$$W_{cal} = A\omega^2_{fr} = A\,(2\pi f_{fr})^2.$$

For further calculations, it is useful to convert the liner vibration acceleration thus obtained into a dimensionless quantity,

using the following expression:

$$S_c = W_{cal} / g.$$

33: Determination of Absolute Liner Weight Losses

From experience we know that when $S_c < 20$, cavitation damage to cylinder liners proceeds slowly and is commensurable with the service life of a liner based on wear of the cylinder surface.

When $S_c > 20$, cavitation damage proceeds intensively, and the higher S_c, the faster the damage process.

To estimate the intensity of cavitation damage to cylinder liners in diesel engines, let us use an empirical function characterizing the intensity of damage to cylinder liners (based on their weight loss) as a function of vibration acceleration and service time.

$$\Delta\bar{G} = \frac{\Delta G_x}{\Delta G_0} = 5 \cdot 10^{-7} t^{1,45} S_c^{\left[0,6 - \frac{16}{(S_c - 15)^2}\right]}, \qquad (32)$$

where $\Delta\bar{G}$ is a dimensionless coefficient characterizing the weight loss of the cylinder liner;

$\Delta G_x = 10^{-3}$ kg are the weight losses of the cylinder liner during its service;

$\Delta G_o = 10^{-3}$ kg is the weight loss of the liner taken as the zero threshold;

$\bar{t}$ is the dimensionless coefficient characterizing the service period of the cylinder liner; $t = t_x / t_o$ (here t_x is the service period of the liner in hours; t_o is the service period of the liner taken as the zero threshold in which processes of cavitation damage begin).

Data for the empirical function (32) were obtained from experiments on diesel engines and on specimens tested on magnetostrictive vibrators and are plotted in Figure 81.

Figure 81: Nomogram for Estimating Weight Losses

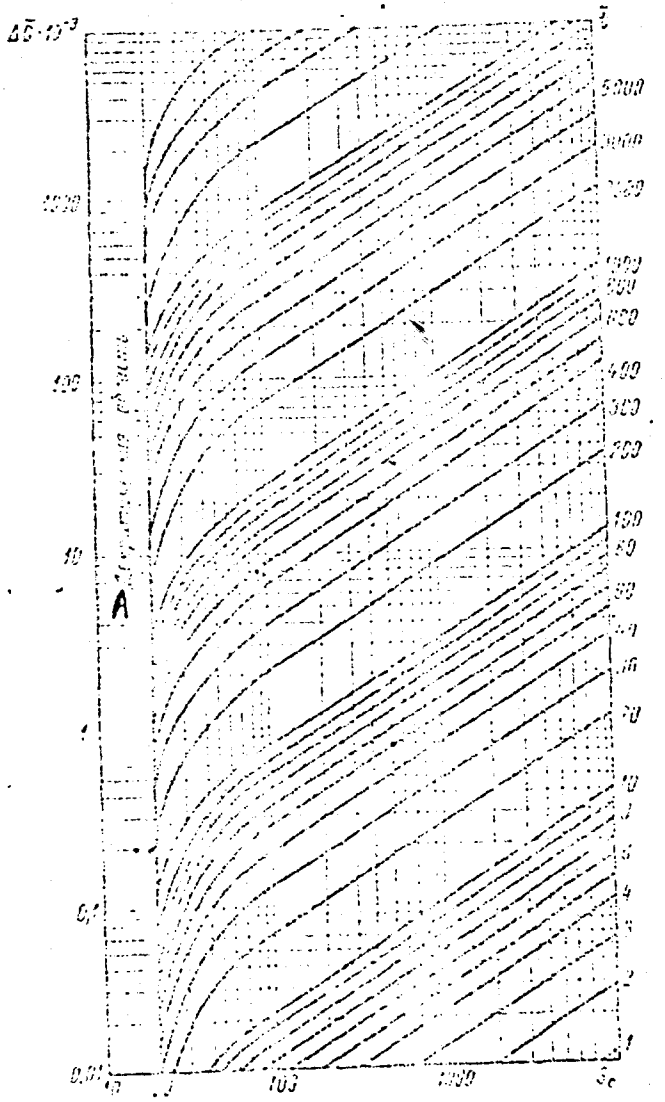

Key: A: Precritical region

Since the intensification of cavitation damage is significantly affected by the temperature of the coolant liquid, one must take its effect into account in the calculation, since the cooling temperature can differ in different diesel engines.

Data characterizing damage intensity, represented as the empirical formula (25) were obtained for a 65 - 75°C diesel engine cooling temperature, that is, for some moderate effect of temperature on cavitation damage.

In general form, the dependence of cavitation damage on temperature is shown in Figure 82.

Figure 82: Damage to a Surface As a Function of Cooling Temperature

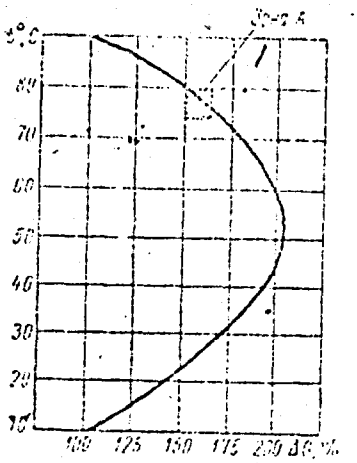

Key: 1 - Zone A

The actual cooling temperature of diesel engines in extended tests in operating conditions is 75 - 80°C (Zone A , Figure 82). At this temperature cavitation then occurs at the surfaces of liners swept by water. Therefore, it is useful to introduce the dimensionless

coefficient I, characterizing the true damage to liners at any cooling temperature, but even at 75 - 80°C, into the derived empirical formula for $\overline{\Delta G}$. . Table 19 lists the values of the coefficient I.

Damage to cylinder liners in diesel engines, with allowance for the fact of temperature, can be determined from

$$\overline{\Delta G} = 5 \cdot 10^5 I \left(\frac{t_x}{t_0}\right)^{1,15} S_c^{\left|0,6 - \frac{10}{(S_c - 15)^2}\right|}. \qquad (33)$$

In its final form, the absolute damage to cylinder liners is found as follows:

$$\Delta G_x = \Delta G_0 5 \cdot 10^5 I \left(\frac{t_x}{t_0}\right)^{1,15} S_c^{\left|0,6 - \frac{10}{(S_c - 15)^2}\right|}. \qquad (34)$$

Table 19: Values of the Coefficients I

1 Температура охлаждения в °С	20	25	30	35	40	45	50	55
2 Коэффициент I	0,97	1,07	1,12	1,2	1,22	1,24	1,26	1,29
1 Температура охлаждения в °С	60	65	70	75	80	85	90	95
2 Коэффициент I	1,26	1,14	1,13	1,04	1,0	0,89	0,645	0,58

Key: 1. Cooling temperature in °C.
2. Coefficient I

Considering the experimental data, the surface finish, gaseous composition of the coolant liquid, flow rate of the liquid and the use of additives increasing the damping properties of the water play a definite role in the buildup of cavitation damage, by attenuating or

intensifying it. However, these factors are not taken into account in the calculation, since they play a lesser role than the coolant temperature. Their effect must be allowed for, additionally, by experimental means.

34: Determination of the Maximum Service Time of the Cylinder Liner Before It Is Replaced Because of Cavitation Damage

Considering that the maximum allowable damage to a cylinder liner is the damage for which the liner is cavitated to three-fourths of the wall thickness in the most dangerous location and has to be replaced, a function (Figure 43) of the dimensionless coefficient ξ, characterizing the maximum permissible damage as a function of liner wall thickness was calculated based on operating data

$$\frac{\Delta \bar{G}}{\bar{S}}; \quad \bar{S} = \frac{S_x}{S_0}.$$

Here $S_0 = 10^{-4}$ m^2 is the area taken as the unit area for the maximum allowable damage.

Considering that the liner surface cavitates at specific locations, the extent of the cavitation area of a liner S_x was selected as a function of the cylinder liner dimensions:

$$S_x = 0.025 \pi D_{ou} l \text{ m}^2,$$

where D_{ou} is the external diameter of the cylinder liner, in m;
l is the length of the cylinder liner, in m.

Thus, the time required for the onset of the maximum allowable damage is determined from the expression (33) with $\Delta \bar{G} = \xi \bar{S}$

$$t_{max} = \sqrt{\frac{3 \cdot 10^2 \cdot D_{ou} l}{S_x / S_c \left[0.6 - \frac{10}{(S_c - 15)^2}\right]}} \, t_0 \text{ hr.} \qquad (35)$$

The main factors affecting the intensity of cavitation damage to cylinder liners - vibration intensity and coolant temperature - are allowed for in the proposed method. The rate of damage to cylinder liners is also affected by the thickness of the layer of water in the water jacket, the pressure in the cooling system, the flow rate of the water, the composition of the water, and other factors whose allowance in general form is difficult at the present time. Their effect must be taken into account by experimental means, as the diesel engine undergoes final adjustments.

35: Examples of Liner Calculation in Which the Maximum Service Period Was Determined

To calculate the cavitation damage to a liner, one must know its linear dimensions, as well as the characteristics of its material. The calculation is carried out in the MKGSS system. As an example, let us calculate a liner with the dimensions given below.

$a = 7.8 \cdot 10^{-2}$ m is the mean radius of the cylinder liner;

$l = 0.277$ m is the liner length;

$h = 6 \cdot 10^{-3}$ m is the thickness of the cylinder liner;

$\sigma = 0.26$ is Poisson's ratio for the steel 38KhMYuA;

$\rho = 8.67 \cdot 10^{2}$ kg $\cdot$ sec^2/m^2 is the density of the steel 38KhMYuA;

$E = 2 \cdot 10^{10}$ kg/m^2 is Young's modulus of the steel 38KhMYuA;

$g = 9.8$ m/sec^2 is the acceleration due to gravity;

$D_{ou} = 0.162$ m is the external diameter of the liner

$\delta = 3.3 \cdot 10^{-4}$ m is the thermal gap between the piston and the liner of an operating diesel engine with a 100% load;

m_o = 0.626 kg $\cdot sec^2/m$ is the mass of bodies in translation;

n = 1500 rpm is the diesel engine rpm (rated);

λ' = 0.28 is the ratio of the crank radius to the connecting rod length

$p_e = 7.85 \cdot 10^4$ kg/m^2 is the mean effective pressure of the diesel engine

$F_p = 1.76 \cdot 10^{-2}$ m^2 is the piston area

$c_o = 7.1 \cdot 10^{-2}$ m is the distance between the piston pin axis and the upper edge of the liner when the piston is in the TDC;

$H = 1.8 \cdot 10^{-1}$ m is the piston stroke;

n_1 = 2; 3 is the number of cylindrical waves;

m = 1; 2 is the number of axial half-waves;

$\beta = h^2/12a^2 = 36/\ 12 \cdot 6084 = 0.000493$ is a coefficient;

P_{max} = 1050 kg is the maximum side force.

The time required for a 15° crank angle from TDC is

$$T = \varphi/6n = 0.0016 \text{ sec.}$$

The distance from the upper edge to the piston pin axis for a 30° crank angle is $c_1 = c_o = 0.067\ H = 8.3 \cdot 10^{-2}$ m.

The further calculation is presented in Table 20.

Thus, according to the calculation, a liner can function in diesel engines for 3090 hours, after which it must be replaced. In practice, liners function for 2800 ~ 3200 hours in diesel engines.

The time required for the onset of the maximum allowable damage can even be somewhat less if one considers that the temperature regime of cooling is somewhat lower than the regime assumed in the calculation.

A cooling regime of 70°C was assumed in the calculation. Actually, in several sectors of the national economy diesel engines operate with cooling temperatures 55 - 70°C. This reduces liner surface life.

Table 20: Calculation of Quantities

Величины [1]	$n_1 = 2;\ m = 1$	$n_1 = 3;\ m = 1$	$n_1 = 2;\ m = 2$
λ	0,885	0,885	1,77
K_0	0,2877	1,5125	3,758
K_1	10,977	30,756	21,359
K_2	7,55	14,4	10,775
Δ	0,0267	0,0593	0,1015
f_{fr} в гц [2]	1680	2010	4100
τ в сек [3]	$0,06 \cdot 10^{-4}$	$4,97 \cdot 10^{-4}$	$2,44 \cdot 10^{-4}$
ω^2 в $1/сек^2$ [4]	$1,07 \cdot 10^8$	$1,64 \cdot 10^8$	$6,62 \cdot 10^8$
$\sin^2 \frac{\pi n_1 \tau}{T}$	0,654	0,654	0,9
A в м [5]	$4,44 \cdot 10^{-6}$	$23,7 \cdot 10^{-7}$	$3,97 \cdot 10^{-7}$
$W_{кр}$ в $м/сек^2$ [6]	475	390	263
S_c в g [7]	48,5	40	26,8
$\varphi = \left[0,6 - \frac{10}{(S_c - 15)^2}\right]$	0,591	0,594	0,529
S_c^2	9,9	8,95	5,25
t_{max} в ч [8]	3600	3310	4790
ΔG в кг [9]	$57,5 \cdot 10^{-3}$	$57,5 \cdot 10^{-3}$	$57,5 \cdot 10^{-3}$

Key: 1. Quantities

2. f_{fr} in Hz

3. τ in sec

4. ω^2 in sec^{-2}

5. A in m

6. W_{cal} in m/sec^2

7. S_c in g

8. t_{max} in hr

9. ΔG in kg

Let us show by the following calculation example that introducing additional intermediate supports dividing a liner into several parts, (two-part in this case) makes it possible to lower the vibrations and eliminate the cavitation damage.

The initial data for the calculation are as follows:

$n_I = 2; 3$ is the number of cylindrical waves;

$m = 1; 2$ is the the number of axial half-waves;

$a = 7.85 \cdot 10^{-2}$ m is the mean radius of the cylinder liner;

$l = 0.11$m is the distance from the upper edge of the liner to its center supporting shoulder;

$D_{ex} = 0.164$ m is the external diameter of the cylinder liner;

$h = 7 \cdot 10^{-3}$ m is the thickness of the cylinder liner;

$\sigma = 0.26$ is the Poisson's ratio for the steel 38 KhMYuA;

$\rho = 8.68 \cdot 10^2$ kg $\cdot$ sec^2/m^4 is the density of the steel;

$E = 2 \cdot 10^{10}$ kg/m^2 is Young's modulus;

$g = 9.8$m/sec^2 is the acceleration due to gravity;

$\delta = 3.3 \cdot 10^{-4}$ m is the thermal gap between the piston and cylinder of the running diesel engine with a 100% load;

$m_o = 0.626$ kg $\cdot$sec^2/m is the mass of the parts in translational motion;

$n = 1500$ rpm is the diesel engine rpm;

$\lambda' = R/L = 0.28$ is the ratio of the crank radius to the connecting rod length;

$p_e = 5.2 \cdot 10^4$ kg/m^2 is the mean effect of pressure;

$F_p = 1.76 \cdot 10^{-2}$ m^2 is the piston area;

$\beta = h^2/12a^2 = 49/12 \cdot 6160 = 0{,}000664$ is a coefficient.

The maximum side pressure acting at a cylinder liner is

$$P_{max} = 2.7 \lambda' P_c F_p = 692 \text{ kg.}$$

The time required for a crank angle of 15°C from the TDC is

$$T = \varphi_1 / 6n = 0.0016 \text{ sec.}$$

The distance from the upper edge of the liner to the axis of the piston pin, for a 30° crank angle is

$$c_1 = c + 0.067 H = 8.3 \cdot 10^{-2} \text{ m.}$$

The further calculation is presented in Table 21.

Table 21: Calculation of Quantities

Величины 1	$n_1 = 2;\ m = 1$	$n_1 = 3;\ m = 1$	$n_1 = 2;\ m = 2$
λ	2,37	2,37	4,74
K_0	12,745	20,8	295
K_1	42,8887	89,1433	289,751
K_2	14,15	21,0	37,3
Δ	0,3261	0,2462	1,1516
$f_{кр}$ в гц 2	5769	5069	16 860
τ в сек 3	$1,74 \cdot 10^{-4}$	$2 \cdot 10^{-4}$	$9,27 \cdot 10^{-5}$
ω^2 в $1/сек^2$ 4	$13,05 \cdot 10^8$	$9,85 \cdot 10^8$	$46 \cdot 10^8$
$\sin^2 \frac{\pi n c_1}{l}$	0,49	0,49	1
A в м 5	$9,65 \cdot 10^8$	$1,465 \cdot 10^{-7}$	$2,97 \cdot 10^{-8}$
$W_{расч}$ в $м/сек^2$ 6	126	144	136
S_2	12,8	14,7	13,9

Key: 1. Quantities

2. f_{fr} in Hz

3. τ in sec

4. ω^2 in sec^{-1}

5. A in m

6. W_{cal} in m/sec^2

The calculation shows that introducing an additional support sharply reduced the liner vibration and shifted it into the postcritical region.

Here the cavitation damage occurs so slowly that the liner must be replaced not because of cavitation damage but because of cylinder surface wear.

36: Parts And Assemblies Whose Service Periods Can Be Limited by Cavitation When Uprating and Increasing the Service Life of Diesel Engines

In spite of the large volume of research on cavitation and cavitation erosion conducted in various fields of technology, there are still a good many questions and directions associated with the physics of the cavitation damage process that remain unclear.

These problems, directly bearing on cavitation damage in diesel engines, can include the following.

1. The mutual role of mechanical and electrochemical processes in cavitation erosion caused by vibrations of various intensities has not been clarified. Neither have the physical basis for the inception and nature of electrochemical processes accompanying cavitation been established with reference to the possible role of the double electrical layer at the surface of the metal being damaged, formation of microcouples with small internal friction when microvolumes undergo deformation at the surfaces of the metal being damaged, and the effect of these on the pressure peaks observed during the collapse of cavitation bubbles, as well as the high temperatures that accompany this process. Clarifying

the mutual role and conditions for mechanical and electrochemical processes in cavitation erosion caused by vibration would promote a more well-defined development of the effect of methods of protecting the cylinder liners and blocks against cavitation damage.

2. According to the major difficulties in measuring the high pressures in microvolumes, the pressure change (with determination of its final value), in cavitation bubbles obtained for different vibration conditions has not yet been adequately studied. The entire mechanism of the gradual buildup of metal damage when exposed to cavitation erosion in conditions when the initial damage foci are present or when they are absent, is not clear enough. No adequate explanation has been given as to why, for the same intensity of vibrations in liners installed in experiments with the same clearances at the very same place, as a rule, zones of cavity accumulation arise, and sometimes only one or two cavities in this site, and in both cases the deepening of cavities proceeds at virtually the same rate.

3. Problems associated with the actual basis for the effect of the properties of a liquid on cavitation damage for vibrations have also not been adequately studied, including the effect of the distance between the vibrating and fixed walls. Only general correlations have been studied in this direction.

4. At the present time, a quantitative account of the mutual effect of changes in flow rate and vibration on the buildup of cavitation erosion is difficult. Clear data on this problem would promote the designing of more rational diesel engine cooling systems. Cavitation erosion is a complicated process that depends on numerous factors.

Therefore, detailed studies of the quantitative and qualitative effect of these factors on damage will assist in operating the reliability and service life of diesel engines.

In recent years there has been a trend to reducing diesel engine weights by operating the rpm and the mean effective pressure. This, in turn, leads to higher vibro-activity of diesel engines, higher liquid flow rate, and an overall rise in the dynamicity of loads on diesel engine assemblies and parts. The potentials for cavitation and cavitation damage are latent in the slip bearings and in the fuel equipment.

Figure 83: Damage to Fuel Pump

There have been cases of premature malfunctioning of bearings in D100 diesel engines and others for reasons of cavitation in the oil wedge, and also in the fuel equipment. Cavitation in these diesel engine

assemblies occurs principally as a result of hydrodynamic factors, which must first of all include pressure drops. Vibrations of these assemblies can promote a buildup of cavitation, but are not the primary factor. The relative pattern of damage in material tested on MSV shows that to lessen cavitation damage in these assemblies, in all cases efforts must be made to reduce the pressure drop.

In several cases, for bearings, it is expedient to somewhat increase the viscosity of the oil or to reduce its outflow through the faces, since when this is done, cavitation damage is diminished. In the event of developed cavitation, this proves inadequate, and it is necessary to use a more cavitation-resistant antifriction alloy for the bearings. It must be noted that subsequent studies made it possible to associate the initial stages of cavitation and cavitation damage in bearings with the velocity of crankshaft journals and the oil wedge, with the pressures at the different points in the oil wedge and also with the design dimensions of the bearing and the extent of its vibration, which permitted devising a method for calculating the functioning of a bearing in a non-cavitation regime.

In fuel equipment, especially in the plunger pairs, cavitation leads to the malfunctioning of the plunger and liner after 10 - 20 hours of operation. Figure 83 shows damage to the plunger of a fuel pump. Work-hardening and damage cause jamming of the plunger pairs and the diesel engine loses its serviceability and malfunctions. Therefore cavitation in a plunger pair is an altogether undesirable phenomenon. At the present time we know that cavitation in fuel equipment can be eliminated only by increasing the duration of the cyclic feed and by

to a metal occurs under the effect of high pressures concentrated over micro-areas, exceeding the strength of the given material, one of the methods of surface protection can be to increase surface hardness. This is especially valuable for diesel engines in which the predominate liner vibration frequency is in the range 800 - 2000Hz. In this frequency range, the mechanical factor is dominant in cavitation damage to surfaces. An increase in liner surface hardness can be achieved by work-hardening, nitriding, and the use of solid coatings.

Chromium has proven itself in solid protective coatings. The use of coatings of porous chromium is most rational, since it provides a uniform layer without micro-cracks that can serve as corrosion foci and subsequent cavitation damage. Micro-cracks can be present when the surface is coated with solid gleaming chromium. However, the intensity of liner vibration is high and the coating with porous chromium does not provide protection against cavitation damage, then a coating with hard gleaming chromium must be used.

Chrome-plated liners are used in various high-rpm diesel engines of the models Ch 8.5/11, Ch 10.5/13, and Ch 15/18, Ch 18/20 and so on. The use of chromium coatings either completely eliminates cavitation damage if individual pressure peaks in the implosion of cavitation bubbles do not exceed the stresses exceeding the strength of the coating, or else considerably prolong the liner surface life. Everything depends on the intensity of the cavitation processes in the specific diesel engine.

Experience shows that in the locations where clusters of cavitation cavities form on uncoated liners, a layer of porous chromium acquires a gleam due to work-hardening during cavitation.

When coatings of porous chromium of different thicknesses were tested on cylinder liners subjected to various vibration intensities, and also in tests of chromium coatings on specimens placed on MSV, curves were plotted of the increase of the liner surface life (Figure 80). These data show that the surface life of a liner increases with coating thickness and decreases with increase in vibration accelerations. A 20 - 25 micron thick layer is the most suitable (with allowance for the time required for chrome-plating). Increasing the thickness of the chromium layer to 50 microns is inadvisable, since cases of layer spalling and scaling due to vibration are observed for thick layers.

When liners coated with a chromium layer are used, one must consider that the energy developing in the implosion of a cavitation bubble is not expended in the failure of the liner surface and is reflected from it. Accordingly, the damage to the opposite walls of a block can increase. Damage to opposite surfaces will be the more severe, the narrower the passage in the water jacket. Accordingly, the passages in a water jacket must be wide. As we can see from the foregoing and from inspecting Figure 80, the use of chromium coatings increases the surface life of cylinder liners.

lowering the pressure drop at the point of fuel cut-off. Increasing the hardness of plunger and liner surfaces promotes a reduction in cavitation damage. There is no doubt that cavitation in fuel equipment merits further investigation in order to find the physical causes for its inception and to control it.

BIBLIOGRAPHY

1. Babikov, O. I., Ul'trazvuk i Yego Primeneniye v Promyshlennosti (Ultrasound and Its Industrial Applications), Moscow, Fizmatgiz, 1958.

2. Basin, A. M., and Anfimov, V. N., Gidrodinamika Sudna (Hydrodynamics of the Ship), Leningrad, Rechnoy Transport Press, 1961.

3. Bogachev, I. N., and Mints, R. I., "Increasing the Cavitation Resistance of Machine Parts by Using Surfactants," Izv. Vuzov. Mashinostroyeniye, No. 2, (1963).

4. Bergman, L., Ul'trazvuk (Ultrasound), Moscow, Foreign Lit. Pub. House, 1957.

5. Bochmanov, D. V., Zashchita Tsilindrovykh Vtulok i Blokov so Storony, Omyvayemoy Vodoy, Vspomogatel'nykh Dvigateley Vnutrennego Sgoraniya na Rybopromyshlovykh Sudakh (Protection of Cylinder Liners and Blocks on the Side Swept by Water in Auxiliary Internal Combustion Engines on Fishing Vessels), Vil'nyus, MINTIS Press, 1965.

6. Vedenkin, S. G., "Protection Against Damage to Cylinder Liners and Blocks in Locomotive Diesel Engines," Trudy VNIIZhT (Transactions of the All-Union Scientific Research Institute of Railroad Transportation), No. 87, (1952).

7. Velikson, D. M., "Control of Corrosion of Cylinder Liners and Blocks of Diesel Engines on the Side Swept by Water," Proizvodstvenno-Tekhnicheskiy Sbornik MRF (Production-Engineering Collection of Articles of the Ministry of the River Fleet), Moscow, No. 3, (1959).

8. Voskresenskiy, I. N., Korroziya i Yeroziya Sudovykh Grebnykh Vintov (Corrosion and Erosion of Marine Propellers), Leningrad, Sudpromgiz, 1948.

9. Vysotskiy, A. A., and Zobachev, Yu. Ye., "Protection of Metals Against Cavitation Damage by Using Anticorrosion Additives," Energomashinostroyeniye, No. 4, (1965).

10. Glikman, L. A., Korrozionno-mekhanicheskaya Prochnost' Materialov (Corrosion-Mechanical Strength of Materials), Moscow, Mashgiz, 1955.

11. Gorshkov, A. Ye., and Ruscetskiy, A. A., Kavitatsionnyye Truby (Cavitation Tubing), Leningrad, Sudpromgiz, 1962.

12. Goryunov, Yu. V., Effekt Rebindera (Rebinder Effect), Moscow, Nauka Press, 1966.

13. Grishin, K. S., "Protection of the Cooling Systems of Diesel Locomotive Engines Equipped With Aluminum Blocks Against Damage," Vestnik VNII Zheleznodorozhnogo Transporta, No. 4, (1960).

14. Den, Hartog, Teoriya Kolebaniya (Theory of Vibrations), Moscow-Leningrad, Gostekhteoretizdat, 1942.

15. Dorogov, B. S., Eroziya Lopatok v Parovykh Turbinakh (Erosion of Blades in Steam Turbines), Moscow-Leningrad, Energiya Press, 1965.

16. Zinchenko, V. I., Shum Sudovykh Dvigateley (Noise in Marine Engines), Leningrad, Sudpromgiz, 1958.

17. Ivanchenko, N. N., "Vibrations of the Liners of Light Diesel Engines and Their Effect on the Pitting of Water-Swept Walls," Trudy TsNIDI (Transactions of the Central Scientific Research Diesel Institute), Nos. 20, 23, 26, Leningrad, Mashgiz, (1952).

18. Ivanchenko, N. N., "Effect of Diesel Engine Design and Its Operating Conditions on the Cavitation Erosion of Cylinder Liners and Blocks," Energomashinostroyeniye, No. 12, (1965).

19. Ivanov, V. P., "Studies of the Vibration of Cylinder Liners of the Model 11D45 Diesel Engine," Zhurnal Teplovoznaya i Elektricheskaya Tyaga, No. 3, (1964).

20. Karpenko, G. V., Prochnost' Stali v Korrozionnoy Srede (Strength of Steel in a Corrosive Medium), Moscow-Leningrad, Mashgiz, 1963.

21. Karelin, A., Ul'trazvuk, Moscow, Foreign Literature Pub. House, 1960.

22. Konstantinov, V. A., "Problems of the Physical Nature of Cavitation and Erosion," Izv. AN SSSR, Otdel Tekhnicheskikh Nauk, Moscow, No. 6, (1949).

23. Kozyrev, S. P., Gidroabrazivnyy Iznos Metallov pri Kavitatsii i Erozii (Hydroabrasive Wear of Metals in Cavitation and Erosion), Moscow, Mashinstroyeniye Press, 1964.

24. Kornfel'd, M., Uprugost' i Prochnost' Zhidkostey (Elasticity and Strength of Liquids), Moscow, Gostekhteoretizdat, 1951.

25. Kochergin, S. M., and Vyaseleva, G. V., Elektroosazhdeniye Metallov v Ul'trazvukovom Pole (Electrodeposition of Metals in an Ultrasonic Field), Moscow, Vysshaya Shkola Press, 1964.

26. Kudryavtsev, B. B., Ul'traakusticheskiye Metody Issledovaniya Veshchestva (Ultrasonic Methods of Investigating Materials), Moscow, Uchpedgiz, 1961.

27. Metter, I., "Physical Nature of Cavitation and the Mechanism of Cavitation Damage," Uspekhi Fizicheskikh Nauk, No. 2, Moscow, USSR Academy of Sciences Press, Vol. 35, 1948.

28. Morz, F., Kolebaniya i Zvuk (Vibrations and Sound), Moscow, Gostekhteoretizdat, 1949.

29. Nikitin, M. D., Poristokhromovoye Pokrytiye Detaley Dvigatelya (Porous-Chrome Coating of Engine Parts), Moscow-Leningrad, Mashgiz, 1950.

30. Pernik, A. D., Problemy Kavitatsii (Problems of Cavitation), Leningrad, Sudpromgiz, 1966.

31. Pronin, M. V., Udlineniye Sroka Sluzhby Dvigatelya 3D6 (Extending the Service Life of Engine Model 3D6), Moscow, Rechnoy Transport Press, 1962.

32. Rozenfel'd, N. L., and Akimov, G. V., "Mechanism of Chromate Protection of Iron Against Corrosion," Trudy Instituta Fizicheskoy Khimii (Transactions of the Institute of Physical Chemistry), No. 2, Moscow, USSR Academy of Sciences Press, 1951.

33. Semerchan, A. A., and Vereshchagin, L. F., "Theory of the Destructive Action of Cavitation," Inzhenerno-Fizicheskiy Zhurnal, No. 3, (1960).

34. Skuridin, A. A., "Cylinder-Piston Group as a Source of Diesel Engine Vibrations," Transportnoye Mashinostroyeniye, No. 4, (1960).

35. Skurdin, A. A., and Nikitin, M. D., Kavitatsionnaya Eroziya Detaley Dizeley, Omyvayemykh Okhlazhdayushchey Zhidkost'yu (Cavitation Erosion of Diesel Engine Parts Swept by Coolant), Moscow, NIIinformtyazhmash, 1966.

36. Chernyy, F., and Lebl', K., "Erosion Resistance of Solid Alloys Used for Sealing Surfaces of Water-Steam Fittings," Elektricheskiye Stantsii, No. 4, (1957).

37. Shimanskiy, Yu. A., Dinamicheskiy Raschet Sudovykh Konstruktsiy (Dynamic Calculation of Ship Structures), Leningrad, Sudpromgiz, 1948.

38. Shul'man, Z. P., "Comparative Testing of the Erosion Resistance of Certain Grades of Steel and Cast Iron," Energomashinostroyeniye, No. 4, (1958).

39. Evans, Yu. R., Korroziya, Passivnost' i Zashchita Metallov (Corrosion, Passivation, and Protection of Metals), Moscow, Metallurgizdat, 1941.

40. Epshteyn, L., "Cavitation -- Is It Only a Disadvantage?" Tekhnika Molodezhi, No. 8, (1965).

41. Ekspress-Informatsiya. Porshnevyye i Gazovyye Dvigateli, Moscow, VVINTI, No. 2, (1965).

42. Yushkin, V. V., Gidravlika (Hydraulics), Minsk, Vysshaya Shkola Press, 1964.

43. Arnold, R. N., "Vibration Cylinders," The Institute of Mechanical Engineers, 167(1), (1963).

44. Wilson, R. W., "The Control of Cavitation Damage in Diesel Engines," Paper to be presented to the Shell Symposium in Moscow, London, 1967.

45. Pflug, E., and Piltz, H., "Corrosion and Cavitation in the Water-Cooling Jackets in Uprated Diesel Engines in Railroad Use With Respect to Causes and Corrective Measures," Motortechn. Zeitung, 26(3), (1965).

46. Spengler, G., "Nature and Applications of Ultrasound," Radio und Fernsehen, No. 5, (1956).

47. Collins, H., "Pitting of Diesel Cylinder Liners," Oil Engine, 27(316), (1960).

48. Love, A., Mathematical Theory of Elasticity, fourth edition, Cambridge University, 1939.

49. Mousson, S., "Pitting Resistance of Metal Under Cavitation Conditions," Transactions ASME, 59, (1937).

50. Plesent, M., and Ellis, A., "On the Mechanism of Cavitation Damage," ibid., 77(7), (1955).

51. Ellis, A., "Production of Accelerated Cavitation Damage by Acoustic /illegible/ in Cylindrical Cavities," Acoustical Society of America, 27, (1955).

52. Montgomery, A., "Design for Minimum Corrosion in 'Composite' Engines," SAE Journal, 68(8), (1960).

53. Cropp, T., and Ellrich, W., "Erosion in the Blading of Low-Speed Turbines," Elektrizitatswirtschaft, 30(21), (1931).

54. Rayleigh, A., and Zord, N., Theory of Sound, second edition, Macmillan and Company, Vol. 1, London, 1894.